

Artificial Transfer Hydrogenases Based on Biotin-Streptavidin Technology

Inauguraldissertation

zur Erlangung der Würde eines Doktors der Philosophie

vorgelegt der

Philosophisch-Naturwissenschaftlichen Fakultät

der Universität Basel

von

Tommaso Quinto

Aus Cerignola, Italien

Basel, 2015

Originaldokument gespeichert auf dem Dokumentenserver der Universität Basel

edoc.unibas.ch

Genehmigt von der Philosophisch-Naturwissenschaftlichen Fakultät auf Antrag von:

Prof. Dr Thomas R. Ward

Prof. Dr Catherine Housecroft

Basel, den 19 May 2015

Prof. Dr Jörg Schibler

Dekan

Acknowledgements

It was a long journey personal and professional, during which I had the chance to meet a multitude of people, different culture and various place, that all contribute to my life experience. I'm glad I had the opportunity to perform this journey.

I want to thank Prof. Thomas R. Ward, to give me the possibility to carry out the PhD in a multidisciplinary group and give me the unique opportunity to be part of an international European program.

I'm also grateful to Prof. Catherine Housecroft for accepting to co-referee this thesis, and for being interested in my professional and private life. I also thank Prof. Oliver Wenger for accepting to be the chairman.

Thanks to Daniel Häussinger for the help, understanding and making easier, complicated NMR interpretation and with whom I share the credit for chapter 4 of this thesis.

An immense thanks to Valentin Köhler, for his help, patience, guidance during all my work, for the accurate and meticulous approach to science, for all the discussion about science, and different arguments in life. Thanks for the loud music in the lab also if sometimes it was not my genre.

Thanks to Yvonne Wilson, for all the nice time, discussion and motivation "to continue", that you give me, for the moral support during my knee accident "you will be fast again", and for all the English corrections.

Thanks to my German speaking labmate, Marc Dürrenberger, Tillmann Heinisch, Sascha Keller, Valentin Köhler, for the nice atmosphere in the lab, discussion in science and out of science, for the football time spent together, to tolerate my crazy rumbles in Italian dialect, and for training my ear to the German language. Thanks Sasha for all the time out of the lab, and trip to Belgrade.

Thanks to Marc Creus to express all his happiness all the time, nice anecdotes, and different ways of thinking.

Special thanks to Elisa, to be my friend, in and out of lab, to share nice and bad moment, to encourage and listen reciprocally and travel around Europe during these years. I'm glad I met you.

Thanks to Alessia to be my "terron" friends for your friendship. Thanks to Gaetano (Tano) for the first welcome in Basel, and to be the "commare" whit who to speak about "sophisticated argument" and make far away trip to Riga and leave "nice memory".

Thanks to Martina and Peter, for your Slovak friendship and enthusiasm, for the practical approach to argument, open language, time during trips, and the patience to listen me and to be my favorite bakery. I'm happy I met you!! Ďakujem!!

A big thanks to all of the people in the group past and present, that I met during this year and contribute to create a nice atmosphere in the lab, for discussion and patience, thanks to Cheick, Thibaud, Fabien Monnard, Didier, Gregory, Sabina, Narashima, Maurus, Jeremy, Christian Tagwerker, Livia Knörr, Julian Ruoss, Mark R. Ewa, Anamitra, Maxime, Fabien, Raphael, and all the other that I may be forgotten.

Thanks to Veronica, Elena, Manuele, for all the time, and the wonderful trip along the Danube, it was an inspiring and creative time.

Thanks to Marko and Serbo, for the efficient hard training and nice talk and open language.

Angelo, Ledi, Stefan, thanks for the deep and constructive discussion, different vision and approach to life.

A big thanks to Marie Curie Training Network (FP7-ITN-238531) for the financial support ad give me the possibility to share knowledge and travel round Europe, in a nice experience. Thanks to Biotrains network, for the pleasant time, to the industrial partners, all the PI, Nick Turner, John Woodley, Frank Hollmann, Thomas Ward, Martina Pohl, Dorth Rother, Vincente Gotor- Fernández, Ivàn Lavandera Garcia, Wolfgang Kroutil, Bo Mattiason, Rajni Hatti-Kaul.

Thanks to all the other fellow students to share time, passion, knowledge and discussion around Europe: Elisa, Serena Gargiulo, Ekaterina Churakova, Serena Bisagni, Oksana, Diego, Bas, Kinga, Caroline, Betti Kondor, Georgina, Annika, Elina, Aashrita, Alvaro, Justina, Bart, Watson, Joana.

Thanks to Frank Hollmann to welcome me in Delft and the scientific time. Thanks Katia, to work together in productive collaboration, and whit Serena Gargiulo to make feel like home even if was only 1 month in Delft, and for all the discussion and pleasant time together.

Thanks to Wolfgang Kroutil to welcome me in Graz, and give the opportunity to work in his lab. Thanks to Francesco Mutti, to supervise me and the contagious smiling approach to the science. Thanks to Elina and Aashrita for the nice time in Graz.

Thanks to Richard Lloyd to welcome me in Cambridge at Dr Reddy's and the scientific support. Thanks to Armando and John Waller for the beer and nice time.

Thanks to all the Department, the secretary Beatrice and Isa, and the technical staff from Werkstatt.

Thanks to Luca e Daniela, to share with me nice moment of their life, conversation, and the moral support along this years, and make me part of the family of their life, Daniela to be my favourite hairdresser and Luca to be my "Kröte".

Thanks to my Trentino's friends, Beppe, Matteo, Claudia, Sabrina, Clarissa, Daniele, Letizia (I know you are from Alfero not from Trentino Letizia) for all the pleasant time together, for the moral support, discussion, wonderful time spent in Trentino and around Italy, you are wonderful! Clarissa and Daniela to have the Tommy's room at their home, and Clarissa thanks to listen me, to encourage me, to give me the happiness feeling and good feeling, each time I speak with you, to push me toward positive experience.... Grazie di esserci sempre!!

Stefano, thanks, to be my friend, my special "black", to be there all the time, to listen, from the time you was "isolated" in Fondi, to have the right word at right moment, to push me and act toward difficulties, to the very positive confidence in me. Is time to make the well-deserved trip! Grazie infinite per la tua presenza!!

Grazie alla mia famiglia, mamma, papa, Michele, Giovanni, Federica, per avermi stimolato e incoraggiato, costantemente in tutti i momenti difficili, per aver cercato di portare sempre il sorriso in ogni momento, per la fiducia riposta in me. Il vostro sorriso mi rende felice.

Summary

The importance of metalloenzymes in nature is reflected by their involvement in many fundamental processes (*e.g.* photosynthesis, respiration, nitrogen fixation). The creation of artificial metalloenzymes for chemical and biochemical applications is an intriguing and potentially highly rewarding area of research. As a starting point, a catalytically active transition metal complex or catalyst precursor needs to be incorporated into a host protein thereby generating a hybrid, which exhibits attractive features of biocatalyst and chemocatalyst. Exploiting the biotin (strept)avidin technology for the creation of artificial metalloenzymes, is a convenient means, to ensure the cofactor localisation thanks to the high affinity of biotin for streptavidin. Synthetic cofactor and protein host can be separately modified by chemical- and genetic means, respectively and subsequently combined. The topic of this thesis is to create artificial transfer hydrogenases relying on this technology and to study the resulting constructs. With the ultimate goal of implementing efficient directed evolution protocols for the optimization of artificial metalloenzymes and for their application *in vivo*, the interaction between the active catalyst and the biological environment needs to be evaluated. Mutual inhibition between the synthetic catalyst and enzymes (other than Sav) was identified as one potential problem. After reviewing the main organometallic-based methods for the non-enzymatic regeneration of NADH, a solution for the frequently observed inhibition between the organometallic NADH regeneration system and the NADH dependent enzyme, namely the compartmentalization of the synthetic cofactor in Sav, will be discussed. The incorporation of the active organometallic catalyst [Cp*Ir(biot-*p*-L)Cl] into streptavidin, led to an active ATHase (Artificial Transfer Hydrogenase), utilized for NADH regeneration, which was subsequently successfully coupled in a cascade biocatalysis reaction with HbpA (a NADH and FADH₂ dependent monooxygenase), for the selective hydroxylation of 2-hydroxybiphenyl to 2,3-hydroxybiphenyl. Next, the stereoselectivity of the ATHase

mediated-NAD⁺ reduction with deuterated formate as a deuteride source was investigated resulting in up to 90% *de*.

Finally chemical variants of IrCp*/Sav- or RhCp*/Sav-based transfer hydrogenases were studied. In order to rapidly generate chemical diversity, a new approach for the creation of biotinylated complexes is presented. Tethering the biotin anchor to the Cp* moiety of the organometallic complex, thereby leaving three coordination sites vacant, enabled fast screening of libraries of bidentate ligands, which led to the identification α -amino amides as promising ligands for the asymmetric reduction of cyclic imines.

Impact of the work

The work presented herein was initiated and guided by Prof. Dr Thomas R. Ward at the Chemistry Department of the University of Basel, during the time period from October 2009 to September 2013.

Excerpts from this work have been published in the following journals:

Quinto T., Häussinger D., Köhler, V., Ward T. R. “Artificial metalloenzymes for the diastereoselective reduction of the NAD⁺ to NAD²H”, *Org & Biomol. Chem.*, **2015**, *13*, 357-360.

Quinto T., Schwizer F., Zimbron J. M., Morina A., Köhler V., Ward T. R. “Expanding the chemical diversity in artificial imine reductases based on the biotin-streptavidin technology”, *ChemCatChem.*, **2014**, *6*, 1010-1014.

Quinto T., Köhler V., Ward T. R. “Recent trends in biomimetic NADH regeneration”, *Topic & Catal.*, **2014**, *57*, 321-331.

Köhler V., Wilson Y. M., Dürrenberger M., Ghislieri D., Churakova E., Quinto T., Knörr L., Häussinger D., Hollmann F., Turner N. J., Ward T. R. “Synthetic cascades are enabled by combining biocatalyst with artificial metalloenzymes”, *Nat. Chem.*, **2013**, *5*, 93-99.

Keywords: artificial metalloenzyme, chemo-genetic optimization, asymmetric catalysis, NADH regeneration, compartmentalization, transfer hydrogenation, imine reduction.

Table of contents

Acknowledgements	i
Summary	v
Impact of the wok	vii
Table of contents	viii
Abbreviation	xi
1 Introduction	1
1.1. Generalities about catalysis	1
1.2. Artificial metalloenzymes	4
1.3. Catalytic scope	9
1.3.1. NADH regeneration	9
1.3.2. Transfer hydrogenation: asymmetric imine reduction	11
1.4. Scope of the thesis	14
1.5. References	15
2 Recent trends in biomimetic NADH regeneration	21
2.1. Abstract	22
2.2. Introduction	22
2.3. Pioneering non-enzymatic approaches for the regeneration of nicotinamide adenine dinucleotide phosphate [NAD(P)H]	23
2.4. Recent developments for NAD(P)H and NAD(P) ⁺ regeneration	27
2.5. Mutual inactivation of the organometallic catalyst and the enzyme	32
2.6. Outlook	38
2.7. References	39

3 Synthetic cascades are enabled by combining biocatalysts with artificial metalloenzymes	45
3.1. Preamble	45
3.2. Abstract	48
3.3. Introduction	48
3.4. NADH regeneration for monooxygenases	50
3.5. Outlook	52
3.6. Supporting information	53
3.7. References	64
4 Artificial metalloenzymes for the diastereoselective reduction of NAD⁺ to NAD²H	69
4.1. Abstract	70
4.2. Introduction	70
4.3. Results and discussion	73
4.4. Conclusion	75
4.5. Experimental section	75
4.6. References	77
5 Expanding the chemical diversity in artificial imine reductases based on the biotin-streptavidin technology	79
5.1. Abstract	80
5.2. Introduction	80
5.3. Results and discussion	81
5.4. Conclusion	91
5.5. Experimental section	91

5.6. Supporting Information	92
5.7. References	98
6 Conclusion and outlook	103
Curriculum vitae	107
Appendices	111

Abbreviations

⊂	included in
Ag	silver
AgCl	silver chloride
L/D -AlaNH ₂	L/D -alanine amide
AME	artificial metallo enzymes
aq	aqueous
L/D -ArgNH ₂	L/D -arginine amide
L-AspNH ₂	L-aspartic acide amide
L-AsnNH ₂	L-asparagine amide
ATHase	artificial transfer hydrogenase
atm	atmosphere
β	beta
biot	biotin
Bpy	2,2'-bipyridine
CH ₂ Cl ₂	dichloromethane
Cp*	pentamethylcyclopentadienil (C ₅ Me ₅)
D ₂ O	deuterated water
<i>de</i>	diastereoselective excess
DNA	deoxyribonucleic acid
L-3,4-dehydroProNH ₂	L-proline amide-N-Ethyl
e ⁻	electron (s)
<i>ee</i>	enantiomeric excess
<i>e.g.</i>	for example (from Latin: <i>exempli gratia</i>)
FAD	flavin adenine dinucleotide
GC	gas chromatography
L-GlnNH ₂	L-glutamine amide
glyNH ₂	glycine amide
β-glyNH ₂	β-glycine amide
h	hour (s)
H ₂	hydrogen (gas)
HCOONa	sodium formate
HbpA	hydroxybiphenyl monooxygenase
He	helium

L-HisNH ₂	L-histidine amide
HNEt ₂	diethyl amine
H ₃ N·BH ₃	ammonia borane
H ₂ O ₂	hydrogen peroxide
HPLC	high performance liquid chromatography
L-IleNH ₂	L-isoleucine amide
<i>i</i> -PrOH	isopropanol
Ir	iridium
<i>J</i>	coupling constant in hertz
<i>k_M</i>	Michaelis constant
<i>k_{cat}</i>	catalytic constant
KOH	potassium hydroxide
l	litre
L/D-LeuNH ₂	L/D-leucine amide
LDH	lactate dehydrogenase
L-LysNH ₂	L-lysine amide
M	Molar
μ	micro
MAO-N	monoamine oxidases
Me	methyl
MeOH	methanol
L-MetNH ₂	L-methionine amide
mg	milligrams
ml	milliliter
mM	milli Molar
Mol	mole
MOPS	3-(<i>N</i> -morpholino)propanesulphonic acid
ms	milliseconds
mV	millivolts
N ₂	nitrogen (gas)
NABH ₄	sodium borohydride
NADH	nicotinamide adenine dinucleotide (reduced form)
NAD ⁺	nicotinamide adenine dinucleotide
NAD(P)H	nicotinamide adenine dinucleotide phosphate (reduced form)
NAD(P) ⁺	nicotinamide adenine dinucleotide phosphate
NaH ₂ PO ₄	monosodium phosphate
(NH ₄) ₂ SO ₄	ammonium sulphate

NaOH	sodium hydroxide
Na ₂ SO ₄	sodium sulphate
nm	nanometres
NMR	nuclear magnetic resonance
pD	pH for D ₂ O
L-ProNHethyl	L-proline amide-N-Ethyl
L/D-ProNH ₂	L/D-proline amide
L/D-PheNH ₂	L/D-phenylalanine amide
ppm	part per million
Rh	rhodium
rpm	rotation per minute
Sav	streptavidin
L-SerNH ₂	L-serine amide
T _(ret)	retention time
TEA	triethylamine
TEOA	triethanolamine
L-ThrNH ₂	L-threonine amide
TOCSY	total correlation spectroscopy
TOF	turnover frequency (mol of product/(mol of catalyst x time))
TON	turnover number (mol of product/mol of catalyst)
L-TrpNH ₂	L-tryptophan amide
L-TyrNH ₂	L-tyrosine amide
V	volts
L/D-ValNH ₂	L/D-valine amide
WT	wild-type

Chapter 1

Introduction

1.1 Generalities about catalysis

Enzymes are widely applied for chemical transformations^[1] due to their high activity and selectivity resulting from their complex and well organized three-dimensional structure. Enzymes are able to perform complicated transformations such as photosynthesis, nitrogen fixation, respiration *etc.* Nowadays, the use of enzymes in industry is extensive for the synthesis of complex molecule *e.g.* in the production of pharmaceuticals, agrochemicals and flavours.^[2,3] The preparation of enantiopure compounds from a racemic mixture or prochiral compounds is still considered challenging for a range of transformations.

In 1893, Lord Kelvin was the first to define chirality “*I call any geometrical figure, or group of points, chiral, and say it has chirality, if its image in a plane mirror, ideally realized, cannot be brought to coincide with itself*”.^[4] Chirality is present in nature almost everywhere, and in different types of molecules including DNA, carbohydrates, amino acids, vitamins and alkaloids. Chiral molecules have two enantiomeric forms, which correspond to the respective image or mirror image of the molecule. Pure enantiomers possess the same physical and chemical properties (*e.g.* boiling points, density, solubility, redox potential, pKa, etc.) but interact differently with chiral system (*e.g.* proteins) and with polarized light (Figure 1.1).^[5-7]

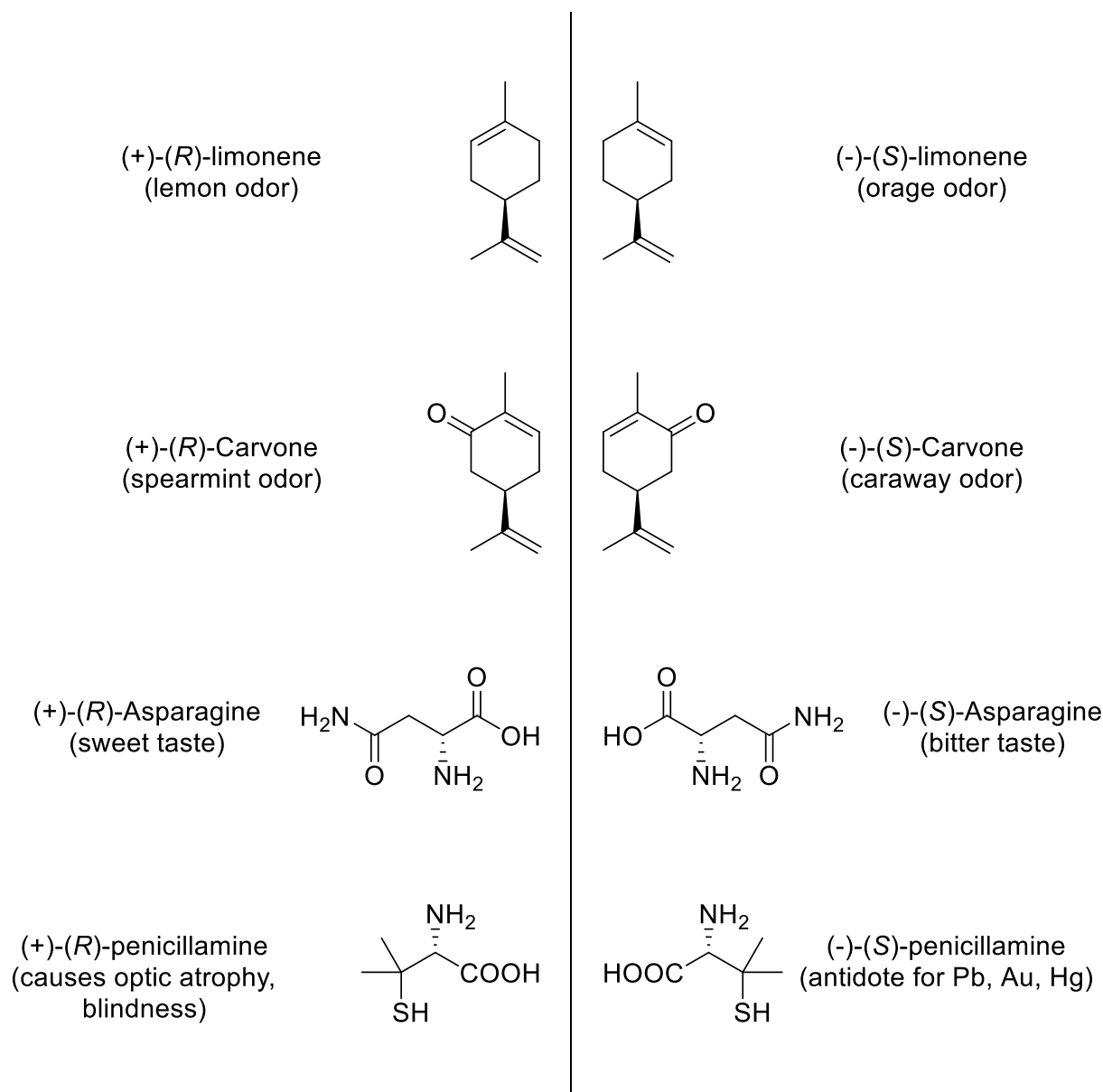


Figure 1.1 — Some examples of the effects of enantiomers on biological systems. The central line indicates a mirror plane

These few examples highlight the importance of chirality, and the importance to generate or isolate single enantiomers. In the context of synthesis, enantioselective catalysis occupies a place of choice. Its aim is to favour the exclusive formation of a single enantiomer starting from a racemic or prochiral starting materials. A common term to describe the ratio between two enantiomers, is the enantiomeric excess (ee) which is defined as (equation 1.1):

$$ee = \frac{([R] - [S])}{([R] + [S])} \cdot 100 \quad (1.1)$$

The determination of *ee* can be achieved with different techniques like polarimetry, NMR-spectroscopy (after derivatization) and chromatographic methods (HPLC or GC).

Commonly three different types of enantioselective catalysis are distinguished: heterogeneous, homogeneous and bio-catalysis. The last two research fields have generated a wide variety of methods for the synthesis of enantiopure compounds.^[1,8]

In homogeneous transition metal catalysis, the enantioselectivity of the reaction is provided by a catalyst consisting of a metal and a small enantiopure ligand directly bound to the metal. The chiral induction for the reaction relies on first coordination sphere interactions between ligand, metal and substrate, respectively. An exact prediction of the stereochemical outcome is difficult, and a screening approach is generally used.^[9] In biocatalysis the chiral environment of the reaction is typically more precisely controlled through additional interactions of the substrate with the protein scaffold (hydrogen bonding, hydrophobic interactions) by the so-called “second coordination sphere”.^[10] These additional interactions contribute to the stabilization of the transition state. Homogeneous catalysis and biocatalysis are complementary in many aspects (Table 1.1).^[8,11]

Table 1.1 Comparison of typical features of homogeneous and enzymatic catalysis.

	Homogeneous catalysis	Bio-catalysis
Substrate scope	large	small
Enantiomers	both enantiomers	single enantiomers
Turnover number	limited	large
Metal involved	any metal	limited (biorelevant)
Reaction repertoire	large	small
Reaction medium	mostly organic	mostly aqueous
Optimization	chemical	genetic
Second coordination sphere	poorly defined	well defined

In line with arguments listed in the table above, biocatalysts can be very active and selective for specific reactions, whereas homogeneous catalysis covers a broader range of reactions. Hence, a catalytic system, which would combine the best aspects of these two approaches, is of high interest.

1.2 Artificial metalloenzymes

The first use of the word “enzyme” dates back to 1876 when German physiologist Wilhelm Kühne identified it as a non-living substance able to perform fermentation.^[12] Enzymes are macromolecules, mostly of proteinic nature, that function as bio-catalysts by increasing the reaction rates^[13] and conform accordingly with the definition of a catalyst, which is “a substance that increases the rate of a chemical reaction without itself being consumed”.^[14]

Metals are essential for all living organisms. They are frequently integrated in proteins where they contribute to structure and also often display catalytic function (such as photosynthesis, respiration, oxygen transport) in so-called metalloproteins.^[15,16]

Metals play a key role in enzymes.^[17] In metalloenzymes, the catalytic metal centre constitutes together with the coordinated moiety of the protein the 1st coordination sphere. The surrounding protein framework, around the 1st coordination sphere, constitutes the 2nd coordination sphere and plays a critical role in catalysis.

The term “Artificial Metalloenzymes” refers to a catalyst resulting from the incorporation of a catalytically active metal ion or complex into a biomolecular host, such as a protein^[11,18–20] or DNA.^[21,22]

In the light of the complementarity between homogeneous and enzymatic catalysis, artificial metalloenzymes appear as a promising alternative as they may combine the best of both worlds.^[23] Artificial metalloenzymes have been successfully applied for a range of chemical reactions.^[24–26]

An artificial metalloenzyme consists of four elements; the biomolecular host, the anchor, the spacer, and the catalytic metal centre (Figure 1.2).

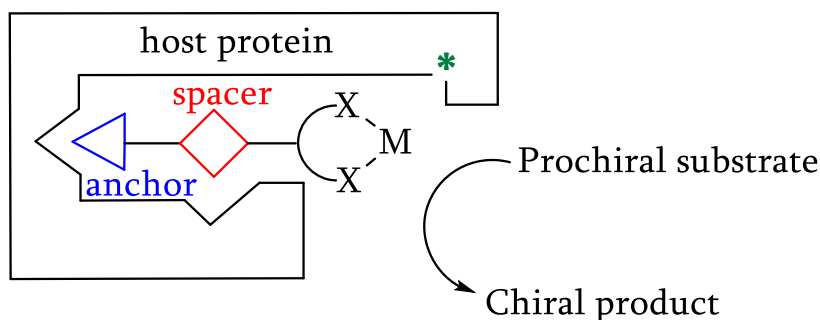


Figure 1.2 — Schematic representation of an artificial metalloenzyme. Chemical optimization is accomplished by modifying the spacer, the metal M, or the ligand scaffold X; genetic optimization is accomplished by site-directed mutagenesis in the proximity of the catalytic centre (*).

There are two possible approaches to create an artificial metalloenzyme: a) *de novo* design, where the catalytic centre is incorporated into a designed polypeptide sequence;^[27,28] b) modification of an existing protein.^[23]

The creation of artificial metalloenzymes needs to take three important parameters into consideration:

1. *The choice of transition metal catalyst*, which is determined by the reaction to be investigated.^[23,29] The catalyst needs to be compatible with biomolecular scaffolds, and to operate under aqueous conditions.
2. *The biomolecular scaffold*, which can be a polypeptide, a protein or a polynucleotide (RNA or DNA).^[24] Apart from structural considerations, pH, temperature stability, and tolerance of the scaffold against organic solvents needs to be taken into account.^[23] So far oxidations and reductions have only been carried out in combination with protein scaffolds, but not with DNA^[23,24] The biomolecular scaffold affects not only the selectivity of the metal cofactor, but can also alter the reaction rate.^[30,31]
3. *The anchoring strategy* for the localization of the metal moiety in the biomolecular scaffold. Three different strategies are commonly distinguished: dative anchoring, covalent anchoring and supramolecular anchoring (Figure 1.3).
 - a. Dative anchoring relies on a metal that is linked to the biomolecular scaffold through a coordinative interaction of one or multiple amino acid side chains present in the host protein. These coordinating groups of the side chain typically stem from histidine, cysteine, methionine, glutamate or aspartate;^[24]
 - b. Covalent anchoring relies on the presence of a suitable electrophile in the ligand moiety, which reacts with accessible cysteine serine histidine residues.^[24,29] The first example of a covalently protein linked metal catalyst was reported by Kaiser;^[32,33]
 - c. Supramolecular anchoring refers to a strong and specific non-covalent interaction between the biomolecular scaffolds and a small molecule ligand, which carries the artificial metal cofactor.^[23,24,29] Whitesides was the first to report the creation of an artificial metalloenzyme by exploiting the high affinity of biotin for avidin.^[34]

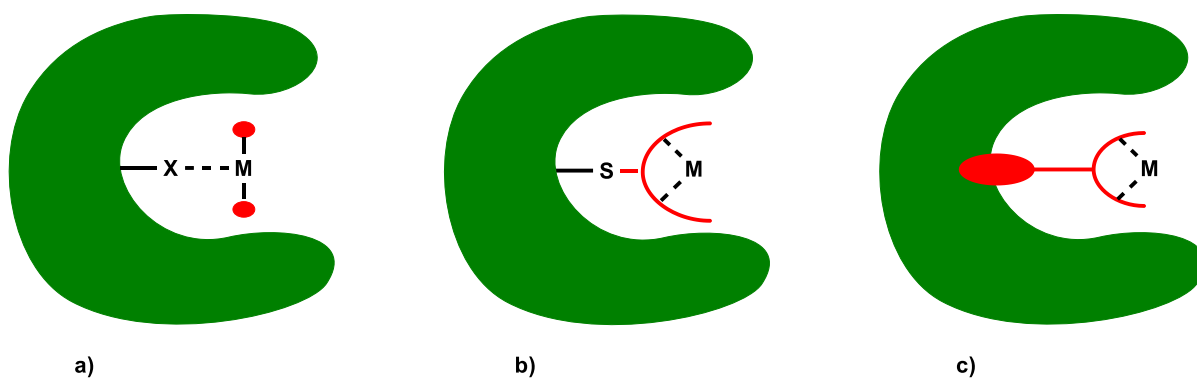


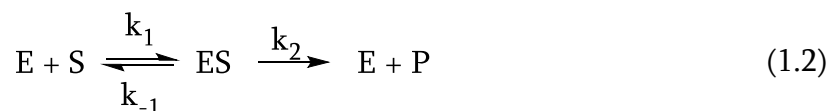
Figure 1.3 — Different anchoring strategies: **a)** dative anchoring; **b)** covalent anchoring; **c)** supramolecular anchoring. M = catalytically active metal centre; the first coordination sphere is highlighted in red; the biomolecular scaffold is schematically depicted in green.

All three different methodologies present distinct advantages and disadvantages. Dative anchoring does not require a chemical step to establish the linkage to the protein, but often suffers from selectivity due to competing coordinating residues on the surface of the protein. Covalent anchoring requires the presence of a unique reactive residue in the host protein for highly selective localization of the metal cofactor. Supramolecular anchoring is achieved by chemical modification of the complex with the ligand which binds to the protein. In principle, any cofactor which can be derivatized with a ligand that displays high affinity for a given protein can be employed, but the choice of scaffolds is accordingly limited to proteins that contain a binding pocket where the modified molecule can bind.^[35]

The creation of artificial metalloenzymes based on the biotin streptavidin technology is a well-established approach.^[20,23–25,36] This technology is based on the strong supramolecular interaction between the host protein streptavidin and the guest molecule biotin (vitamin H). Streptavidin is a homotetrameric protein and each monomer constitutes a β -barrel which can bind a single molecule of biotin in a deep binding pocket leading to unambiguous positioning of the biotin ligand. The affinity of biotin for streptavidin is one of the strongest non-covalent interactions known in nature ($K_a \approx 10^{13} \text{ M}^{-1}$).^[37,38] The introduction of the active catalyst moiety into streptavidin is achieved by derivatization of the valeric acid side chain of the biotin anchor. This derivatization does typically not alter the biotin streptavidin affinity

dramatically.^[39] Streptavidin is stable under harsh conditions such as pH values as low as 1.5, temperature (> 90°C), organic solvents (50% ethanol) and the presence of surfactants like sodium dodecyl sulphate.^[40,41] Streptavidin can be easily expressed in *E. coli* (about 200 mg/L). Furthermore, the protein and cofactor can be modified independently by genetic and chemical means. These characteristics enable the application of artificial metalloenzymes in a wide range of catalytic transformations. Wilson and Whitesides were the first to use the biotin avidin technology for artificial metalloenzymes and incorporated a rhodium diphosphine catalyst for the asymmetric hydrogenation of activated olefins in avidin.^[34] Following this pioneering work, many other catalysts have been incorporated into the structurally related streptavidin and a range of catalytic reactions scrutinized such as hydrogenation,^[42] olefin metathesis,^[43] transfer hydrogenation of ketones, imines and enones,^[44,45] sulfoxidation,^[46] dihydroxylation,^[47] allylic alkylation^[48] and C-H activation.^[31]

To evaluate the performance of artificial metalloenzymes in terms of rate, the kinetic model of Michaelis and Menten is typically applied (equation 1.2). In the first, step the enzyme (E) and the substrate (S) form a complex (ES), (k_1 indicates the association rate and k_{-1} indicates the dissociation rate of the ES complex). In the second step, the reaction takes place and the ES complex is converted into product (P) and free enzyme (k_2 is the rate constant for this step). The K_M equals the dissociation constant of the enzyme substrate complex, if $k_2 \ll k_{-1}$.^[49]



Another assumption is the “steady state” approximation: when the concentration of the substrate is much higher than the concentration of the enzyme ($[S] \gg [E]$), then the concentration of the enzyme-substrate complex ($[ES]$) remains constant in the initial phase of the reaction and the Michaelis–Menten equation can be expressed as (equation 1.3):

$$v = \frac{k_{\text{cat}} \cdot [E]_0 \cdot [S]}{K_M + [S]} \quad (1.3)$$

In the equation above, it is also assumed that the binding step is fast, thus k_2 equals the total catalytic constant k_{cat} which is defined as (equation 1.4):

$$k_{\text{cat}} = \frac{V_{\text{max}}}{[E]_0} \quad (1.4)$$

where $[E]_0$ is the total enzyme concentration. The concentration of the substrate at which $v = 1/2 V_{\text{max}}$ is the K_M . In an optimal case for catalysis, an enzyme shows high specific activity and should show minimal substrate (or other) inhibition.

1.3 Catalytic scope

1.3.1 NADH regeneration

The application of biocatalysis in industrial processes has received increasing consideration.^[50-53] Oxidoreductases present considerable potential and a large application field, due to their high activity and selectivity.^[54,55] For their biological function, oxidoreductases require redox equivalents often provided in the form of cofactors, such as nicotinamide adenine dinucleotide (NAD⁺) or nicotinamide adenine dinucleotide phosphate (NADP⁺) (Figure 1.4).

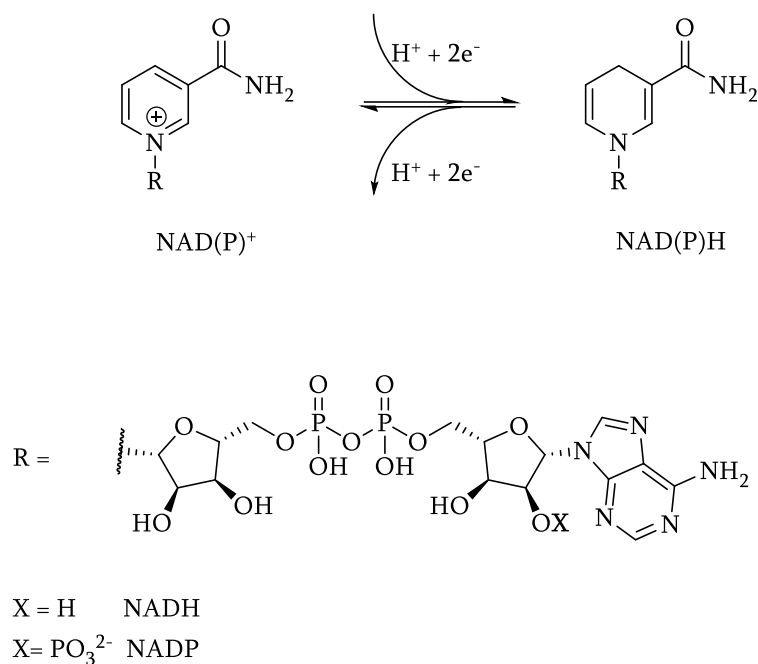


Figure 1.4 — NAD(P): structure and redox chemistry

The regeneration of the cofactor is an important topic in biocatalysis, because the stoichiometric use of NAD(P) is not feasible due to its high cost (Table 1.2). A catalytic amount of cofactor is generally used in NAD(P) or NAD(P)H dependent biotransformations and a concurrent reaction is performed to regenerate the cofactor.

Table 2.2 Cost of cofactors from Alfa-Aesar. Product purity: ^{a)}97%; ^{b)}98%; (April 2015)

Cofactor	€/g
^{a)} NAD ⁺	34
^{b)} NADH	48
^{b)} NAD(P) ⁺	361
^{b)} NAD(P)H	1050

Different strategies are employed for cofactor regeneration: a) the use of whole cells, which provide their own redox equivalents; b) the addition of a sacrificial co-substrate; c) the addition of a second enzyme and a co-substrate^[54,56] The most commonly employed enzymatic regeneration systems for synthetic applications are formate dehydrogenase/formic acid, glucose dehydrogenase/glucose, alcohol

dehydrogenase/sacrificial alcohol or glutamate dehydrogenase/glutamate.^[56-58] In extension to the enzymatic methods mentioned above, further non-enzymatic regeneration approaches, namely chemical, electrochemical, and photochemical regeneration methods have been investigated.^[59-62] Nowadays, none of the non-enzymatic regeneration methods has reached the efficiency provided by enzymatic systems. Non-enzymatic regeneration methods will be discussed in chapter two of this thesis and include the use of artificial metalloenzymes based on the biotin (strept)avidin technology. The employment of artificial metalloenzymes for NADH regeneration will be presented in chapter 3.

1.3.2 Transfer hydrogenation: asymmetric imine reduction

The synthesis of enantiopure amines is of high interest due to the high value of these compounds arising from various applications in the pharmaceutical, agrochemical, and fine chemical industries.^[63,64] Imine reduction is a convenient route to enantioenriched amines it has received increasing attention in the last 30 years.^[65] A prominent role among the reduction methods is held by the asymmetric transfer hydrogenation (ATH) to access such compounds. ATH is an efficacious strategy to reduce ketones or imines with the assistance of homogeneous transition metal catalysis and an alternative to hydrogenation processes (using hazardous H₂).^[66-68]

The first example of asymmetric transfer hydrogenation for the reduction of prochiral ketones or dehydrogenation of chiral alcohols, was reported in the late 1970s from Sinou^[69] and Ohkubo^[70], who used the Wilkinson's catalyst, and either a chiral co-substrate or a chiral ligand. However, these catalytic systems afforded modest results in terms of conversion and enantioselectivity. A remarkable advancement in asymmetric transfer hydrogenation appeared with the introduction of Noyori's ruthenium based catalyst.^[71] The η^6 -arene piano stool complex of Noyori was successfully applied in the asymmetric transfer hydrogenation of ketones,^[67,71] and inspired related complexes bearing amino alcohols,^[72] or C₂-symmetric diphosphines/diamines as ligands,^[73] formic

acid/triethylamine mixtures were also successfully employed instead of isopropanol as a hydride source.^[74] Noyori's ruthenium (II) based catalysts and analogous catalysts such as $[\eta^5\text{-Cp}^*\text{M}(\text{TsDPEN})\text{Cl}]$ (M=Ir, Rh)^[75-77] are probably the most prominent catalysts for the asymmetric transfer hydrogenation of ketone substrates.

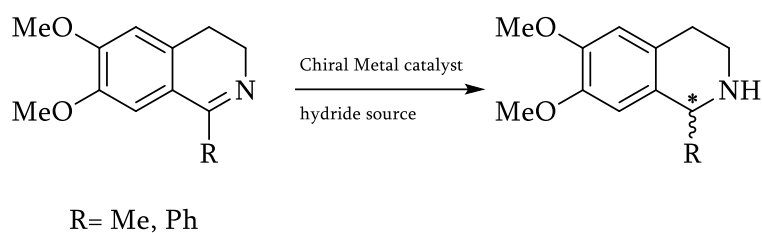
Imine reduction by transfer hydrogenation is generally carried out using either isopropanol, formic acid or formate salts as reducing agents and ruthenium, iridium or rhodium based catalysts.^[65] Grigg *et al.* reported in 1981 the use of Wilkinson's catalyst for the transfer hydrogenation of aldimines to secondary amines, using isopropanol as the hydride source.^[78] Jones *et al.* reported in the late 1980s the ruthenium catalyst precursor $\text{Ru}_3(\text{CO})_{12}$ for the transfer hydrogenation of benzylideneaniline.^[79]

The Shvo's diruthenium complex^[80] was utilized for the ATH of imines and investigated by Casey^[81,82] and Bäckvall.^[83-85]

The introduction of the Noyori's ruthenium (II) based catalyst brought improved results in the ATH of imine.^[86] Different isoquinolines and other cyclic and non-cyclic imines were reduced with up to 97% *ee* using formic acid-triethylamine as a hydride source. The reactivity of the catalyst was much higher for imine reduction compared to ketone reduction.

In the last 2 decades, a range of ligands and many successful catalysts have been developed for the ATH of ketones and imines.^[68,87] The increasing demand for efficient and environmentally-friendly chemistry encouraged also the development of water compatible catalysts.^[88] Deng *et al.* reported the first examples for asymmetric transfer hydrogenation in water, employing Noyori's ruthenium (II) TosDPEN piano stool complex for the reduction of a range of cyclic and a few acyclic imines with good to excellent *ee* using HCO_2Na as a hydride source and sulfonated analogue of the ligand for improved water solubility.^[89] Modified versions of the complex for improved water solubility were also investigated in further studies.^[90,91] Investigation on the influence of the pH for the ATH in water, were conducted from Xiao in catalytic systems for ketone and^[92] and quinoline reduction.^[93] The reduction of dihydroisoquinoline-based

scaffolds can be considered as a model reaction for the evaluation of new catalysts. (Scheme 1.1).



Scheme 1.1 — Asymmetric transfer hydrogenation of cyclic imine.

By anchoring a related complex with an achiral ligand moiety bound to a M-arene fragment inside a protein scaffold and subsequent chemo-genetic optimization, artificial transfer hydrogenases (ATHases) were developed by the Ward group for the reduction of cyclic imines.^[45] A range of three-legged piano stool complexes of Rh, Ir^[77] and Ru^[67] are highly active in the asymmetric transfer hydrogenation of imines. Considering the robustness of the Cp* moiety^[94,95] and aiming at the fast generation of large artificial cofactor libraries, a new strategy to link the catalyst through the Cp* moiety to biotin, was employed.^[96] This concept is discussed in more detail in chapter 5 of this thesis.

1.4 Scope of the thesis

The goals of this thesis are to improve and explore the potential of artificial transfer hydrogenases (ATHases) for new applications. The use of $[(\eta^p\text{-arene})M(\text{ligand})]$ ($M = \text{Rh, Ru, Ir}$) complexes as catalysts for the creation of ATHases has been successfully demonstrated for several applications in the Ward group. In the light of these reliable ATHases, the objective of this thesis are:

1. Employ the ATHases for NADH regeneration in coupled enzymatic transformations to overcome the mutual inhibition between an organometallic catalyst and an enzyme.
2. Investigate the stereoselectivity of the ATHase in NAD^+ reduction
3. Explore new strategies towards increasing the chemical diversity of ATHases

1.5 References

- (1) Faber, K. *Biotransformations in organic chemistry*, Springer-Verlag, Ed.; Sixth edit.; Berlin: Heidelberg, 2011.
- (2) Bornscheuer, U. T.; Huisman, G. W.; Kazlauskas, R. J.; Lutz, S.; Moore, J. C.; Robins, K. *Nature* **2012**, *485*, 185–194.
- (3) Torrelo, G.; Hanefeld, U.; Hollmann, F. *Catal. Letters* **2015**, *145*, 309–345.
- (4) White, L. L. *Nature* **1958**, *182*, 198.
- (5) Brenna, E.; Fuganti, C.; Serra, S. *Tetrahedron Asymmetry* **2003**, *14*, 1–42.
- (6) Koskinen, A. M. P. *Asymmetric synthesis of natural products*, Hoboken, Ed.; Second edi.; John Wiley & Sons: New Jersey, 2012.
- (7) Schreier, P.; Bernreuther, A.; Huffler, M. *Analysis of chiral organic molecules: methodology and applications*, Berlin, Ed.; Walter de Gruyter: New York, 1995.
- (8) Ward, T. R. *Chem. - Eur. J.* **2005**, *11*, 3798–3804.
- (9) *Comprehensive Asymmetric Catalysis*; Jacobsen, E. N.; Pfaltz, A.; Yamamoto, H., Eds.; First Ed.; Springer Verlag: Berlin, 1999.
- (10) Bommarius, A. S.; Riebel, B. R. *Biocatalysis: Fundamentals and Applications*; Bommarius, A. S.; Riebel, B. R., Eds.; Wiley-VCH Verlag GmbH & Co. KGaA, 2004.
- (11) Ward, T. R. *Acc. Chem. Res.* **2011**, *44*, 47–57.
- (12) Silverman, R. B. *The Organic Chemistry of Enzyme Catalyzed Reaction*; Second ed.; Elsevier Science: San Diego, California, 2002.
- (13) Gold, V. IUPAC Compendium of Chemical Terminology **2014**, 1670.
- (14) Hartwig, J. F. *Organotransition Metal Chemistry - From Bonding to Catalysis*; University Science Books, Ed.; Sausalito, California, 2010.
- (15) Guengerich, F. P. *J. Biol. Chem.* **2012**, *287*, 13508–13509.
- (16) Yannone, S. M.; Hartung, S.; Menon, A. L.; Adams, M. W. W.; Tainer, J. A. *Curr. Opin. Biotechnol.* **2012**, *23*, 89–95.

- (17) Waldron, K. J.; Rutherford, J. C.; Ford, D.; Robinson, N. J. *Nature* **2009**, *460*, 823–830.
- (18) Creus, M.; Ward, T. R. *Org. Biomol. Chem.* **2007**, *5*, 1835–1844.
- (19) Podtetenieff, J.; Taglieber, A.; Bill, E.; Reijerse, E. J.; Reetz, M. T. *Angew. Chem. Int. Ed.* **2010**, *49*, 5151–5155.
- (20) Onoda, A.; Hayashi, T.; Salmain, M. In *Bioorganometallic Chemistry: application in Drug discovery, Biocatalysis, and Imaging*; Jaouen, G.; Salmain, M., Eds.; Wiley-VCH Verlag GmbH & Co. KGaA, 2015; pp. 305–337.
- (21) Roelfes, G.; Feringa, B. L. *Angew. Chemie Int. Ed.* **2005**, *44*, 3230–3232.
- (22) Megens, R. P.; Roelfes, G. *Org. Biomol. Chem.* **2010**, *8*, 1387–1393.
- (23) Rosati, F.; Roelfes, G. *ChemCatChem* **2010**, *2*, 916–927.
- (24) Hamels, D. R.; Ward, T. R. *Compr. Inorg. Chem. II (Second Ed. From Elem. to Appl.* **2013**, *6*, 737–761.
- (25) Dundas, C. M.; Demonte, D.; Park, S. *Appl. Microbiol. Biotechnol.* **2013**, *97*, 9343–9353.
- (26) Bos, J.; Roelfes, G. *Curr. Opin. Chem. Biol.* **2014**, *19*, 135–143.
- (27) Zastrow, M. L.; Peacock, A. F. A.; Stuckey, J. A.; Pecoraro, V. L. *Nat. Chem.* **2012**, *4*, 118–123.
- (28) Zastrow, M. L.; Pecoraro, V. L. *Coord. Chem. Rev.* **2013**, *257*, 2565–2588.
- (29) Ward, T. R.; Pordea, A. *Comp. Chirality* **2012**, *7*, 516–552.
- (30) Collot, J.; Humbert, N.; Skander, M.; Klein, G.; Ward, T. R. *J. Organomet. Chem.* **2004**, *689*, 4868–4871.
- (31) Hyster, T. K.; Knörr, L.; Ward, T. R.; Rovis, T. *Science* **2012**, *338*, 500–503.
- (32) Yamamura, K.; Kaiser, E. T. *J. Chem. Soc. Chem. Commun.* **1976**, 830.
- (33) Kaiser, E. T.; Lawrence, D. S. *Science* **1984**, *226*, 505–511.
- (34) Wilson, M. E.; Whitesides, G. M. *J. Am. Chem. Soc.* **1978**, *100*, 306–307.
- (35) Wilson, Y. M.; Marc, D.; Ward, T. R. In *Protein Engineering Handbook*; Lütz, S.; Bornscheuer, U. T., Eds.; Wiley-VCH: Weinheim, 2012.

- (36) Dürrenberger, M.; Ward, T. R. *Curr. Opin. Chem. Biol.* **2014**, *19*, 99–106.
- (37) Green, N. *Adv. Protein Chem.* **1975**, *29*, 65–133.
- (38) Weber, P. C.; Ohlendorf, D. H.; Wendoloski, J. J.; Salemme, F. R. *Science* **1989**, *243*, 85–88.
- (39) Loosli, A.; Rusbandi, U. E.; Gradinaru, J.; Bernauer, K.; Schlaepfer, C. W.; Meyer, M.; Mazurek, S.; Novic, M.; Ward, T. R. *Inorg. Chem.* **2006**, *45*, 660–668.
- (40) Sano, T.; Cantor, C. R. *Proc. Natl. Acad. Sci. U. S. A.* **1990**, *87*, 142–146.
- (41) Cantor, C. R.; Fidelio, G. D. *Mol. Biol.* **1997**, *272*, 11288–11294.
- (42) Collot, J.; Gradinaru, J.; Humbert, N.; Skander, M.; Zocchi, A.; Ward, T. R. *J. Am. Chem. Soc.* **2003**, *125*, 9030–9031.
- (43) Lo, C.; Ringenberg, M. R.; Gnanndt, D.; Wilson, Y.; Ward, T. R. *Chem. Commun.* **2011**, *47*, 12065.
- (44) Letondor, C.; Humbert, N.; Ward, T. R. *Proc. Natl. Acad. Sci.* **2005**, *102*, 4683–4687.
- (45) Dürrenberger, M.; Heinisch, T.; Wilson, Y. M.; Rossel, T.; Nogueira, E.; Knörr, L.; Mutschler, A.; Kersten, K.; Zimbron, M. J.; Pierron, J.; Schirmer, T.; Ward, T. R. *Angew. Chem. Int. Ed.* **2011**, *50*, 3026–3029.
- (46) Pordea, A.; Creus, M.; Panek, J.; Duboc, C.; Mathis, D.; Novic, M.; Ward, T. R. *J. Am. Chem. Soc.* **2008**, *130*, 8085–8088.
- (47) Köhler, V.; Mao, J.; Heinisch, T.; Pordea, A.; Sardo, A.; Wilson, Y. M.; Knörr, L.; Creus, M.; Prost, J. C.; Schirmer, T.; Ward, T. R. *Angew. Chemie Int. Ed.* **2011**, *50*, 10863–10866.
- (48) Pierron, J.; Malan, C.; Creus, M.; Gradinaru, J.; Hafner, I.; Ivanova, A.; Sardo, A.; Ward, T. R. *Angew. Chemie Int. Ed.* **2008**, *47*, 701–705.
- (49) Fersht, A. *Structure and Mechanism in Protein Science: a guide to Enzyme Catalysis and Protein folding*; Freeman, W. H., Ed.; First Ed.; New York, 1998.
- (50) Breuer, M.; Ditrich, K.; Habicher, T.; Hauer, B.; Keßeler, M.; Stürmer, R.; Zelinski, T. *Angew. Chem. Int. Ed.* **2004**, *43*, 788–824.
- (51) Schmid, A.; Dordick, J. S.; Hauer, B.; Kiener, A.; Wubbolts, M.; Witholt, B. *Nature* **2001**, *409*, 258–268.

- (52) Schmid, A.; Hollmann, F.; Park, J. B.; Bühler, B. *Curr. Opin. Biotechnol.* **2002**, *13*, 359–366.
- (53) Koeller, K. M.; Wong, C. H. *Nature* **2001**, *409*, 232–240.
- (54) Hollmann, F.; Arends, I. W. C. E.; Holtmann, D. *Green Chem.* **2011**, *13*, 2285–2313.
- (55) Monti, D.; Ottolina, G.; Carrea, G.; Riva, S. *Chem. Rev.* **2011**, *111*, 4111–4140.
- (56) Wichmann, R.; Vasic-Racki, D. *Adv. Biochem. Eng. Biotechnol.* **2005**, *92*, 225–260.
- (57) Donk, W. A. Van Der; Zhao, H. *Curr. Opin. Biotechnol.* **2004**, *14*, 421–426.
- (58) Kroutil, W.; Mang, H.; Edegger, K.; Faber, K. *Adv. Synth. Catal.* **2004**, *346*, 125–142.
- (59) Hollmann, F.; Hofstetter, K.; Schmid, A.; Care, D.; Specialties, S.; Ag, G. *TRENDS in Biotech.* **2006**, *24*, 163–171.
- (60) Maenaka, Y.; Suenobu, T.; Fukuzumi, S. *J. Am. Chem. Soc.* **2012**, *134*, 367–374.
- (61) Hildebrand, F.; Lütz, S. *Chem. Eur. J.* **2009**, *15*, 4998–5001.
- (62) Poizat, M.; Arends, I. W. C. E.; Hollmann, F. *J. Mol. Catal. B Enzym.* **2010**, *63*, 149–156.
- (63) Höhne, M.; Bornscheuer, U. T. *ChemCatChem* **2009**, *1*, 42–51.
- (64) Nugent, T. C.; El-Shazly, M. *Adv. Synth. Catal.* **2010**, *352*, 753–819.
- (65) Wills, M. In *Modern Reduction Methods*; Andersson, P. G.; Munslow, I. J., Eds.; Wiley-VCH, 2008; pp. 1–501.
- (66) Gladiali, S.; Alberico, E. *Chem. Soc. Rev.* **2006**, *35*, 226–236.
- (67) Noyori, R.; Hashiguchi, S. *Acc. Chem. Res.* **1997**, *30*, 97–102.
- (68) Bartoszewicz, A.; Ahlsten, N.; Martín-Matute, B. *Chem. Eur. J.* **2013**, *19*, 7274–7302.
- (69) Descotes, G.; Sinou, D. *Tetrahedron Lett.* **1976**, 4083–4086.
- (70) Ohkubo, K.; Hirata, K.; Yoshinaga, K. *Chem. Lett.* **1976**, 183–184.

- (71) Hashiguchi, S.; Fujii, A.; Takehara, J.; Ikariya, T.; Noyori, R. *J. Am. Chem. Soc.* **1995**, *117*, 7562–7563.
- (72) Takehara, J.; Hashiguchi, S.; Fujii, A.; Inoue, S.; Ikariya, T.; Noyori, R. *Chem. Commun.* **1996**, 233–234.
- (73) Gao, J.; Ikariya, T.; Noyori, R. *Organometallics* **1996**, *15*, 1087–1089.
- (74) Fujii, A.; Hashiguchi, S.; Uematsu, N.; Ikariya, T.; Noyori, R. *J. Am. Chem. Soc.* **1996**, *118*, 2521–2522.
- (75) Mashima, K.; Abe, T.; Tani, K. *Chem. Lett.* **1998**, 1201–1202.
- (76) Mashima, K.; Abe, T.; Tani, K. *Chem. Lett.* **1998**, 1199–1200.
- (77) Murata, K.; Ikariya, T.; Noyori, R. *J. Org. Chem.* **1999**, *64*, 2186–2187.
- (78) Grigg, R.; Mitchell, T. R. B. *Synthesis* **1981**, *6*, 442–444.
- (79) Basu, A.; Bhaduri, S.; Sharma, K.; Jones, P. G. *J. Chem. Soc., Chem Commun.* **1987**, *3*, 1126–1127.
- (80) Shvo, Y.; Czarkie, D.; Rahamim, Y.; Chodosh, D. F. *J. Am. Chem. Soc.* **1986**, *108*, 7400–7402.
- (81) Casey, C. P.; Singer, S. W.; Powell, D. R.; Hayashi, R. K.; Kavana, M. *J. Am. Chem. Soc.* **2001**, *123*, 1090–1100.
- (82) Casey, C. P.; Johnson, J. B. *J. Am. Chem. Soc.* **2005**, *127*, 1883–1894.
- (83) Samec, J. S. M.; Bäckvall, J. E. *Chem. Eur. J.* **2002**, *8*, 2955–2961.
- (84) Ell, A. H.; Johnson, J. B.; Bäckvall, J.-E. *Chem. Commun.* **2003**, 1652–1653.
- (85) Samec, J. S. M.; Ell, A. H.; Bäckvall, J.-E. *Chem. Commun.* **2004**, 2748–2749.
- (86) Uematsu, N.; Fujii, A.; Hashiguchi, S.; Ikariya, T.; Noyori, R. *J. Am. Chem. Soc.* **1996**, *118*, 4916–4917.
- (87) Wang, C.; Wu, X.; Xiao, J. *Chem. Asian J.* **2008**, *3*, 1750–1770.
- (88) Wei, Y.; Wu, X.; Wang, C.; Xiao, J. *Catal. Today* **2015**, *247*, 104–116.
- (89) Wu, J.; Wang, F.; Ma, Y.; Cui, X.; Cun, L.; Zhu, J.; Deng, J.; Yu, B. *Chem. Commun.* **2006**, 1766–1768.

- (90) Li, L.; Wu, J.; Wang, F.; Liao, J.; Zhang, H.; Lian, C.; Zhu, J.; Deng, J. *Green Chem.* **2007**, *9*, 23–25.
- (91) Canivet, J.; Süß-Fink, G. *Green Chem.* **2007**, *9*, 391–397.
- (92) Wu, X.; Li, X.; King, F.; Xiao, J. *Angew. Chem. Int. Ed.* **2005**, *44*, 3407–3411.
- (93) Wang, C.; Li, C.; Wu, X.; Pettman, A.; Xiao, J. *Angew. Chem. Int. Ed.* **2009**, *48*, 6524–6528.
- (94) Wu, X.; Li, X.; Zanotti-Gerosa, A.; Pettman, A.; Liu, J.; Mills, A. J.; Xiao, J. *Chem. Eur. J.* **2008**, *14*, 2209–2222.
- (95) Wu, X.; Xiao, J. In *Metal-Catalyzed Reactions in Water*; Dixneuf, P. H.; Cadierno, V., Eds.; WILEY-VCH: Weinheim, 2013; pp. 173–242.
- (96) Zimbron, J. M.; Heinisch, T.; Schmid, M.; Hamels, D.; Nogueira, E. S.; Schirmer, T.; Ward, T. R. *J. Am. Chem. Soc.* **2013**, *135*, 5384–5388.

Chapter 2

Recent trends in biomimetic NADH regeneration

Tommaso Quinto, Valentin Köhler and Thomas R. Ward

This chapter was published in: *Top & Catal.*, **2014**, *57*, 321-331.

DOI 10.1007/s11244-013-0187-y

Reproduced by permission of the Springer

<http://dx.doi.org/10.1007/s11244-013-0187-y>

2.1 Abstract

Nicotinamide adenine dinucleotide (NADH) and nicotinamide adenine dinucleotide phosphate [NAD(P)H] constitute a major cost factor in preparative biotransformations. The development of efficient methods for their regeneration with cheap reducing equivalents has been an area of intense research in the last decades. Methods explored include chemical, electrochemical, and photochemical approaches. None of the methods to regenerate NADH has reached efficiency comparable with enzymatic regeneration (*e.g.* formate dehydrogenase), which remains the method of choice for most applications.

In this review, we summarize primarily organometallic-based approaches for NADH regeneration methods which include non-enzymatic steps, before moving on to the most recent developments in synthetic NADH related transformations. We highlight the frequent problem of mutual inactivation between the organometallic catalyst for NADH regeneration and the corresponding NADH dependent downstream enzyme. Potential remedies are discussed, such as the compartmentalization of the organometallic complex.

2.2 Introduction

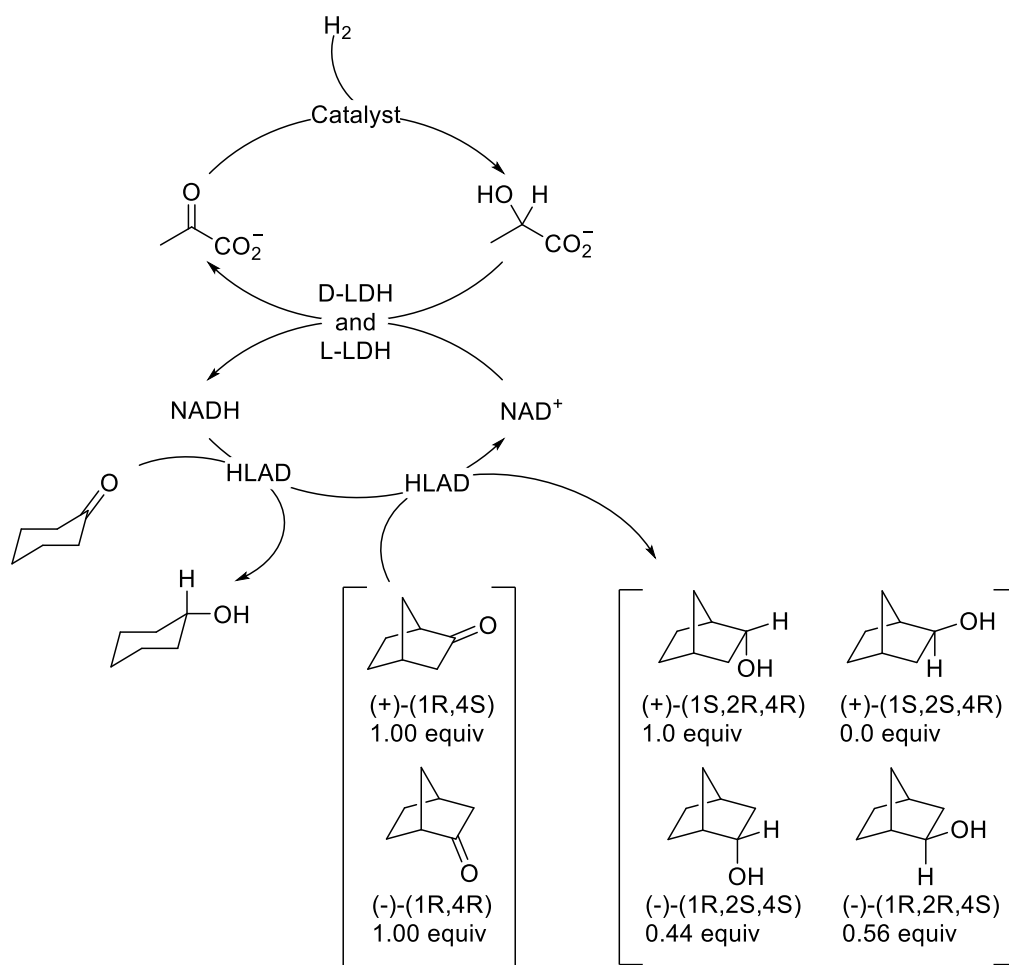
Ever since the groundbreaking work by Abril and Whitesides^[1] and Steckhan and colleagues^[2] on metal mediated nicotinamide adenine dinucleotide (NAD⁺) regeneration the field has blossomed and has been reviewed extensively.^[3-12] While numerous metal-catalysts have been reported for the efficient reduction of the pyridinium moiety, several studies to date were performed on NAD⁺ (or analogs thereof) in the absence of the nicotinamide adenine dinucleotide (NADH) dependent enzyme. Indeed, combining both enzyme and organometallic catalyst often lead to deactivation of one or both catalytic systems. In this context and following a selection

of historically relevant abiotic NADH regeneration systems, we present the most promising means to overcome the mutual inhibition challenge.

2.3 Pioneering non-enzymatic approaches for the regeneration of nicotinamide adenine dinucleotide phosphate [NAD(P)H]

The first electro-enzymatic regeneration of NAD(P)H was reported by the group of Whitesides. For this purpose, they relied on a tungsten cathode to reduce either a disulfide to the corresponding dithiol^[13] or methyl viologen^[14] to provide the reducing equivalents for the enzymatic reduction of NAD⁺ or nicotinamide adenine dinucleotide phosphate (NADP⁺) with either lipoamide dehydrogenase or ferredoxin NADP reductase, respectively. This indirect approach allowed to overcome problems encountered in the direct electrochemical reduction, such as insufficient regioselectivity and radical dimerization.^[15] The NADH produced served for the concurrent reduction of pyruvate with lactate dehydrogenase. The methyl viologen mediated NADPH regeneration was coupled to the glutamic dehydrogenase catalyzed formation of glutamate from α -ketoglutarate.

The first example of indirect chemical regeneration of NADH, was also reported by Whitesides' group in 1981. They employed a water soluble organometallic diphosphine rhodium(I) catalyst, to convert pyruvate to lactic acid using H₂ (2.72 atm) as reducing agent. In the presence of lactate dehydrogenase, NAD⁺ was reduced to NADH, thus enabling the stereoselective reduction of (1*R*,4*S*)-Norcamphor with horse liver alcohol dehydrogenase (Figure 2.1).^[1] They note that the efficiency of the system is limited by the modest activity (TOF) of the rhodium complex in the pyruvate reduction (TOF \approx 10 h⁻¹, TON = 1500), which nevertheless enables high productivity (TON). The deactivation of the rhodium complex by free thiol groups present on the enzymes was hypothesized. The addition of a fresh batch of the complex was required to complete the reaction.



D(L)-LDH = D(L), lactate dehydrogenase; HLADH = horse liver alcohol dehydrogenase

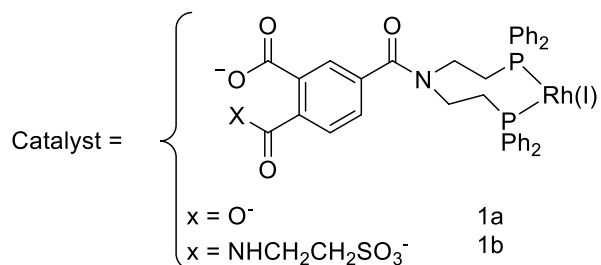


Figure 2.1 — The first example of NADH regeneration involving a metal-catalyzed step.^[1]

One of the first attempts to regenerate NADH by a photochemical reduction was reported by Kiwi in 1981. Here, $[\text{Ru}(\text{bpy})_3]^{2+}$ was activated by irradiation with visible light, in the presence of TEA which served as the electron donor (Figure 2.2).^[16] In contrast to their proposed final disproportionation step of the NAD radicals to NAD^+ and NADH ,^[17] Steckhan subsequently showed that the radical dimerises practically exclusively to yield the non-active $(\text{NAD})_2$.^[18]

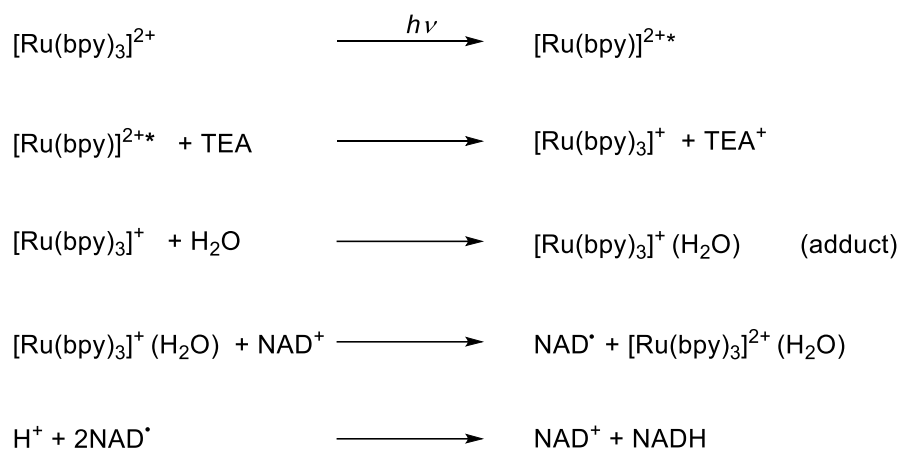
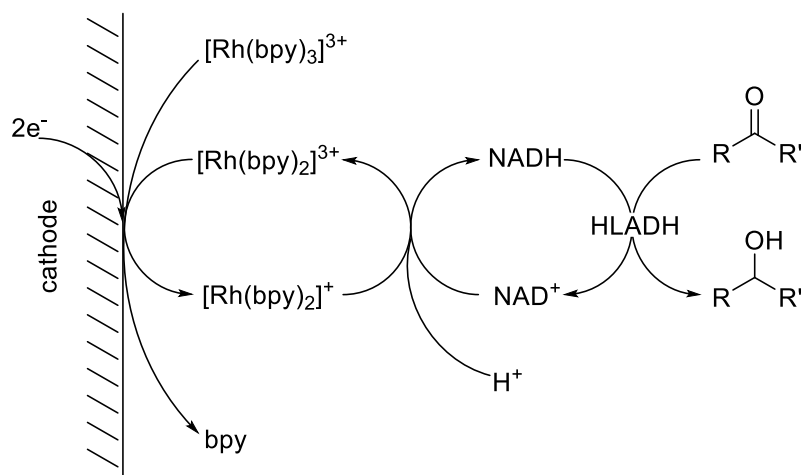


Figure 2.2 — Proposed photochemical NADH regeneration with $[\text{Ru}(\text{bpy})_3]^{2+}$ as catalyst.^[16]

Steckhan was the first to report an indirect electrochemical NADH regeneration method. In this system, a $[\text{Rh}(\text{bpy})_3]^{3+}$ catalyst is reduced electrochemically to $[\text{Rh}(\text{bpy})_2]^+$ which subsequently reduces NAD^+ in buffered aqueous medium which serves as a proton source (Figure 2.3). The system was coupled to horse liver alcohol dehydrogenase (HLAD) catalyzed ketone reduction.^[19] The use of a $[\text{Rh}(\text{bpy})_3]^{3+}$ mediator prevents the formation of NAD radicals. Indeed, the direct electrochemical reduction of NAD^+ , requires a potential of > -1.1 V *vs.* the Ag/AgCl electrode, potentially leading to side-products, including the NAD dimer. In the presence of the redox-mediator, the potential can be reduced to -850 mV *vs.* Ag/AgCl electrode. The authors identified a passivation of the cathode due to the deposition of $[\text{Rh}(\text{bpy})_2(\text{H}_2\text{O})_2]\text{Cl}$ or $[\text{Rh}(\text{bpy})_2(\text{OH})_2]\text{Cl}$ leading to low TONs with respect to Rh (TON = 2.2). Lacking enzyme activity as a possible cause for the low productivity was excluded.



HLADH = horse liver alcohol dehydrogenase

Figure 2.3 — First example of an indirect electrochemical NADH regeneration using an organometallic mediator.^[19]

Subsequently, Steckhan reported a photochemical system similar to Kiwi's whereby $[\text{Ru}(\text{bpy})_3]^{2+}$ (used as sensitizer) is activated by visible light.^[18] In the presence of TEOA, $[\text{Rh}(\text{bpy})_3]^{3+}$ is converted to $[\text{Rh}(\text{bpy})_2]^+$ and reduces NAD^+ . In subsequent work, they reported an improved version of the electrochemical regeneration. The improvement was mainly achieved by tuning the ligand: substituting the bipyridine by bipyridyl-5-sulfonic acid, allowed to reduce the reduction potential to $-730 \text{ mV vs. Ag/AgCl}$ thereby overcoming the formation of NAD radicals. A TOF of 0.5 h^{-1} and a TON of 19 with respect to Rh were achieved in the coupled reduction of cyclohexanone to cyclohexanol by HLAD.^[20]

Importantly, Steckhan introduced $[\text{Cp}^*\text{Rh}(\text{bpy})\text{Cl}]^+$ to the arena of NADH regeneration. Compared to previous systems, the coupling of this catalyst with LDH shows 20 times higher reduction rates (TOF = 5 h^{-1} , TON = 14 in respect to Rh) in the conversion of pyruvate.^[2]

In the latter system, the hydride $[\text{Cp}^*\text{Rh}(\text{bpy})\text{H}]^+$ is the species responsible for NAD^+ and NAD(P)^+ reduction. Instead of using electrochemical means of production from $[\text{Cp}^*\text{Rh}(\text{bpy})\text{Cl}]^+$, it can be generated by ligand substitution using sodium formate as hydride source in a purely chemical regeneration system (Figure 2.4).^[21] For NADH and NADPH regeneration at 38°C the reported TOF is 82. It should be noted that sodium

formate had been introduced previously by Whitesides as a preparative stoichiometric reagent for the enzymatic regeneration of NAD^+ with formate dehydrogenase.^[22]

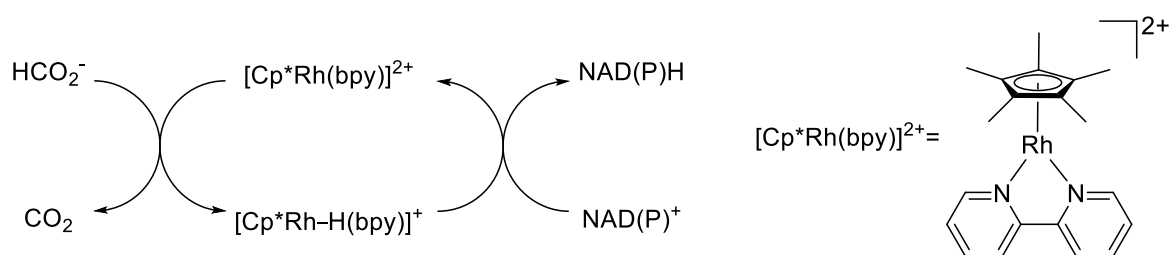


Figure 2.4 — Regeneration of NAD(P)H with $[\text{Cp}^*\text{Rh}(\text{bpy})]^{2+}$ using formate as chemical hydride source.^[21]

2.4 Recent developments for NAD(P)H and NAD(P)⁺ regeneration

The initial examples of NAD(P)H regeneration involving non-enzymatic steps, rely largely on rhodium—and ruthenium-based catalysts. Numerous other studies have been published in the past 20 years. Metals investigated for the reduction and oxidation of NAD^+/NADH or analogues (in solution or as electrode materials) include Co,^[23–25] Mn,^[26] Fe,^[27] Pd-Au,^[28] Pt-C,^[29] Ni-C,^[29] Cu, Au, Pt-Au,^[30] Re,^[31,32] Cu-Hg.^[33]

Recent reports feature increasingly iridium as the active metal center and address additionally the reverse reaction – the catalytic non-enzymatic oxidation of NAD(P)H under the simultaneous formation of metal hydrides.

Fukuzumi and co-workers^[34] reported an efficient system where a [C-N] cyclometalated complex $[\text{Cp}^*\text{Ir}(4-(1H\text{-pyrazol-1-yl})\text{benzoic acid})\text{H}_2\text{O}]\text{SO}_4$ can regenerate NADH under mild conditions (pH 6–8) utilizing H_2 as the hydride source at room temperature and ambient pressure (Figure 2.5). A TON of 9.3 at pD 8.0 was reported for an NMR experiment at high conversion after 90 min. Under moderately acidic conditions, the same complex catalyzes the oxidation of NADH (*i.e.* the microscopic reverse reaction). The TON was determined with 6.3 after 20 min. at a pD

of 4.6 and at high conversion. This offers interesting opportunities for catalysis in a biological environment since the hydride is transferred to the metal complex, before combining with a proton from the solvent to release H₂. It is believed that the change in pH leads to protonation of the carboxylate group on the ligand, which modifies the electronic properties of the ligand and alters the total charge of the complex. Regeneration of NADH with this complex can also be accomplished with alcohols as reductants under basic aqueous conditions (pH 8.5-10) yielding the corresponding carbonyl compounds as 'byproducts'.^[35]

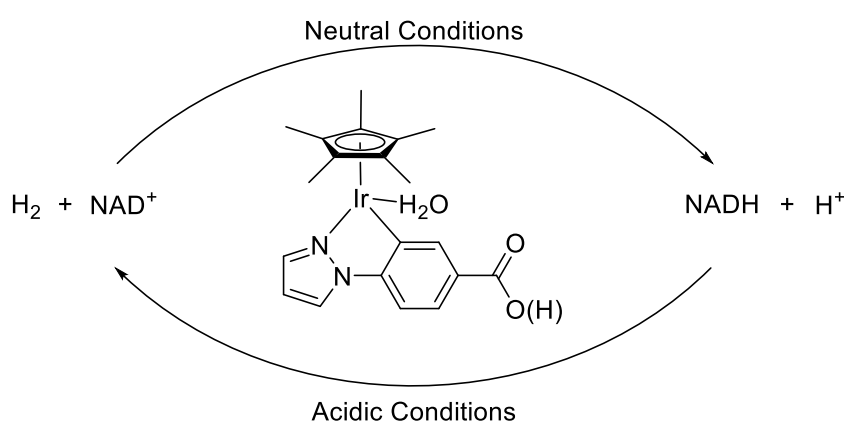


Figure 2.5 — NAD⁺ reduction (neutral conditions) and NADH oxidation (acidic conditions) with a cyclometallated pincer complex.^[34]

Shortly thereafter, Sadler showed that an organometallic ruthenium- or iridium catalyst can be employed for the reduction of pyruvate with NADH as the hydride source, thus mimicking the activity of lactate dehydrogenase.^[36] In particular, the organometallic complexes $[(\eta^6\text{-hmb})\text{Ru}(\text{bpm})\text{Cl}]\text{PF}_6$ (hmb=hexamethylbenzene, bpm=2,2'-bipyrimidine) and $[\text{Cp}^{\text{xph}}\text{Ir}(\text{phen})\text{Cl}]\text{PF}_6$ (xph= $\eta^5\text{-C}_5\text{Me}_4\text{C}_6\text{H}_5$, phen=1,10-phenanthroline) are two functional mimics of lactate dehydrogenase (for the iridium complex, a TON of 75 was reached) (Figure 2.6). The complex $[\text{Cp}^*\text{Ir}(\text{phen})\text{Cl}]\text{PF}_6$ was employed to catalyze the reduction of quinones in a biomimetic reaction of ubiquinone oxidoreductase.^[37] Sadler analyzed the influence of the nature of the arene cap and the *N,N*-bidentate ligand for Noyori type ruthenium complexes. The activity of the complex for NADH oxidation was particularly high when benzene was used as an arene cap and the chelating aminosulfonamide ligand carried electron poor

sulfonamides.^[38] The oxidation of NADH to NAD⁺ was further performed in aqueous solution with the osmium containing pianostool complex $[(\eta^6\text{-}p\text{-cym})\text{Os}(\text{Impy-NMe}_2)\text{Cl}]\text{PF}_6$ ($p\text{-cym}$ = *para*-cymene, Impy=iminopyridine).^[39] In preceding work, Sadler and co-workers^[40] reported the application of different ruthenium complexes for the generation of NADH under physiological conditions using formate as reducing agent.

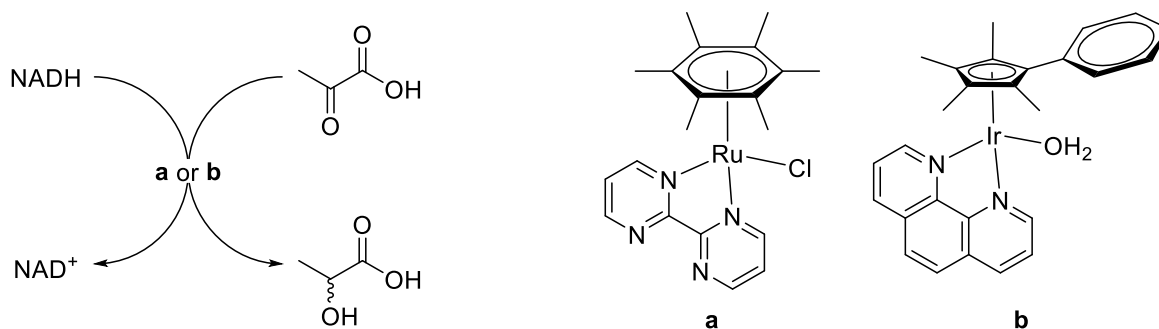


Figure 2.6 — NADH oxidation coupled with pyruvate reduction. The resulting systems present lactate dehydrogenase activity.^[36]

An iron(III) porphyrin complex was introduced by Gröger for the oxidation of NAD(P)H.^[41] This water soluble organometallic catalyst is able to oxidize both NADH and NAD(P)H with molecular O₂ from air as the electron acceptor reaching a TON of 48-50 (Figure 2.7). Efficient alcohol oxidation was achieved in conjunction with an alcohol dehydrogenase. Tests for H₂O₂ were negative, which accordingly did not need to be decomposed by the addition of a catalase. No mutual deactivation of metalloporphyrin and enzyme was reported.

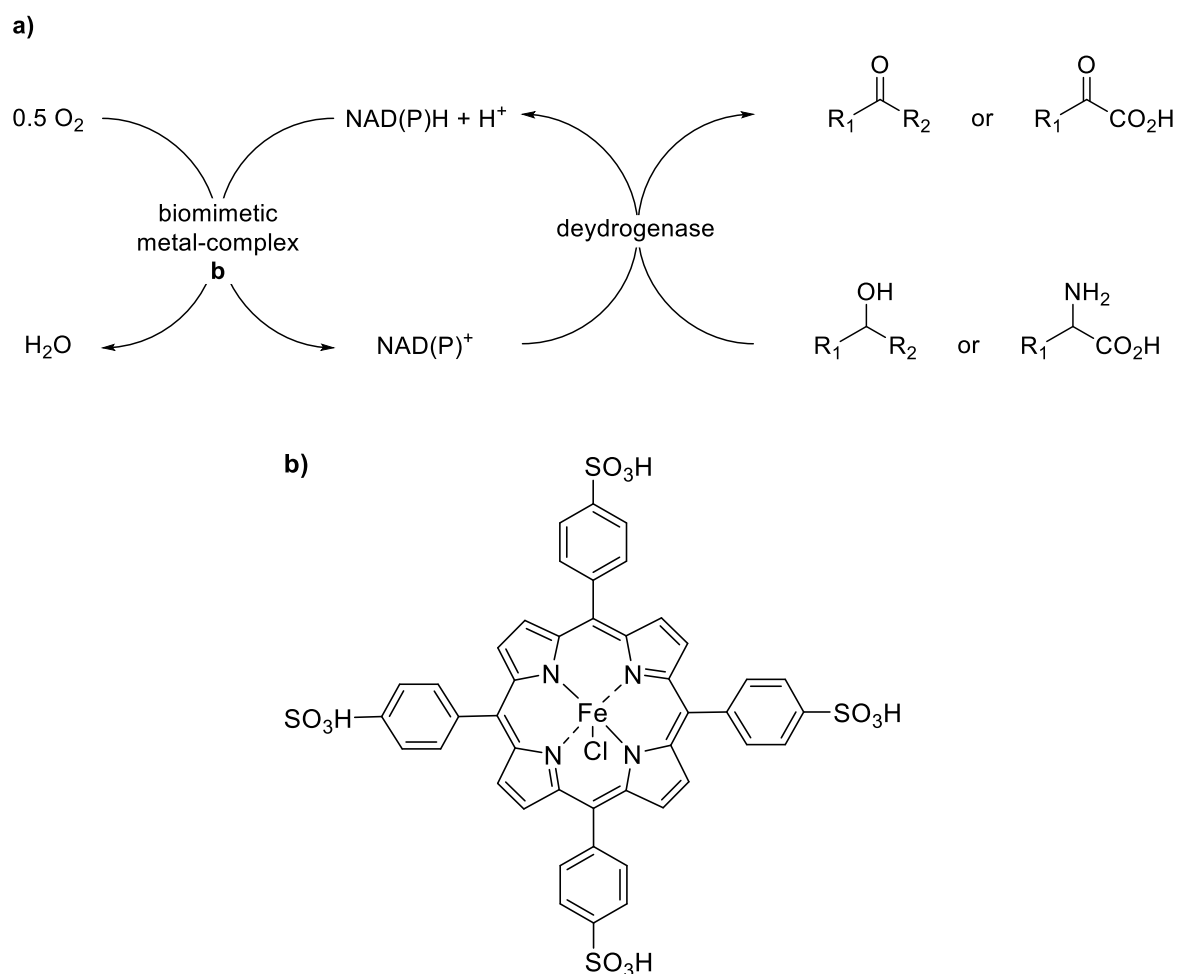
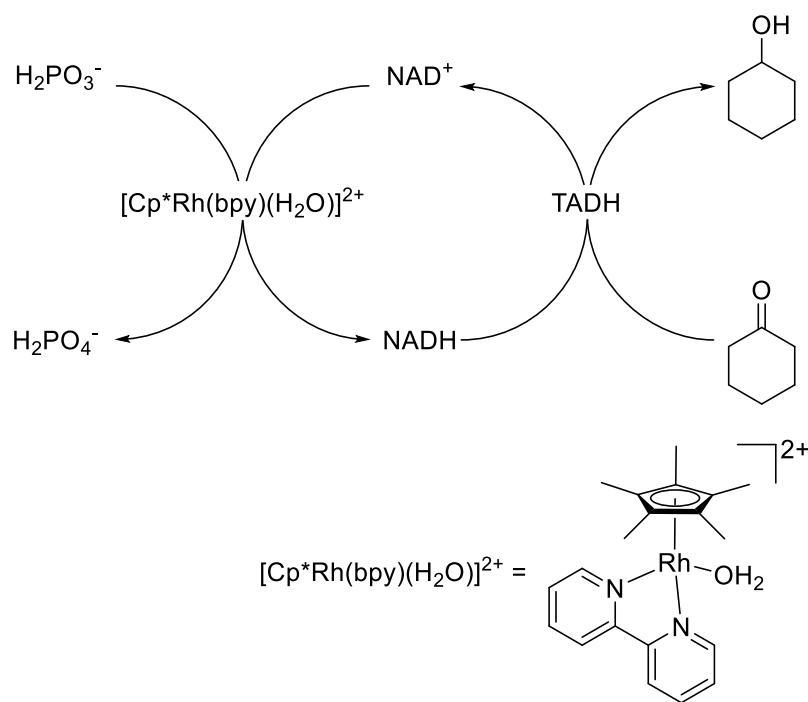


Figure 2.7 — a) NAD(P)H oxidation by a biomimetic organometallic complex; b) water soluble iron(III) porphyrin for NAD(P)H oxidation.^[41]

Hollmann has been very active in the field of cofactor regeneration. He recently reported on coupling the well-established $[\text{Cp}^*\text{Rh}(\text{Bpy})(\text{H}_2\text{O})]^{2+}$ catalyst for NADH regeneration with cyclohexanone reduction catalysed by alcohol dehydrogenase from thermophile *Thermus* sp. ATN1 (TADH) (Figure 2.8). Instead of formate, he relied on phosphite as the stoichiometric reducing agent reaching a TOF of 21 h^{-1} .^[42] Phosphite had previously been reported for enzymatic NADH regeneration with phosphite dehydrogenase.^[43] While the authors observe product inhibition for the enzyme, no inactivation of the rhodium complex or of the enzyme was mentioned.

Hollmann and co-workers^[44] also reported the use of a Noyori-type rhodium catalyst $[\text{Cp}^*\text{Rh}(\text{TsDPEN})\text{Cl}]$, immobilized on polyethylene solid support, for the regeneration of NADH with a TOF of 2.5 h^{-1} .



TADH = alcohol dehydrogenase

Figure 2.8 — Chemical NADH regeneration using phosphite as hydride source, coupled with enzymatic alcohol dehydrogenase.^[42]

A photochemical approach employing flavin as photosensitizer for the regeneration of NADH was reported by Park. Electrons are provided by TEOA and $[Cp^*Rh(bpy)(H_2O)]^{2+}$ serves once again as organometallic mediator. The NADH regeneration system was coupled to an enzymatic reaction for the formation of L-glutamate from α -ketoglutarate with GDH (L-glutamate dehydrogenase) (Figure 2.9).^[45] No inactivation of enzyme or mediator was reported.

In successive investigations, they used different photosensitizers such as Eosin-Y or dot-coated silica beads, the former also in conjunction with NAD^+ analogues.^[46,47] A related photochemical regeneration of NADPH was recently coupled with cytochrome P450 catalyzed the O-dealkylation. In this case, the author mentions the inactivation of the cytochrome P-450 by $[Cp^*Rh(bpy)(H_2O)]^{2+}$.^[48]

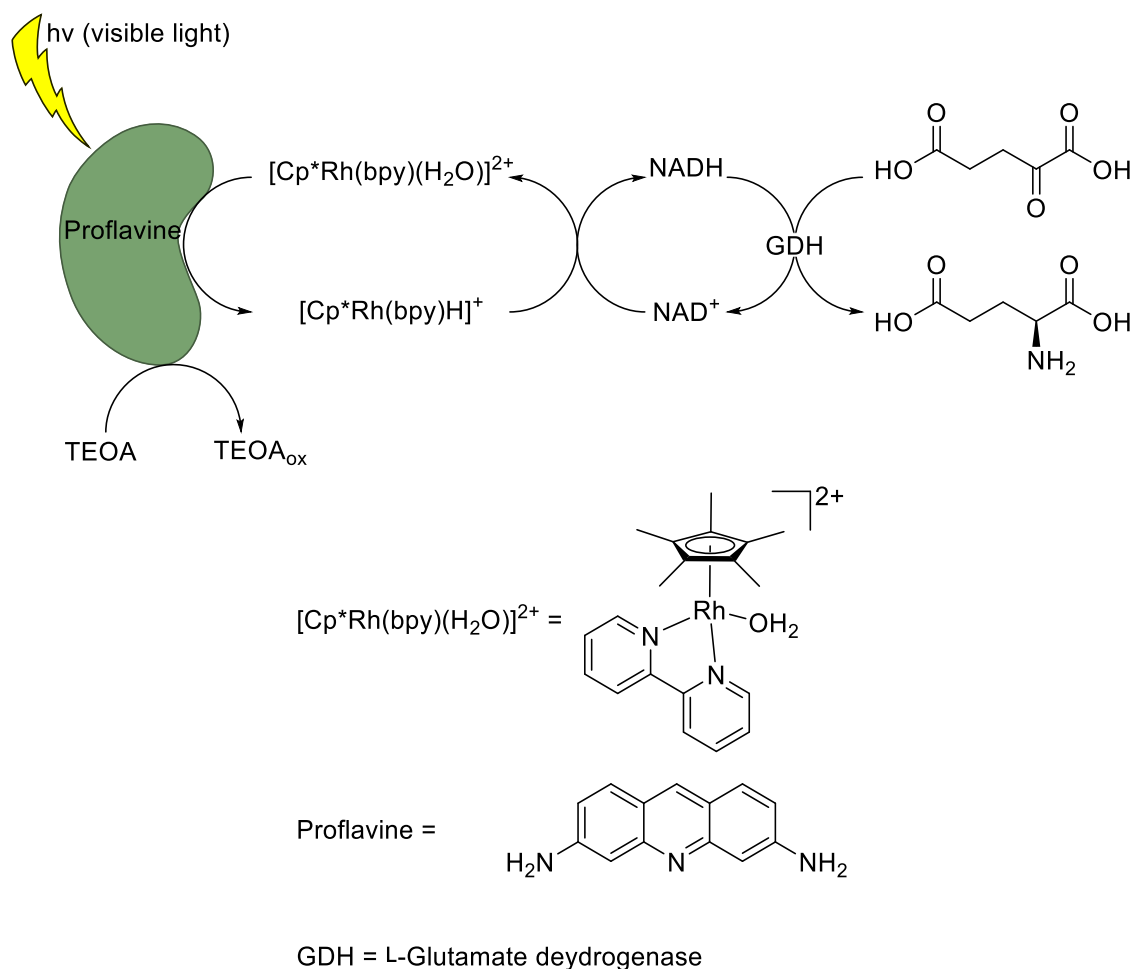


Figure 2.9 — NADH regeneration induced by visible light, mediated from organometallic rhodium catalyst, coupled with an enzymatic L-glutamate dehydrogenase.^[45]

2.5 Mutual inactivation of the organometallic catalyst and the enzyme

A challenge, often encountered in combining transition metal-based NAD(P)H regeneration with enzymatic NAD(P)H-dependent processes is the mutual deactivation of the organometallic catalyst and the enzyme.

Some of the publications summarized above, mention low TONs and suggest that this may be due to the limited compatibility of organometallic and enzymatic catalysts. We present below a selection of studies aimed at addressing this problem specifically.

To the best of our knowledge, Schmid and Fish were the first to highlight the mutual inactivation between $[Cp^*Rh(bpy)(H_2O)]^{2+}$ and an NADH dependent enzyme.^[49] The

model system they investigated was the $[\text{Cp}^*\text{Rh}(\text{bpy})(\text{H}_2\text{O})]^{2+}$ mediated regeneration of an NADH mimic with the enzymatic hydroxylation of 2-hydroxybiphenyl to the corresponding catechol catalysed by 2-hydroxybiphenyl-3-monooxygenase (HbpA) (Figure 2.10).

Upon combining the organometallic cofactor regeneration system with the monooxygenase, no product formation was detected. The authors suggest that the interaction between the accessible nucleophilic amino acid residues (i.e. lysine (-NH₂) and cysteine (-SH)) of the enzyme (HbpA) and the soft metal center of the organometallic catalyst causes deactivation of the rhodium catalyst.

To overcome the problem, they immobilized the enzyme on a polymer support flanked with epoxide moieties which react with exposed nucleophilic amino acid residues. The resulting coupled system enabled substantial hydroxylation when natural NAD⁺ was employed.

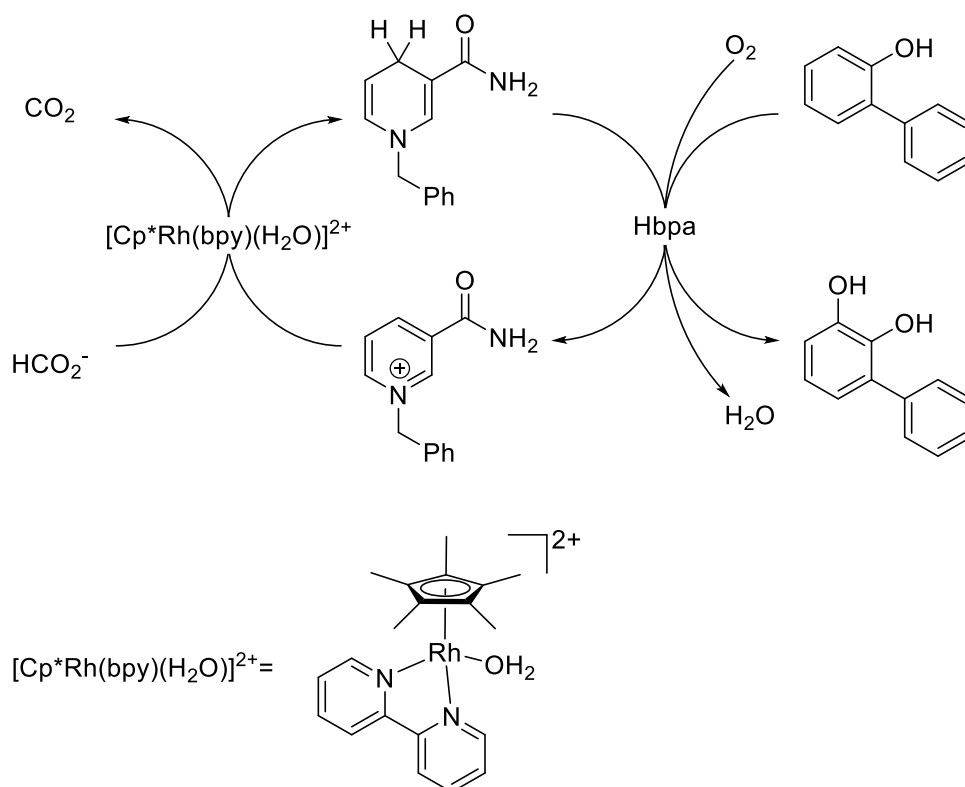
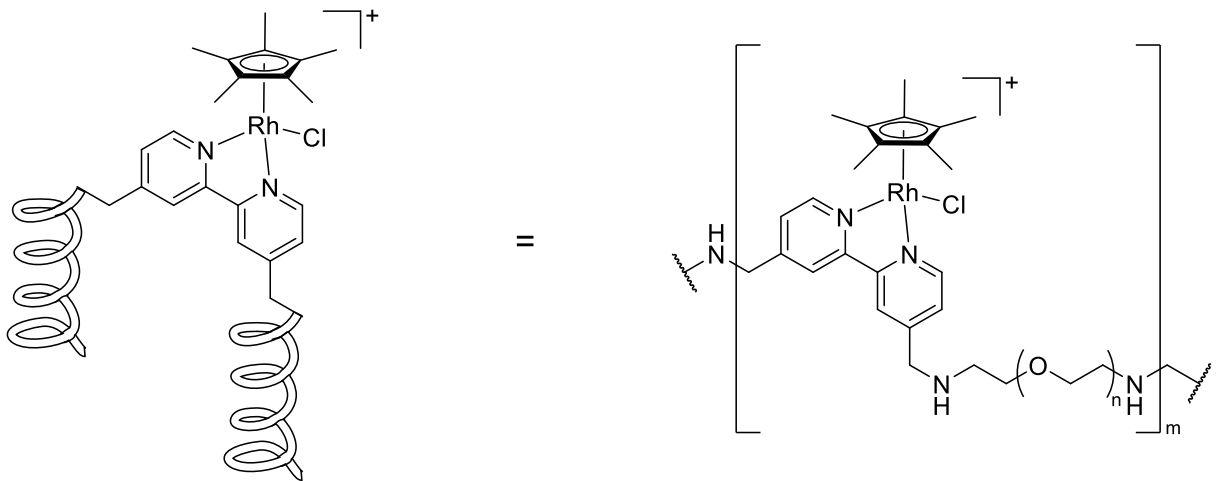
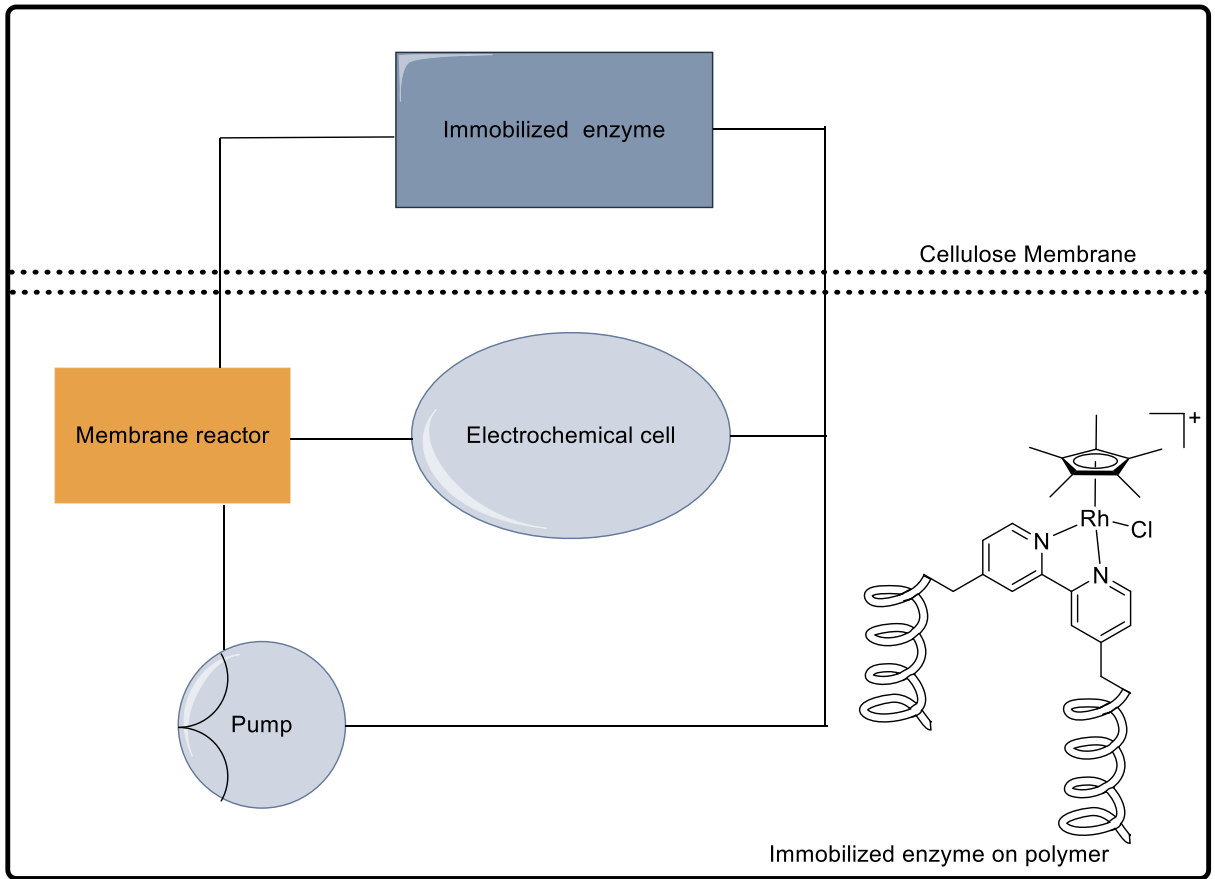


Figure 2.10 — Organometallic regeneration of a mimic NADH coupled with enzymatic monooxygenase.^[49]

Lütz and coworkers investigated in detail the problem of mutual inactivation between the organometallic mediator $[\text{Cp}^*\text{Rh}(\text{bpy})(\text{H}_2\text{O})]^{2+}$ and an alcohol dehydrogenase from *Lactobacillus brevis* (*Lb*-ADH) and proposed a compartmentalization of the two entities.^[50]

For this purpose, they scrutinized the interaction of the piano stool complex with isolated amino acids to evaluate their influence. Interestingly, he identified tryptophan, in addition to the traditional suspects histidine and cysteine that lead to strong deactivation of the pianostool moiety. Compartmentalization was achieved by immobilizing the organometallic mediator used for the electrochemical regeneration as part of a water-soluble polymer and the enzyme on Sephabeads[®]. Additionally, a cellulose membrane, permeable only to NADH and substrate, was introduced to physically separate both catalysts (Figure 2.11). Based on recovered mediator after the reaction they calculated a feasible turnover number of >200.



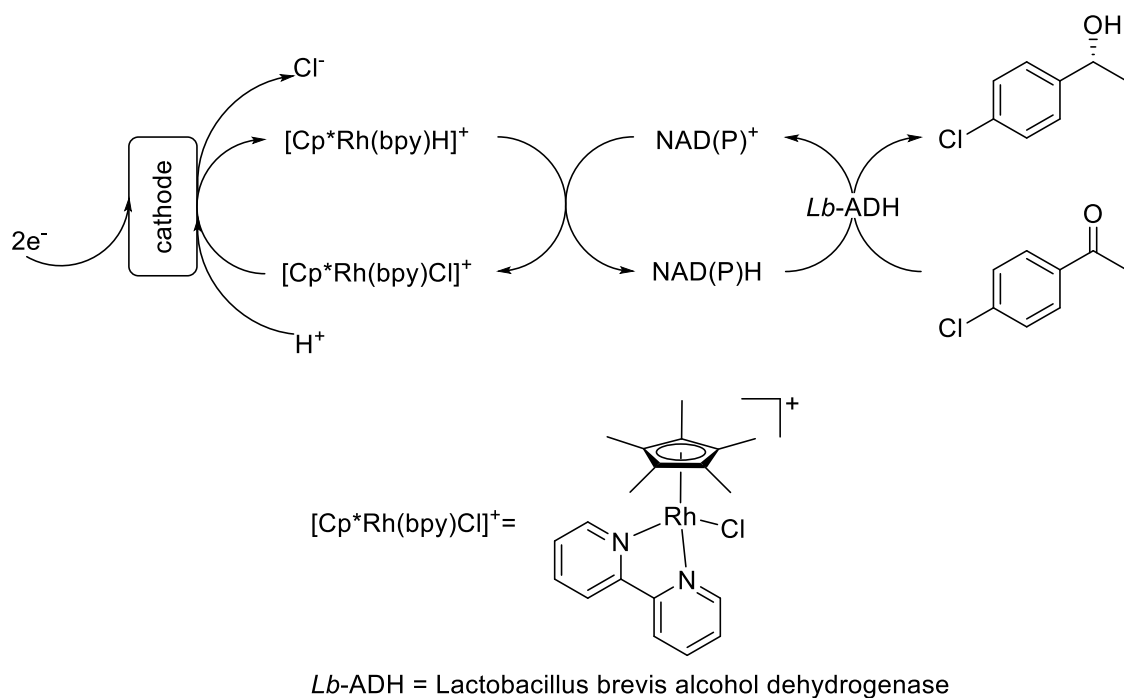


Figure 2.11 — Electroenzymatic reactor with separation of electrochemical NADH-regeneration and enzymatic reaction for the production of *p*-chloro-(*R*)-phenylethanol with *Lb*-ADH.^[50]

Building on previous observations, Hollmann and coworkers investigated the inactivation of various enzymes upon addition of $[\text{Cp}^*\text{Rh}(\text{bpy})(\text{H}_2\text{O})]^{2+}$. In addition to the spatial separation described above, they scrutinized the use of coordinating buffers as a potential remedy to mutual inactivation. They found that addition of $(\text{NH}_4)_2\text{SO}_4$ leads to an increased compatibility between the enzyme and the pincer catalyst $[\text{Cp}^*\text{Rh}(\text{bpy})(\text{H}_2\text{O})]^{2+}$. Unfortunately, the catalytic NADH regeneration using formate was eroded. In stark contrast, the electrochemical regeneration in the presence of $(\text{NH}_4)_2\text{SO}_4$ remained satisfying.^[51]

More recently, Bergman, Raymond and Toste presented an original supramolecular compartmentalization strategy to prevent mutual inactivation. For this purpose, they encapsulated the pincer moiety $[\text{CpRu}(\text{NCMe})_2\text{PMe}_3]^+$ (Cp = cyclopentadiene) within a supramolecular tetrahedral host cage. As a proof of principle, they developed a tandem catalytic process where the organometallic guest $[\text{CpRu}(\text{NCMe})_2\text{PMe}_3]^+$ catalyses the isomerization of allylic alcohol to the corresponding aldehyde which is subsequently reduced by an alcohol dehydrogenase to the saturated alcohol. A formate

dehydrogenase provides the NADH equivalents for the process (Figure 2.12).^[52] Although this system does not constitute an artificial NADH regeneration systems, it highlights the improved compatibility of an organometallic catalyst with enzymes upon incorporation into a supramolecular host, to avoid the interaction with free amino acid residues from enzyme.

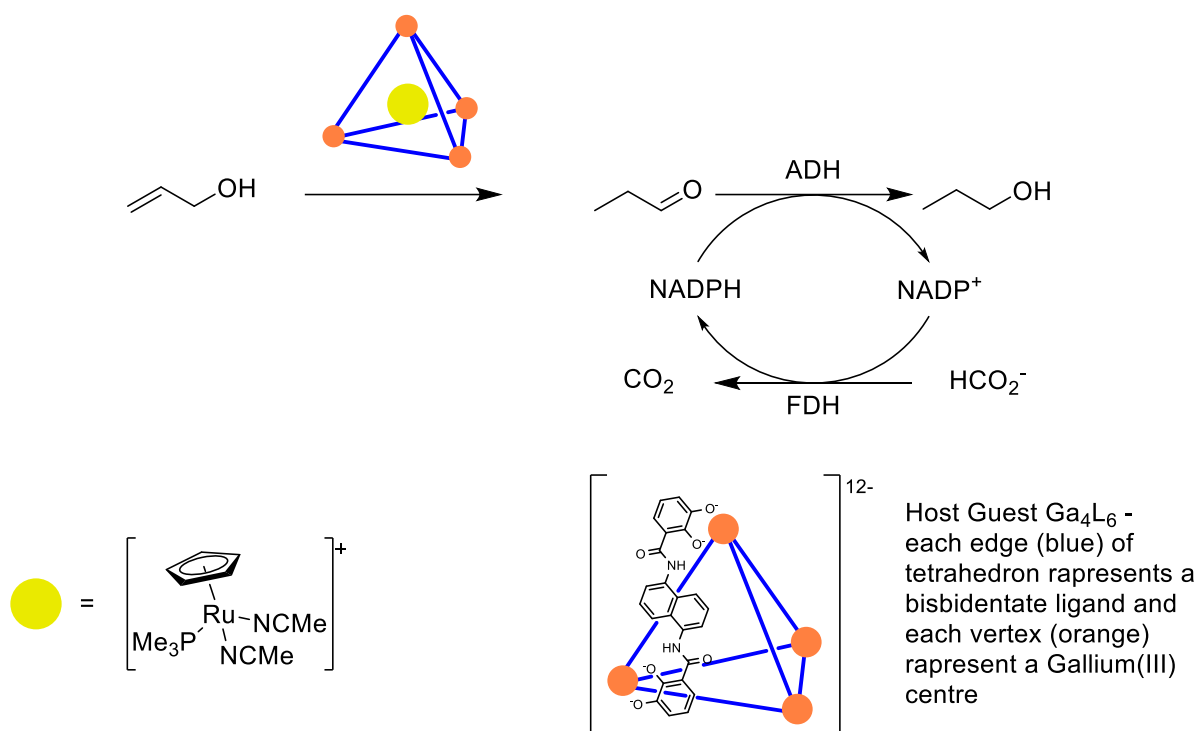


Figure 2.12 — Encapsulation of a ruthenium piano-stool catalyst in a supramolecular cage allows to combine a metal-catalyzed allylic isomerization with an enzyme cascade consisting of an NADPH-dependent alcohol dehydrogenase (ADH) and formate dehydrogenase (FDH).^[52]

An alternative approach to address the problem of mutual inactivation was reported by Hollmann, Turner and Ward. They incorporated an Ir-piano stool complex for NAD^+ regeneration into streptavidin, thereby creating an artificial metalloenzyme and efficiently compartmentalizing the NADH dependent downstream enzyme and the Ir-complex.^[53] The incorporation was realized by exploiting the biotin streptavidin technology.^[54]

In the same study it was observed that the catalyst $[\text{Cp}^*\text{Ir}(\text{biot-}p\text{-L})\text{Cl}]$ is significantly more active in NADH regeneration than the well-established $[\text{Cp}^*\text{Rh}(\text{bpy})(\text{H}_2\text{O})]^{2+}$. By

incorporation of the iridium catalyst into a streptavidin mutant S112A, the system was coupled to the hydroxybiphenyl monooxygenase (HbpA) catalyzed hydroxylation; efficient hydroxylation was achieved under relevant biological conditions (pH 7.5, 30°C, open air) (Figure 2.13) with a TON of >100 in respect to $[\text{Cp}^*\text{Ir}(\text{biot-}p\text{-L})\text{Cl}]$.

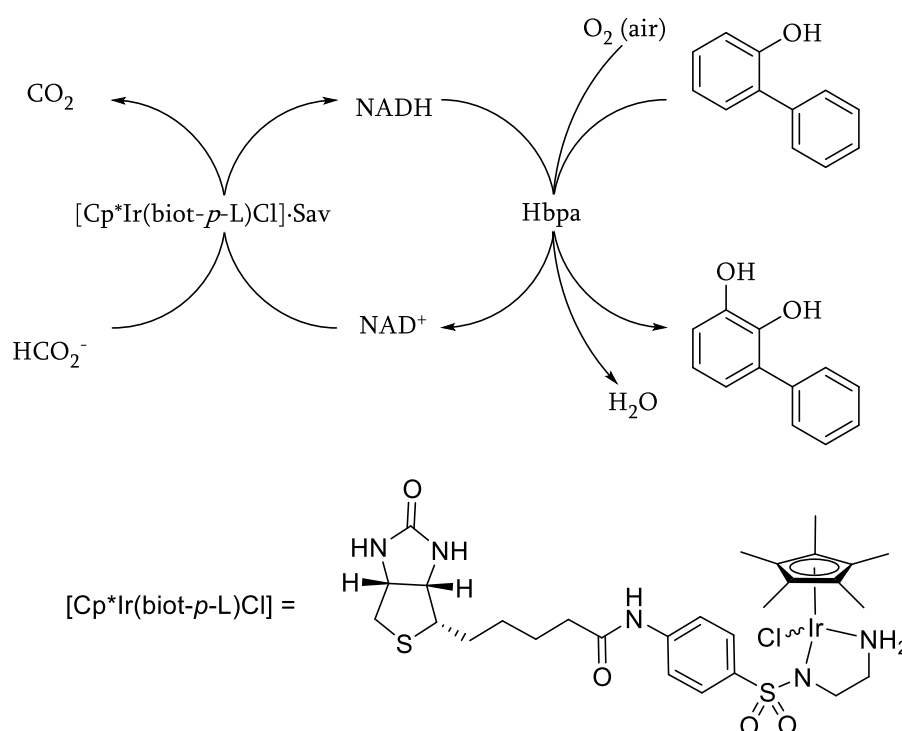


Figure 2.13 — An artificial metalloenzyme for the NADH regeneration fully compatible with hydroxybiphenyl monooxygenase (HbpA).^[53]

2.6 Outlook

Having identified the underlying principles of mutual inhibition, several complementary compartmentalization strategies have been developed in recent years: polymer immobilization, selective membranes, supramolecular encapsulation and anchoring within a macromolecular scaffold. Thus far however, the most promising organometallic regeneration systems rely on precious metals: rhodium and iridium occupying a place of choice. The next step will be to implement the above strategies to base-metals.

2.7 References

- (1) Abril, O.; Whitesides, G. M. *J. Am. Chem. Soc.* **1982**, *104*, 1552–1554.
- (2) Ruppert, R.; Herrmann, S.; Steckhan, E. *Tetrahedron Lett.* **1987**, *28*, 6583–6586.
- (3) Hollmann, F.; Arends, I. W. C. E.; Buehler, K. *ChemCatChem* **2010**, *2*, 762–782.
- (4) Mcskimming, A.; Colbran, S. B. *Chem. Soc. Rev.* **2013**, *42*, 5439–5488.
- (5) Kochius, S.; Magnusson, A. O.; Hollmann, F.; Schrader, J.; Holtmann, D. *Appl. Microbiol. Biotechnol.* **2012**, *93*, 2251–2264.
- (6) Hollmann, F.; Hofstetter, K.; Schmid, A.; Care, D.; Specialties, S.; Ag, G. *TRENDS in Biotech.* **2006**, *24*, 163–171.
- (7) Kohlmann, C.; Wolfgang, M.; Lütz, S. *J. Mol. Catal. B Enzym.* **2008**, *51*, 57–72.
- (8) Rodriguez, C.; Lavandera, I.; Gotor, V. *Curr. Org. Chem.* **2012**, *16*, 2525–2541.
- (9) Truppo, M. D. *Compr. Chirality* **2012**, *7*, 46–70.
- (10) Holtmann, D.; Schrader, J. In *Modern biooxidation. Enzymes, Reactions and Applications*; Schmid, R. D.; B. Urlacher, V., Eds.; WILEY-VCH: Weinheim, 2007; pp. 265–290.
- (11) Lütz, S. In *The Handbook of Homogeneous Hydrogenation*; de Vries, J. G.; Elsevier, C. J., Eds.; WILEY-VCH: Weinheim, 2007; pp. 1471–1482.
- (12) Weckbecker, A.; Gröger, H.; Hummel, W. In *Advances in Biochemical Engineering/Biotechnology*; Scheper, T., Belkin, S., Doran, P.M., Endo, I., Gu, M.B., Hu, W.S., Mattiasson, B., Nielsen, J., Stephanopoulos, G.N., Ulber, R., Zeng, A.-P., Zhong, J.-J., Zhou, W., Ed.; Springer: Heidelberg, 2009; pp. 195–242.

- (13) Shaked, Z.; Barber, J. J.; Whitesides, G. M. *J. Org. Chem.* **1981**, *46*, 4100–4101.
- (14) DiCosimo, R.; Wong, C.-H.; Lacy Daniels; M., G.; Whitesides *J. Org. Chem.* **1981**, *46*, 4622–4623.
- (15) Schmakel, C. O.; Santhanam, K. S. V; Elving, P. J. *J. Am. Chem. Soc.* **1975**, *97*, 5083–5092.
- (16) Kiwi, J. *J. Photochem.* **1981**, *16*, 193–202.
- (17) Land, E. J.; Swallow, A. J. *Biochem.* **1969**, *8*, 2117–2125.
- (18) Wienkamp, R.; Steckhan, E. *Angew. Chem. Int. Ed.* **1983**, *22*, 497.
- (19) Wienkamp, R.; Steckhan, E. *Angew. Chem. Int. Ed.* **1982**, *21*, 782–783.
- (20) Franke, M.; Steckhan, E. *Angew. Chem. Int. Ed.* **1988**, *27*, 265–267.
- (21) Ruppert, R.; Herrmann, S.; Steckhan, E. *J. Chem. Soc., Chem. Commun.* **1988**, *1*, 1150–1151.
- (22) Shaked, Z.; Whiteside, G. M. *J. Am. Chem. Soc.* **1980**, *102*, 7104.
- (23) Fukuzumi, S.; Kitano, T. *J. Chem. Soc. Perkin Trans.* **1991**, 41–45.
- (24) Hilt, G.; Steckhan, E. *J. Chem. Soc., Chem Commun.* **1993**, 1706–1707.
- (25) Kim, J. A.; Kim, S.; Lee, J.; Baeg, J.; Kim, J. *Inorg. Chem.* **2012**, *51*, 8057–8063.
- (26) Fukuzumi, S.; Kotani, H.; Prokop, K. A.; Goldberg, D. P. *J. Am. Chem. Soc.* **2011**, *133*, 1859–1869.
- (27) Fukuzumi, S.; Kotani, H.; Lee, Y.-M.; Nam, W. *J. Am. Chem. Soc.* **2008**, *130*, 15134–15142.

- (28) Gopalan, A.; Ragupathy, D.; Kim, H.; Manesh, K. M.; Lee, K. *Spectrochim. Acta Part A* **2009**, *74*, 678–684.
- (29) Ali, I.; Gill, A.; Omanovic, S. *Chem. Eng. J.* **2012**, *188*, 173–180.
- (30) Damian, A.; Maloo, K.; Omanovic, S. *Chem. Biochem. Eng. Q.* **2007**, *21*, 21–32.
- (31) Kobayashi, A.; Takatori, R.; Kikuchi, I.; Konno, H.; Sakamoto, K.; Ishitani, O. *Organometallics* **2001**, *20*, 3361–3363.
- (32) Kobayashi, A.; Konno, H.; Sakamoto, K.; Sekine, A.; Iida, M.; Ishitani, O. *Chem. Eur. J.* **2005**, *11*, 4219–4226.
- (33) Munteanu, G.; Dempsey, E.; McCormac, T.; Munteanu, C. *J. Electroanal. Chem.* **2012**, *665*, 12–19.
- (34) Maenaka, Y.; Suenobu, T.; Fukuzumi, S. *J. Am. Chem. Soc.* **2012**, *134*, 367–374.
- (35) Maenaka, Y.; Suenobu, T.; Fukuzumi, S. *J. Am. Chem. Soc.* **2012**, *134*, 9417–9427.
- (36) Betanzos-lara, S.; Liu, Z.; Habtemariam, A.; Pizarro, A. M.; Qamar, B.; Sadler, P. *J. Angew. Chem. Int. Ed.* **2012**, *51*, 3897–3900.
- (37) Liu, Z.; Deeth, R. J.; Butler, J. S.; Habtemariam, A.; Newton, M. E.; Sadler, P. J. *Angew. Chem. Int. Ed.* **2013**, *52*, 4194–4197.
- (38) Soldevila-barreda, J. J.; Bruijninx, P. C. A.; Habtemariam, A.; Clarkson, G. J.; Deeth, R. J.; Sadler, P. J. *Organometallics* **2012**, *31*, 5958–5967.
- (39) Fu, Y.; Romero, J. M.; Habtemariam, A.; Snowden, M. E.; Song, L.; Clarkson, G. J.; Qamar, B.; Pizarro, A. M.; Unwin, P. R.; Sadler, P. J. *Chem. Sci.* **2012**, *3*, 2485–2494.

- (40) Yan, Y. K.; Melchart, M.; Abtemariam, A.; Peacock, A. F. A.; Sadler, P. J. *J. Biol. Inorg. Chem.* **2006**, *11*, 483–488.
- (41) Maid, H.; Böhm, P.; Huber, S. M.; Bauer, W.; Hummel, W.; Jux, N.; Gröger, H. *Angew. Chem. Int. Ed.* **2011**, *50*, 2397–2400.
- (42) Grau, M. M.; Poizat, M.; Arends, I. W. C. E.; Hollmann, F. *Appl. Organomet. Chem.* **2010**, *24*, 380–385.
- (43) Vrtis, J. M.; White, A. K.; Metcalf, W. W.; Donk, W. A. Van Der; V, S. M. A.; On, H. *J. Am. Chem. Soc.* **2001**, *123*, 2672–2673.
- (44) Torres, M. De; Dimroth, J.; Arends, I. W. C. E.; Keilitz, J.; Hollmann, F. *Molecules* **2012**, *17*, 9835–9841.
- (45) Nam, D. H.; Park, C. B. *Chembiochem* **2012**, *13*, 1278–1282.
- (46) Lee, S. ha; Ryu, J.; Nam, D. H.; Park, C. B. *Chem. Comm.* **2011**, *47*, 4643–4645.
- (47) Lee, S. H.; Lee, H. J.; Won, K.; Park, C. B. *Chem. Eur. J.* **2012**, *18*, 5490–5495.
- (48) Lee, S. H.; Kwon, Y.-C.; Kim, D.-M.; Park, C. B. *Biotechnol. & Bioeng.* **2013**, *110*, 383–90.
- (49) Lutz, J.; Hollmann, F.; Vinh, T.; Schnyder, A.; Fish, R. H.; Schmid, A. *J. Organomet. Chem.* **2004**, *689*, 4783–4790.
- (50) Hildebrand, F.; Lütz, S. *Chem. Eur. J.* **2009**, *15*, 4998–5001.
- (51) Poizat, M.; Arends, I. W. C. E.; Hollmann, F. *J. Mol. Catal. B Enzym.* **2010**, *63*, 149–156.
- (52) Wang, Z. J.; Clary, K. N.; Bergman, R. G.; Raymond, K. N.; Toste, F. D. *Nat. Chem.* **2013**, *5*, 100–103.

- (53) Köhler, V.; Wilson, Y. M.; Dürrenberger, M.; Ghislieri, D.; Churakova, E.; Quinto, T.; Knörr, L.; Häussinger, D.; Hollmann, F.; Turner, N. J.; Ward, T. R. *Nat. Chem.* **2013**, *5*, 93–9.
- (54) Ward, T. R. *Acc. Chem. Res.* **2011**, *44*, 47–57.

Chapter 3

Synthetic cascades are enabled by combining biocatalysts with artificial metalloenzymes

3.1 Preamble

With the aim of performing *in vivo* catalysis, i.e. employing catalytic organometallic chemistry in biological systems, the activity of the corresponding catalyst in the cellular environment needs to be assured. Therefore, one needs to consider that the catalyst will interact with the cellular matrix. In order to perform directed evolution of artificial transfer hydrogenases, one of the challenges that needs to be overcome consists of the often detrimental interaction between cellular proteins and the synthetic metal complex. Mutual inactivation between organometallic catalyst and enzymes is an event that occurs frequently when these two catalytic systems are brought together. This is mainly due to the interactions of nucleophilic amino acid side chain functions on the protein surface (stemming *e.g.* from histidine, cysteine) and the metal catalyst.^[1,2] To overcome this problem, the active organometallic catalyst [Cp*Ir(biot-*p*-l)Cl] was incorporated into streptavidin mutants to shield it from the enzymatic tandem catalysis partner and thereby prevent inhibitory interactions. To validate this concept, the resulting artificial transfer hydrogenases (ATHase) were tested for the regeneration of NADH coupled with the concurrent action of 2-hydroxybiphenyl monooxygenase (HbpA), which performs the *ortho*-specific hydroxylation of an α -substituted phenol to the corresponding catechol and requires NADH as a redox equivalent (Scheme 3.1).

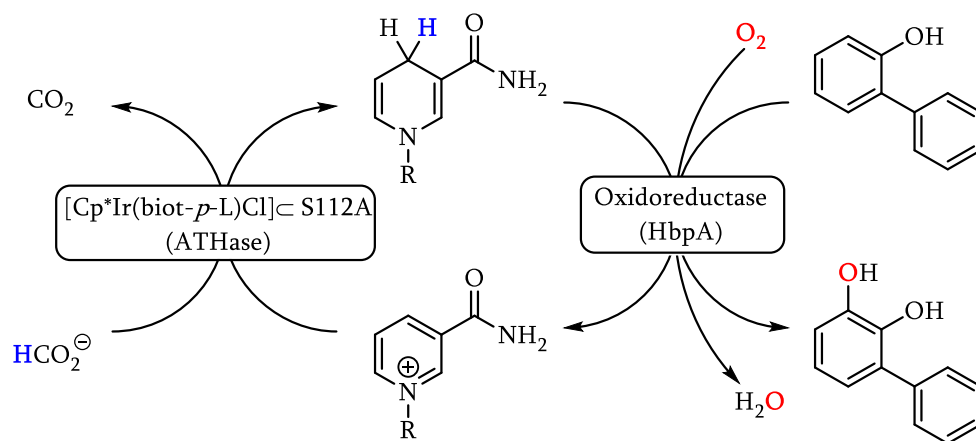


Figure 3.1 — Hydroxylation of 2-hydroxybiphenyl, coupled to ATHase-catalysed NADH regeneration.

Synthetic cascades are enabled by combining biocatalysts with artificial metalloenzymes

V. Köhler,¹ Y. M. Wilson,¹ M. Dürrenberger,¹ D. Ghislieri,² E. Churakova,³ T. Quinto,¹ L. Knörr,¹ D. Häussinger,¹ F. Hollmann,^{*,3} N. J. Turner,^{*,2} and T. R. Ward^{*,1}

¹Department of Chemistry, University of Basel, Spitalstrasse 51, CH-4056 Basel, Switzerland

²School of Chemistry, University of Manchester, Manchester Interdisciplinary Biocentre, 131 Princess Street, Manchester, M1 7DN, United Kingdom

³Department of Biotechnology, Delft University of Technology, Julianalaan 136, 2628BL Delft, The Netherlands

This chapter is based on the publication in: *Nature Chemistry*, **2013**, *5*, 93-99.

DOI 10.1038/NCHEM.1498

Reproduced with permission of the Nature Publishing Group

3.2 Abstract

Enzymatic catalysis and homogeneous catalysis offer complementary means to address synthetic challenges, both in chemistry and in biology. Despite its attractiveness, the implementation of concurrent cascade reactions which combine an organometallic catalyst with an enzyme has proven challenging, due to the mutual inactivation of both catalysts. To address this, we show that incorporation of a α^{δ} -piano stool complex within a host protein affords an artificial transfer hydrogenase (ATHase) which is fully compatible with and complementary to natural enzymes, thus enabling efficient concurrent tandem catalysis. To illustrate the generality of the approach, the ATHase was combined with various NADH-, FAD- and heme-dependent enzymes resulting in orthogonal redox cascades. Up to three enzymes were integrated in the cascade and combined with the ATHase with a view to achieving i) a double stereoselective amine deracemisation, ii) a horseradish peroxidase-coupled readout of the transfer hydrogenase activity towards its genetic optimization iii) the formation of L-pipecolic acid from L-lysine and iv) regeneration of NADH to promote a monooxygenase-catalyzed oxyfunctionalization reaction.

3.3 Introduction

Cellular biochemistry requires the orchestration of metabolic pathways in which many enzyme-catalysed processes are able to function simultaneously, resulting in the production of a wide range of primary and secondary metabolites within the cell. In an attempt to construct artificial cells, using the principles of synthetic biology, compartmentalization of cellular processes will need to be mimicked in order to allow cascade reactions to take place in parallel in an efficient manner.^[3-8] Whereas enzymes have evolved in concert and in complex media, problems and mutual inactivation are often encountered upon combining chemocatalyst with biocatalysts.^[9-11] Such incompatibility may be circumvented by performing cascades in sequential steps or by site-isolation of the individual catalysts through immobilization, heterogeneous or

biphasic reaction conditions, encapsulation and so on.^[12-26] Recently, we have described one approach to cellular compartmentalization in which an *E. coli* cell was engineered to simultaneously express an intracellular enzyme (monoamine oxidase) and also bind palladium nanoparticles in its outer membrane, thereby allowing efficient chemo-enzymatic deracemisation of amines^[26] Artificial metalloenzymes which result from encapsulation of an organometallic catalyst within a protein scaffold, have been shown to combine attractive features of both chemocatalysts and biocatalysts for single-step transformations^[27-34] In the context of concurrent cascade reactions, we reasoned that the artificial cofactor may be effectively shielded by its host protein, thus preventing the mutual inactivation commonly encountered upon combining an organometallic catalyst with an enzyme (Figure 3.1). To test the validity of the concept, we examined the combination of an artificial transfer-hydrogenase (ATHase) and a monooxygenase (Figure 3.2). For this purpose, we rely on the incorporation of a biotinylated [Cp*Ir(Biot-*p*-L)Cl] complex within streptavidin (Sav hereafter) as ATHase using sodium formate as hydride source (Figures 3.1 and 3.2).

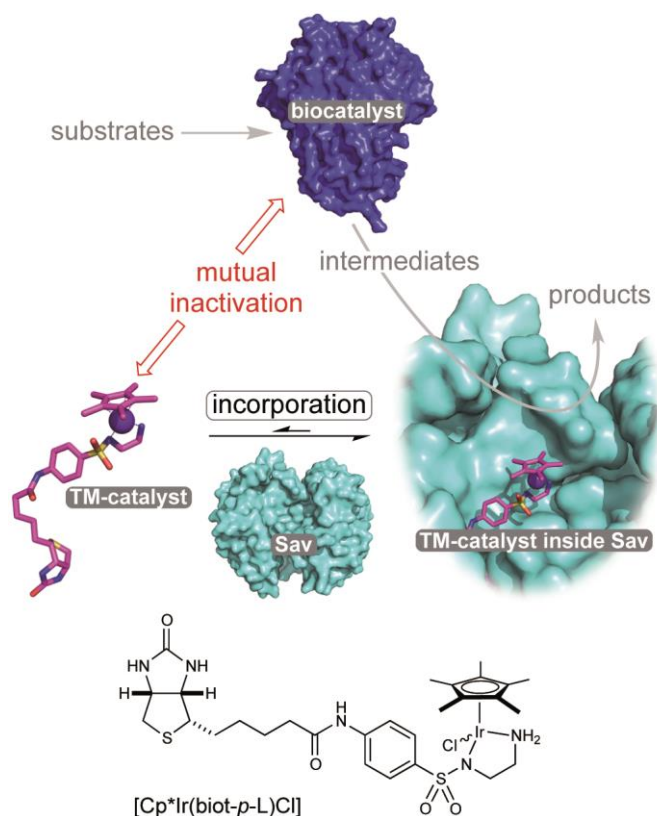


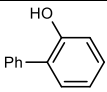
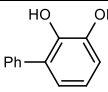
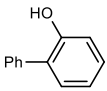
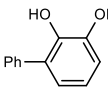
Figure 3.1 — Reaction cascades resulting from combining an ATHase with a biocatalyst. The organometallic transfer-hydrogenation catalyst $[\text{Cp}^*\text{Ir}(\text{biot-}p\text{-L})\text{Cl}]$ and biocatalyst suffer from mutual inactivation thus precluding the implementation of reaction cascades. Relying on the strength of the biotin-streptavidin interaction, incorporation of the biotin-bearing complex $[\text{Cp}^*\text{Ir}(\text{biot-}p\text{-L})\text{Cl}]$ within streptavidin (Sav) affords an ATHase which is fully compatible with and complementary to a variety of natural enzymes thus leading to the development of concurrent orthogonal redox cascades.

3.4 NADH regeneration for monooxygenases

The chemical and electrochemical recycling of NAD(P)H and analogues has been intensively investigated as an alternative to enzymatic regeneration.^[1,2,14,35–40] In this context, $[\text{Cp}^*\text{Rh}(\text{bipy})\text{Cl}]^+$ has emerged as redox mediator or catalyst of choice. However, in the presence of the downstream enzyme, mutual inactivation is commonly encountered.^[1,2] To test the validity of the molecular compartmentalization concept outlined in Figure 3.1, we investigated the regeneration of NADH in the presence of an NADH-dependent enzyme using an ATHase. Although significantly

more active than $[\text{Cp}^*\text{Rh}(\text{bipy})\text{Cl}]^+$ for the NADH regeneration in the absence of an NADH-dependent enzyme, $[\text{Cp}^*\text{Ir}(\text{Biot-}p\text{-L})\text{Cl}]$ was rapidly deactivated in the presence of 2-hydroxybiphenyl monooxygenase (HbpA from *Pseudomonas azaleica*, an NADH- and FAD-dependent enzyme). In the presence of Sav, however, the mutual inactivation of $[\text{Cp}^*\text{Ir}(\text{Biot-}p\text{-L})\text{Cl}]$ and HbpA was efficiently prevented and robust hydroxylation activity was achieved (Table 3.1, Figure 3.2). We conclude that Sav shields the ATHase from the downstream enzyme, allowing the NADH regeneration with formate as hydride source ($K_{\text{M}(\text{app})} = 165 \mu\text{M}$ ($\pm 6 \mu\text{M}$), $k_{\text{cat}(\text{app})} = 1.37 \text{ min}^{-1}$ ($\pm 0.01 \text{ min}^{-1}$), Supporting Information Figure 3.7). Full conversion of 2-hydroxybiphenyl to 2,3-dihydroxybiphenyl was accomplished in 2 h with a crude enzyme extract (Figure 3.2 and Table 3.1) and Supporting Information Figure 3.5).

Table 3.1 Orthogonal redox cascade combining ATHase with monooxygenases.

Entry	Substrate	Product	Sav-Mutant	Monooxygenase	Conv. ^(a) (%)
1			–	HbpA	3
2			S112A	HbpA	>99

a) Conversion determined by HPLC

The system could be run either in pure aqueous phase or as a biphasic system with 1-decanol functioning as a substrate reservoir and product sink, thereby highlighting the applicability of the ATHase under a variety of reaction conditions. The biphasic system displayed again strong inactivation in the absence of Sav, whereas a TON of > 100 (versus $[\text{Cp}^*\text{Ir}(\text{Biot-}p\text{-L})\text{Cl}]$) was achieved when Sav was present (Supporting information Figure 3.6).

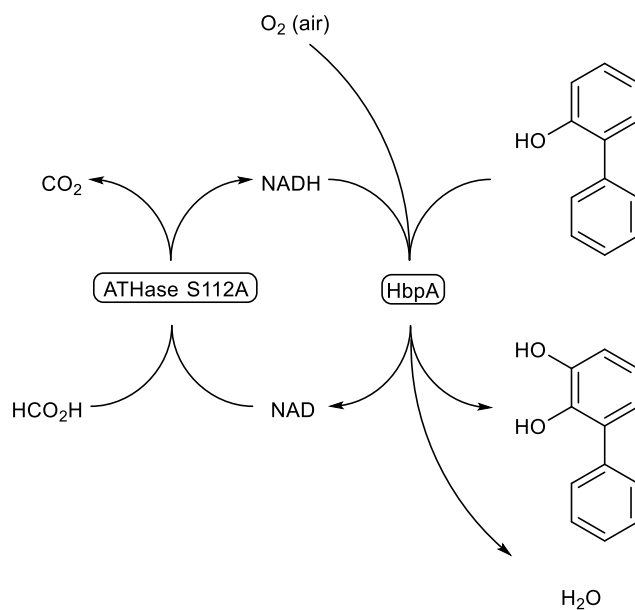


Figure 3.2 — Expanding the concept of orthogonal redox cascades to include other enzymes. Concurrent regeneration of NADH by the ATHase in the presence of a monooxygenase.

3.5 Outlook

We have demonstrated herein that an ATHase consisting of [Cp*Ir(Biot-*p*-L)Cl] anchored within streptavidin mutants is complementary and compatible with a variety of redox enzymes relying on NADH, FADH₂ and heme cofactors. Such artificial metalloenzymes display attractive features which are reminiscent of both biocatalysts and chemocatalysts: precious metal reactivity, genetic optimization potential and well-defined second coordination sphere provided by a protein scaffold. This last feature could be further exploited with a view to achieving the immobilization of the entire enzyme cascade.

To optimize such cascades, directed evolution protocols are highly desirable. With this goal in mind, we have shown that the ATHase can be integrated with a colorimetric coupled assay, leading to the identification of a genetically improved ATHase. These proof-of-principle examples open fascinating perspectives towards complementing biocatalytic cascades with molecularly compartmentalized organometallic catalysts.

3.6 Supporting Information

General Information

Chemicals were purchased from Sigma-Aldrich, Acros and TCI and used as received. Streptavidin (Sav) mutants were produced, purified and characterised as previously described.^[41] The Sav used in this work and on which all variants were based was T7-tagged core Sav described by Gallizia et al.^[42] and here we refer to this as wild-type Sav. The corresponding ATHase is also referred to as wild-type (WT). For a detailed synthesis procedure of [Cp*Ir(Biot-*p*-L)Cl] see reference.^[43] Commercial enzyme preparations were purchased from Sigma. MAO-Nmutants used in this study are described elsewhere.^[44,45] *rac*-2-cyclohexylpyrrolidine was prepared from 2-cyclohexyl-1-pyrroline by reduction with NaBH₄ in MeOH. 2-cyclohexyl-1pyrroline was prepared according to literature procedure.^[46] Pseudooxynicotine was prepared as described in reference.^[47] 2,3-dihydroxybiphenyl was a kind gift from Prof. Dr. Andreas Schmid (TU Dortmund, Dortmund, Germany). L-lysine-¹³C₂ HCl (99% ¹³C) was obtained from Sigma. NMR Experiments were performed at 25°C (MeOH calibration) on Bruker Avance III NMR spectrometers operating at 600, 500 or 400 MHz proton frequency. All were equipped with direct (600 and 400 MHz) or inverse (500MHz) dual channel broadband probe-heads with z-gradients. Chemical shifts were referenced to residual proton solvent peak (4.773 ppm for H₂O, 7.26 for CHCl₃). The quantitative constant time HSQC experiment was performed using 2048 data points in the F2 and 1024 data points in the F1 dimension, corresponding to acquisition time of 155ms in F2 and 34 ms in F1. Each increment was recorded with 8 scans resulting in a total experiment time of 2h 45min. HPLC measurements were performed on Agilent (or hp) machines equipped with modules from the 1100 and 1200 series and diode array detectors, if not indicated otherwise. HPLC columns were used with the appropriate guard columns, if not indicated otherwise. Column and conditions are indicated for each compound separately. GC measurements were performed on Agilent GCs of the 6890 series equipped with FIDs.

NAD reduction and HbpA coupled hydroxylation of 2-hydroxybiphenyl

Stock solutions: Potassium phosphate buffer (KPi) was prepared by dissolving K_2HPO_4 (114.8 mg) and KH_2PO_4 (590.2 mg) in distilled water (100mL, final conc. 50 mM, pH 6.0). Then sodium formate was dissolved in phosphate buffer (final 200mM). The pH was adjusted with NaOH. Stock solutions of lyophilized streptavidin S112A (Sav S112A) corresponding to 1 mM free binding sites (assuming 3 free binding sites per tetramer) were prepared by dissolving Sav S112A (21.9 mg) in H_2O (1 mL) directly before the experiment. The mixture was stirred until all protein was dissolved. The stock solutions of the metal complexes were prepared in DMF to the final concentration of 1 mM. NAD^+ and NADH stock solutions were prepared in H_2O to the final concentration of 10 mM and stored at $-20^\circ C$. FAD stock solutions were prepared in water to the final concentration of 1 mM.

HbpA preparation

The enzyme 2-hydroxybiphenyl-3-monooxygenase (HbpA, E.C.1.14.13.44) was kindly supplied by Prof. Dr. Andreas Schmid (TU Dortmund, Dortmund, Germany). The enzyme had been produced using *Escherichia coli* recombinantly expressing HbpA (*E. coli* JM101 pHBP461 containing hbpA) following a published procedure.^[48,49] For enrichment, the cell crude extracts (cell disruption was achieved by two passages through a French Press) were submitted to anion exchange chromatography (Streamline DEAE anion exchanger - Pharmacia). HbpA was eluted with 20 mM Tris HCl pH 7.5 using a linear gradient of NaCl from 0 to 1 M NaCl. HbpA was recovered in pooled fractions at 150 to 200 mM NaCl. The final enzyme preparation (pooled fractions) contained partially purified HbpA. Specific activities of purified fractions were determined at $30^\circ C$, 0.1 mM 2-hydroxybiphenyl and 0.1 mM NADH.^[48,49] HbpA was stored as a lyophilised powder at $-20^\circ C$. HbpA-preparation (typically 12.5 mg/mL) was dissolved directly before the experiments in KPi buffer (50 mM, pH 7.5).

NADH regeneration activity of [Cp*Ir(Biot-*p*-L)Cl]; [Cp*Ir(Biot-*p*-L)Cl]₂Sav with [Cp*Rh(Biot-*p*-L)Cl]

The activity measurements of the biotinylated metal-complexes (in the absence or presence of SAV) for NADH regeneration was carried out in disposable UV cuvettes (polystyrene) at 30°C (Shimadzu UV-2401 PC spectrophotometer; Julabo F12 Refrigerated/Heating Circulator). The reaction buffer (980 µL (or 970 µL for the reaction with SAV), 50 mM KPi, 200 mM NaHCO₂, pH 7.5) was supplemented with [Cp*Ir(Biot-*p*-L)Cl] or [Cp*Rh(Biot-*p*-L)Cl], respectively (10 µL of a 1 mM solution in DMF). If indicated, SAV-S112A stocksolution (10 µL, 1 mM in free binding sites in H₂O; 3 free binding sites per tetramer assumed) was added and the mixture was incubated at ambient temperature for 15 min. to allow for binding of the metal complex to SAV. The reactions were started by addition of NAD (10 µL of a 10 mM solution in H₂O). The reaction progress was followed spectrophotometrically by recording UV spectra or simply by following the absorption change at 340 nm. For quantification of NADH formed, the molar absorption coefficient of 6220 M⁻¹ cm⁻¹ was used.^[50]

Representative UV spectra of the [Cp*Ir(Biot-*p*-L)Cl] and of the [Cp*Ir(Biot-*p*-L)Cl]₂Sav mediated reduction of NAD are shown in Figure 3.3. The time courses of NAD reduction for all three regeneration catalysts are shown in Figure 3.3 (right) and initial rates compared in Table 3.2.

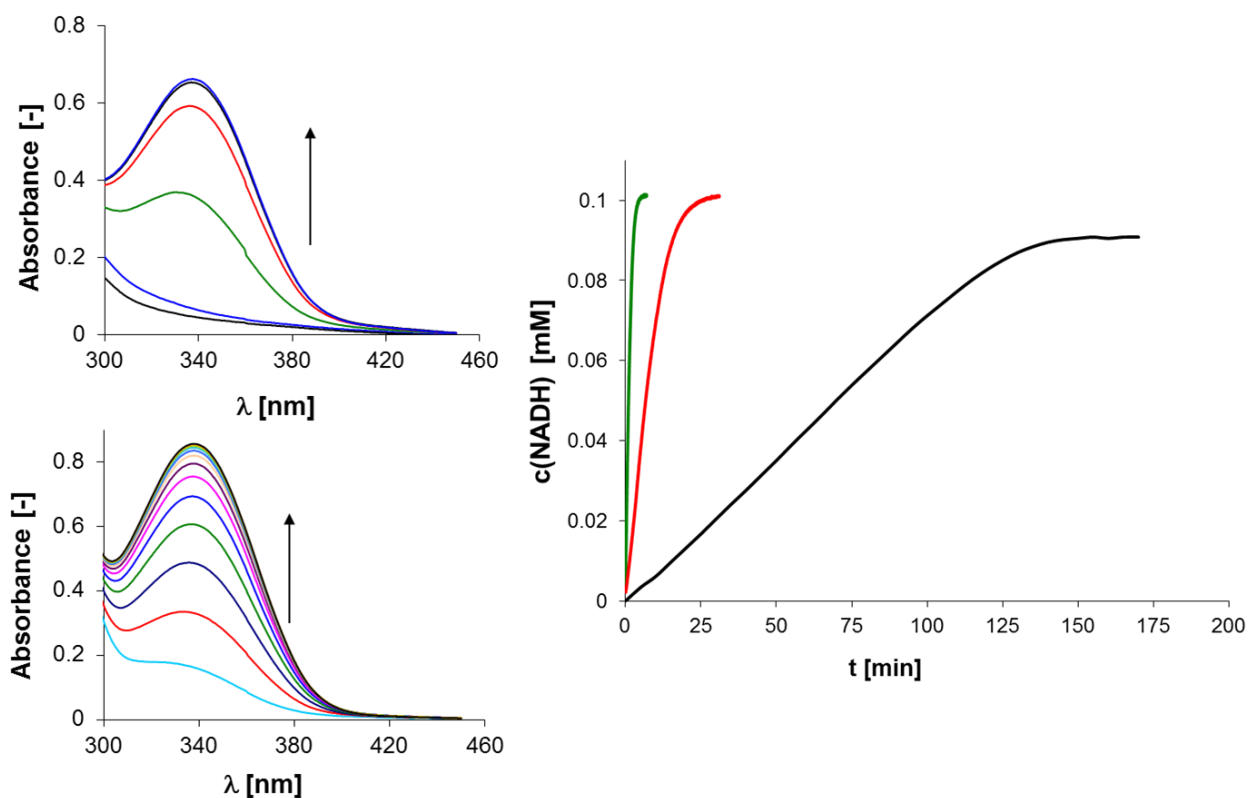


Figure 3.3 — Left: UV-spectra recorded during the $[\text{Cp}^*\text{Ir}(\text{Biot-}p\text{-L})\text{Cl}]$ (top left) and $[\text{Cp}^*\text{Ir}(\text{Biot-}p\text{-L})\text{Cl}]_{\text{cSAV}}$ (bottom left)-mediated reduction of NAD. Spectra were recorded at 10 sec and 60 sec intervals in case of $[\text{Cp}^*\text{Ir}(\text{Biot-}p\text{-L})\text{Cl}]$ (top left) and $[\text{Cp}^*\text{Ir}(\text{Biot-}p\text{-L})\text{Cl}]_{\text{cSAV}}$ (bottom left), respectively. Right: Time course of the metal-catalyzed reductions of NAD. $[\text{Cp}^*\text{Ir}(\text{Biot-}p\text{-L})\text{Cl}]$: green; $[\text{Cp}^*\text{Ir}(\text{Biot-}p\text{-L})\text{Cl}]_{\text{cSAV(S112A)}}$: red; $[\text{Cp}^*\text{Rh}(\text{Biot-}p\text{-L})\text{Cl}]$: black.

Table 3.2 Comparison of initial rates for graph in Figure 3.3 (right).

Compound	TOF [h^{-1}]	relative activity [%]
$[\text{Cp}^*\text{Rh}(\text{Biot-}p\text{-L})\text{Cl}]$	4.3	100
$[\text{Cp}^*\text{Ir}(\text{Biot-}p\text{-L})\text{Cl}]$	276.0	6420
$[\text{Cp}^*\text{Ir}(\text{Biot-}p\text{-L})\text{Cl}]_{\text{cSAV(S112A)}}$	42.5	988

Effect of Sav-S112A on the robustness of the chemoenzymatic hydroxylation reactions

In a first set of experiments the mutual inactivation of $[\text{Cp}^*\text{Ir}(\text{Biot-}i>P\text{-L})\text{Cl}]$ and HbpA as well as the protecting effect of $[\text{Cp}^*\text{Ir-biot-}i>P\text{-L})\text{Cl}]_{\text{cSAV(S112A)}}$ was examined. For this, spectrophotometric activity assays were performed: To phosphate buffer (1560 μL , 50 mM, pH 7.5) was added $[\text{Cp}^*\text{Ir}(\text{Biot-}i>P\text{-L})\text{Cl}]$ (20 μL of a 1 mM solution in DMF) and either SAV-S112A (20 μL , 1 mM free binding sites in H_2O ; 3 free binding sites per tetramer assumed) or H_2O (20 μL), respectively. Subsequently the mixtures were supplemented with HbpA stock solution (400 μL , 1 mg/mL in 50 mM KPi buffer, pH 7.5). These mixtures were incubated in a shaking incubator at 30°C. At 1 and 2 hours aliquots were taken to measure the residual activity. Residual HbpA activity: An aliquot of the incubated mixture (200 μL) was added to a mixture of phosphate buffer (740 μL , 50 mM, pH 7.5), NADH stock (30 μL of a 10 mM solution in H_2O) and FAD (10 μL of a 1 mM solution in H_2O) in a disposable UV-cuvette (polystyrene). The resulting solution was placed in a UV spectrometer at 30°C and background activity was recorded for 1.5 min. Residual substrate-related activity was followed after adding 2-hydroxybiphenyl (20 μL of a 25 mM methanolic solution) by the decrease in absorption at 340nm (NADH). For residual $[\text{IrCp}^*(\text{Biot-}i>P\text{-L})\text{L}]$ activity an aliquot of the incubated mixture (100 μL) was added to formate containing buffer (890 μL , 50 mM in KPi, 200 mM in NaHCO_2 , pH 7.5) and the reactions were started by addition of NAD (10 μL of a 10 mM solution H_2O). Table 3.3 summarizes the residual activities observed for the metal- and biocatalyst.

Table 3.3 Residual activity of HbpA and Ir-catalyst after co-incubation.

	residual HbpA activity [%]		residual Ir-activity [%]	
	incubation time			
	1h	2h	1h	2h
[Cp*Ir(biot- <i>p</i> -L)Cl]	<1	0	29	0
[Cp*Ir(biot- <i>p</i> -L)Cl] _c S112A	62	49	68	57
Potassium phosphate buffer	98	94	100	100

Both HbpA and [Cp*Ir(Biot-*p*-L)L] were rapidly deactivated when brought into contact. The deactivation was largely alleviated if the Ir-catalyst was preincubated with SAV-S112A. Hence, we concluded that indeed, SAV shielded the Ir-complex efficiently from interaction with HbpA and thereby protected both catalysts from mutual deactivation.

The effect of SAV-S112A on the chemoenzymatic hydroxylation of 2-hydroxybiphenyl

A first set of experiments was performed in aqueous medium: formate containing buffer solution (1.68 ml of 50 mM KPi, 200 mM NaHCO₂, pH adjusted to 7.5 with NaOH) was placed in a 2 mL PP-tube, SAV-S112A stock solution (40 μL, 1 mM free binding sites in H₂O; 3 free binding sites per tetramer assumed) was added, followed by [Cp*Ir(Biot-*p*-L)Cl] (40 μL, 1 mM in DMF). This mixture was incubated for 15 minutes at room temperature. Afterwards, the mixture was supplemented with FAD solution (20 μL of a 1 mM solution in H₂O) and HbpA stock solution (80 μL, 12.5 mg/ml, 11 U/ml in KPi buffer). After addition of the substrate 2-hydroxybiphenyl (40 μL of a 25 mM stock solution in methanol) the reaction was started by addition of NAD (100 μL of a 10 mM stock solution in H₂O). The reaction mixtures were placed in a thermoshaker (TWISTER comfort) and incubated at 30°C and 400 rpm. Samples of 50 μL were

withdrawn at the indicated time points, diluted with ACN/water (0.95 mL of a 50:50 (v/v) mixture containing 0.1% TFA) and analysed by RP-HPLC. (Shimadzu LC-20 system with a Shimadzu SPD-20A Photo Diode Array detector using a Waters Xterra column (RP18, 3.5 μ M, 4.6 \times 150 mm). The temperature was controlled to 40°C by a Shimadzu CTO-20AC column oven. The eluent was acetonitrile/water (50/50) isocratic and contained 0.1% TFA; flow rate: 1.1 mL/min, detection wavelength 254 nm). The quantification was based on calibration curves using authentic standards. Typical chromatograms are shown in Figure 3.4.

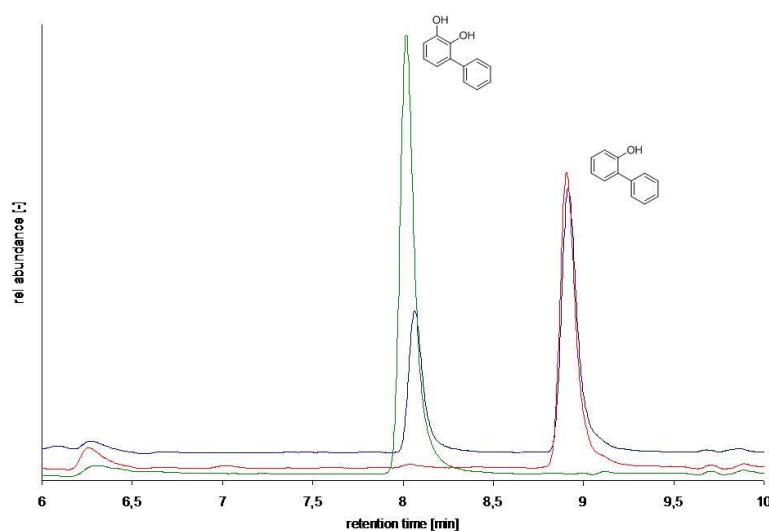


Figure 3.4 — Chromatograms of a typical chemoenzymatic hydroxylation reaction. **Red:** Sample taken immediately after initiation of the reaction, **blue:** sample taken after 40 min reaction time, **green:** sample taken after 24 h reaction time.

The reaction without Sav S112A was performed under identical conditions but leaving out the SAV-S112A addition step. The time courses of performing the reaction in the presence and absence of Sav S112A are compared in Figure 3.5. If Sav S112A was absent from the reaction mixture, accumulation of the product ceased soon after start of the reaction yielding less than 5% conversion of the starting material. However, in the presence of SAV-S112A, the reaction progressed smoothly to full conversion, accumulating the desired product only.

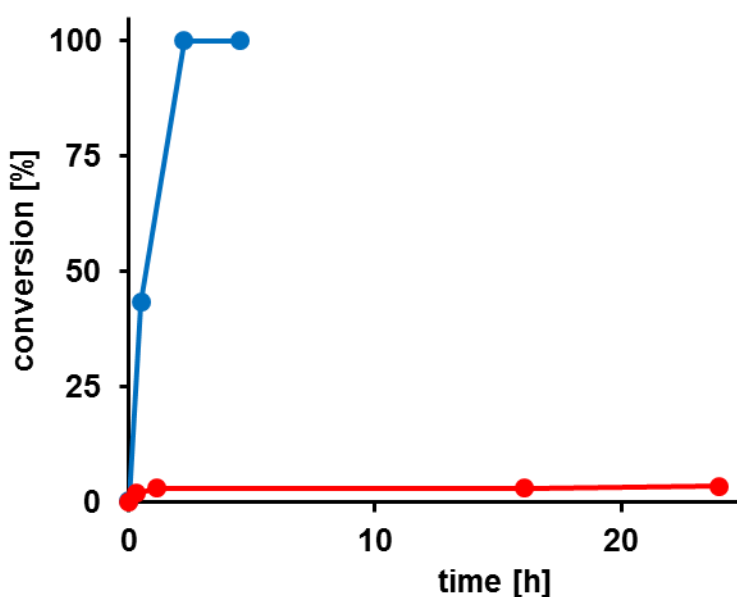


Figure 3.5 — Comparison of the chemoenzymatic hydroxylation of 2-hydroxybiphenyl in the presence (blue) and absence (red) of Sav S112A.

Due to the low solubility of the substrate (2-hydroxy biphenyl) in aqueous reaction media, the performance of the catalysts was somewhat limited. Therefore, we investigated the cascade reaction in a biphasic system (2LS) wherein a hydrophobic organic solvent (*e.g.* 1-decanol) serves as substrate reservoir and product sink (Figure 3.6). A typical procedure was: to a buffered solution of NaHCO₂ (712 μ L, 200 mM in NaHCO₂, 50 mM in KPi, pH adjusted with NaOH to 7.5) was added [Cp*Ir-biot-*p*-L]Cl (50 μ L of a 1 mM solution in DMF) and either Sav S112A (50 μ L, 1 mM free binding sites in H₂O; 3 free binding sites per tetramer assumed) or H₂O (50 μ L), respectively. The mixture was then supplemented with an FAD solution (10 μ L of a 1 mM solution in H₂O) as well as HbpA stock solution (128 μ L, 12.5 mg/mL, 6.9U/mL in KPi buffer, pH of buffer 7.5). Immediately afterwards 2-hydroxybiphenyl in 1-decanol (1 mL of a 100 mM solution) was added. The reaction mixtures were placed in a thermoshaker and incubated at 30°C and 800 rpm. After a short mixing period (approx. 1 minute) a sample (0.1 mL) was withdrawn and centrifuged to induce phase separation. 10 μ L of the organic phase were withdrawn (the remaining sample was added back to the reaction mixture), diluted with ACN/water (0.99 mL of a 50:50 (v/v) mixture containing 0.1%

TFA) and analysed by RP-HPLC as described above. The reaction was subsequently initiated by addition of NAD stock solution (50 μ L of a 10 mM solution in H₂O). Samples were taken at the indicated time points (Figure 3.6) and treated as described above. For analysis, only the substrate and product concentrations in the organic phase were considered.

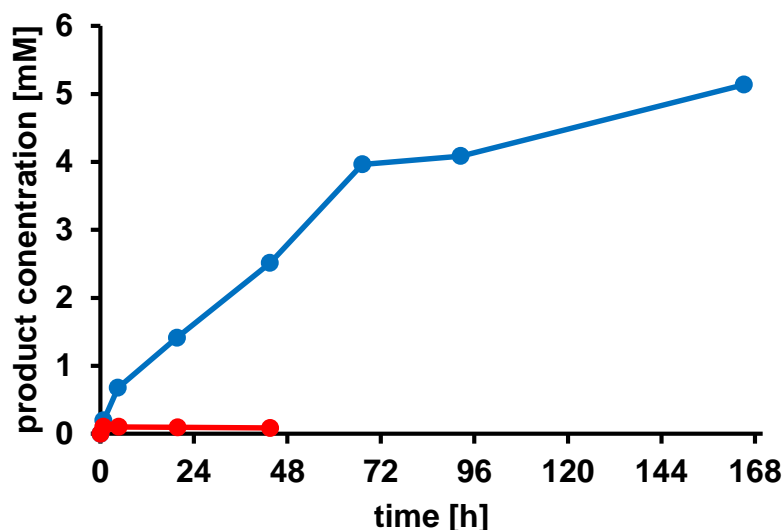


Figure 3.6 — Time course of chemoenzymatic hydroxylation of 2-hydroxybiphenyl under biphasic (2LPS) conditions in the presence (blue) and absence (red) of Sav S112A.

Determination of apparent kinetic constants of ATHase catalyzed NAD reduction

Note: the reaction conditions for the kinetic measurement (50 mM KPi-buffer, 200 mM NaHCO₂) are not identical to the conditions used in the monophasic reaction set-up (42 mM KPi-buffer, 168 mM NaHCO₂). Stock solution:

- **Buffer 1:** phosphate buffer 50mM pH 7.5
- **Buffer 2:** phosphate/formate buffer (50mM in phosphate, 200mM in NaHCO₂ pH adjusted with NaOH to 7.5)
- NAD⁺: 10mM in **buffer1** (29.27 mg, purity 90%, contains 10% H₂O) was dissolved 3.970ml of **buffer1**.
- **Buffer 3:** stock of NAD⁺ diluted to various concentrations (see Table 3.4).

- [Cp*Ir(Biot-*p*-L)Cl]: stock 1mM (MW 803, weight 2.32mg in 2.889 ml of DMF)
- ATHase: 10.2 mg of Sav S112A were dissolved in buffer 1 (4.209 mL) and Ir-stock solution (467 μ L) were added. This leads to a final concentration of 100 μ M and a ratio of Ir/free binding sites of 1/3(3 free binding sites per tetramer assumed).

Table 3.4 Volumes and concentrations

entry	volume buffer 1 [μ L]	volume buffer 3 with NAD ⁺ [μ L]	NAD concentration of buffer 3 [μ M]	volume ATHase [μ L]	volume buffer 2 [μ L]	final conc. of NAD ⁺ [μ M]
1	450	0	0	50	500	0
2	250	200	25	50	500	5
3	250	200	50	50	500	10
4	250	200	75	50	500	15
5	250	200	100	50	500	20
6	250	200	150	50	500	30
7	250	200	250	50	500	50
8	250	200	400	50	500	80
9	250	200	500	50	500	100
10	250	200	1000	50	500	200
11	250	200	2000	50	500	400
12	250	200	4000	50	500	800
13	250	200	6000	50	500	1200
14	250	200	8000	50	500	1600

15	250	200	10000	50	500	2000
----	-----	-----	-------	----	-----	------

The sample was prepared in the cuvette (polystyrene) by adding first **buffer 1** (prewarmed to 30°C), followed by the ATHase, and then **buffer 3** (prewarmed to 30°C). The reactions were started by the addition of formate containing **buffer 2** (prewarmed to 30°C).

Each measurement was performed in triplicate in a Shimadzu UV-1800 UV spectrophotometer (at 30°C) and analysed with UV probe, version 2.34. Absorption was detected at 340nm and an absorption coefficient of $6220\text{M}^{-1}\text{cm}^{-1}$ for NADH was used for calculation of the kinetic parameters.^[50] Rates were determined by considering the linear part of increase in absorbance over time. The apparent Michaelis-Menten parameters V_{max} , K_{m} and K_{i} were obtained applying non-linear regression (least squares method) using GraphPad Prism 5.0® corresponding to the mMichaelis-Menten equation.^[51]

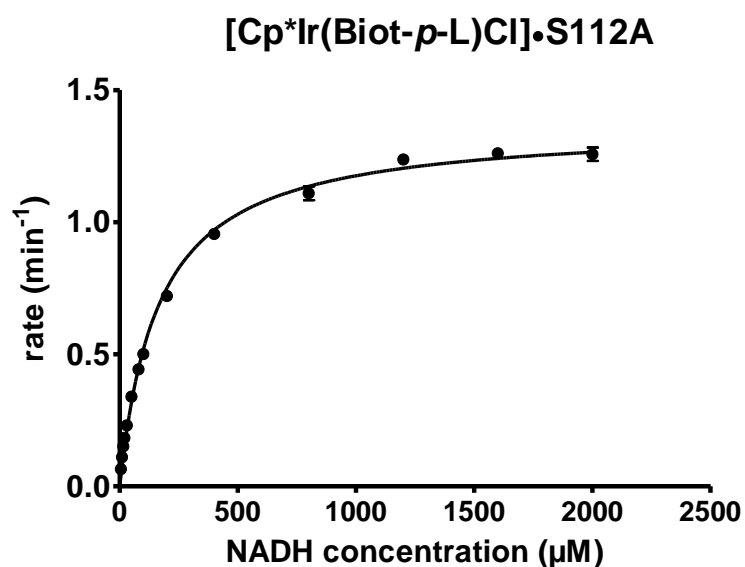


Figure 3.7 — Saturation kinetics of ATHase S112A in the reduction of NAD. Errors bars indicate ± 1 standard deviation, determined from the triplicate measurement of each rate.

3.7 References

- (1) Poizat, M.; Arends, I. W. C. E.; Hollmann, F. *J. Mol. Catal. B Enzym.* **2010**, *63*, 149–156.
- (2) Hildebrand, F.; Lütz, S. *Chem. Eur. J.* **2009**, *15*, 4998–5001.
- (3) Wörsdörfer, B.; Woycechowsky, K. J.; Hilvert, D. *Science* **2011**, *331*, 589–592.
- (4) Choudhary, S.; Quin, M. B.; Sanders, M. a.; Johnson, E. T.; Schmidt-Dannert, C. *PLoS One* **2012**, *7*, e33342.
- (5) Dueber, J. E.; Wu, G. C.; Malmirchegini, G. R.; Moon, T. S.; Petzold, C. J.; Ullal, A. V.; Prather, K. L. J.; Keasling, J. D. *Nat. Biotechnol.* **2009**, *27*, 753–759.
- (6) Keasling, J. D. *ACS Chem. Biol.* **2008**, *3*, 64–76.
- (7) Bromley, E. H. C.; Channon, K.; Moutevelis, E.; Woolfson, D. N. *ACS Chem. Biol.* **2008**, *3*, 38–50.
- (8) Weissman, K. J.; Leadlay, P. F. *Nat. Rev. Microbiol.* **2005**, *3*, 925–936.
- (9) Mutti, F. G.; Orthaber, A.; Schrittwieser, J. H.; de Vries, J. G.; Pietschnig, R.; Kroutil, W. *Chem. Commun.* **2010**, *46*, 8046–8048.
- (10) Haak, R. M.; Berthiol, F.; Jerphagnon, T.; Gayet, A. J. a; Tarabiono, C.; Postema, C. P.; Ritleng, V.; Pfeffer, M.; Janssen, D. B.; Minnaard, A. J.; Feringa, B. L.; de Vries, J. G. *J. Am. Chem. Soc.* **2008**, *130*, 13508–13509.
- (11) Maid, H.; Böhm, P.; Huber, S. M.; Bauer, W.; Hummel, W.; Jux, N.; Gröger, H. *Angew. Chem. Int. Ed.* **2011**, *50*, 2397–2400.
- (12) Wasilke, J. C.; Obrey, S. J.; Baker, R. T.; Bazan, G. C. *Chem. Rev.* **2005**, *105*, 1001–1020.

- (13) Zhou, J. *Chem. Asian J.* **2010**, *5*, 422–434.
- (14) Betanzos-lara, S.; Liu, Z.; Habtemariam, A.; Pizarro, A. M.; Qamar, B.; Sadler, P. *J. Angew. Chem. Int. Ed.* **2012**, *51*, 3897–3900.
- (15) Wingstrand, E.; Laurell, A.; Fransson, L.; Hult, K.; Moberg, C. *Chem. Eur. J.* **2009**, *15*, 12107–12113.
- (16) Simons, C.; Hanefeld, U.; Arends, I. W. C. E.; Maschmeyer, T.; Sheldon, R. a. *Top. Catal.* **2006**, *40*, 35–44.
- (17) Wieczorek, B.; Träff, A.; Krumlinde, P.; Dijkstra, H. P.; Egmond, M. R.; Koten, G. Van; Bäckvall, J. E.; Gebbink, R. J. M. K. *Tetrahedron Lett.* **2011**, *52*, 1601–1604.
- (18) Rocha-Martín, J.; Rivas, B. de Las; Muñoz, R.; Guisán, J. M.; López-Gallego, F. *ChemCatChem* **2012**, *4*, 1279–1288.
- (19) Hanefeld, U.; Gardossi, L.; Magner, E. *Chem. Soc. Rev.* **2009**, *38*, 453–468.
- (20) Brady, D.; Jordaan, J. *Biotechnol. Lett.* **2009**, *31*, 1639–1650.
- (21) Mateo, C.; Palomo, J. M.; Fernandez-Lorente, G.; Guisan, J. M.; Fernandez-Lafuente, R. *Enzyme Microb. Technol.* **2007**, *40*, 1451–1463.
- (22) Lopez-Gallego, F.; Schmidt-Dannert, C. *Curr. Opin. Chem. Biol.* **2010**, *14*, 174–183.
- (23) Pàmies, O.; Bäckvall, J. E. *Chem. Rev.* **2003**, *103*, 3247–3261.
- (24) Kim, Y.; Park, J.; Kim, M. J. Dynamic kinetic resolution of amines and amino acids by enzyme-metal cocatalysis. *ChemCatChem* **2011**, *3*, 271–277.

- (25) Yusop, R. M.; Unciti-Broceta, A.; Johansson, E. M. V; Sánchez-Martín, R. M.; Bradley, M. *Nat. Chem.* **2011**, *3*, 239–243.
- (26) Foulkes, J. M.; Malone, K. J.; Coker, V. S.; Turner, N. J.; Lloyd, J. R. *ACS Catal.* **2011**, *1*, 1589–1594.
- (27) Lu, Y.; Yeung, N.; Sieracki, N.; Marshall, N. M. *Nature* **2009**, *460*, 855–862.
- (28) Ward, T. R. *Acc. Chem. Res.* **2011**, *44*, 47–57.
- (29) Bos, J.; Fusetti, F.; Driessen, A. J. M.; Roelfes, G. *Angew. Chemie - Int. Ed.* **2012**, *51*, 7472–7475.
- (30) Jing, Q.; Kazlauskas, R. J. *ChemCatChem* **2010**, *2*, 953–957.
- (31) Podtetenieff, J.; Taglieber, A.; Bill, E.; Reijerse, E. J.; Reetz, M. T. *Angew. Chem. Int. Ed.* **2010**, *49*, 5151–5155.
- (32) Deuss, P. J.; den Heeten, R.; Laan, W.; Kamer, P. C. J. *Chem. Eur. J.* **2011**, *17*, 4680–4698.
- (33) Ueno, T.; Abe, S.; Yokoi, N.; Watanabe, Y. *Coord. Chem. Rev.* **2007**, *251*, 2717–2731.
- (34) Matsuo, T.; Hayashi, A.; Abe, M.; Matsuda, T.; Hisaeda, Y.; Hayashi, T. *J. Am. Chem. Soc.* **2009**, *131*, 15124–15125.
- (35) Hollmann, F.; Hofstetter, K.; Schmid, A.; Care, D.; Specialties, S.; Ag, G. *TRENDS in Biotech.* **2006**, *24*, 163–171.
- (36) Hollmann, F.; Arends, I. W. C. E.; Buehler, K. *ChemCatChem* **2010**, *2*, 762–782.
- (37) Haquette, P.; Talbi, B.; Barilleau, L.; Mandern, N.; Fosse, C.; Salmain, M. *Org. Biomol. Chem.* **2011**, *9*, 5720–5727.

- (38) Maenaka, Y.; Suenobu, T.; Fukuzumi, S. *J. Am. Chem. Soc.* **2012**, *134*, 367–374.
- (39) Canivet, J.; Süß-fink, G.; Petr, S. *Eur. J. Inorg. Chem* **2007**, 4736–4742.
- (40) Ryan, J. D.; Fish, R. H.; Clark, D. S. *ChemBioChem* **2008**, *9*, 2579–2582.
- (41) Köhler, V.; Mao, J.; Heinisch, T.; Pordea, A.; Sardo, A.; Wilson, Y. M.; Knörr, L.; Creus, M.; Prost, J. C.; Schirmer, T.; Ward, T. R. *Angew. Chemie Int. Ed.* **2011**, *50*, 10863–10866.
- (42) Gallizia, a; de Lalla, C.; Nardone, E.; Santambrogio, P.; Brandazza, a; Sidoli, a; Arosio, P. *Protein Expr. Purif.* **1998**, *14*, 192–196.
- (43) Wilson, Y. M.; Marc, D.; Ward, T. R. In *Protein Engineering Handbook*; Lütz, S.; Bornscheuer, U. T., Eds.; Wiley-VCH: Weinheim, 2012.
- (44) Rowles, I.; Malone, K. J.; Etchells, L. L.; Willies, S. C.; Turner, N. J. *ChemCatChem* **2012**, *4*, 1259–1261.
- (45) Atkin, K. E.; Reiss, R.; Koehler, V.; Bailey, K. R.; Hart, S.; Turkenburg, J. P.; Turner, N. J.; Brzozowski, a. M.; Grogan, G. *J. Mol. Biol.* **2008**, *384*, 1218–1231.
- (46) Starr, D. F.; Bulbrook, H.; Xixon, R. M. *J. Am. Chem. Soc.* **1932**, *54*, 3971–3976.
- (47) Dunsmore, C. J.; Carr, R.; Fleming, T.; Turner, N. J. *J. Am. Chem. Soc.* **2006**, *128*, 2224–2225.
- (48) Schmid, A.; Vereyken, I.; Held, M.; Witholt, B. *J. Mol. Catal. - B Enzym.* **2001**, *11*, 455–462.
- (49) Suske, W. a.; Held, M.; Schmid, A.; Fleischmann, T.; Wubbolts, M. G.; Kohler, H. P. E. *J. Biol. Chem.* **1997**, *272*, 24257–24265.

- (50) Dawson, R. M. C.; Elliott, D. C.; Elliott, W. H.; Jones, K. M. In *Data for biochemical research*; Calarendon Press: Oxford, 1986; pp. 122–123.
- (51) Michaelis, L.; Menten, M. L. *Biochem. Z.* **1913**, *49*, 333–369.

Chapter 4

Artificial metalloenzymes for the diastereoselective reduction of NAD⁺ to NAD²H

Tommaso Quinto, Daniel Häussinger, Valentin Köhler and Thomas R. Ward

This chapter was published in: *Organic & Biomolecular Chemistry*, **2015**, *13*, 357-360.

DOI 10.1039/c4ob02071e

Reproduced by permission of the Royal Society of Chemistry

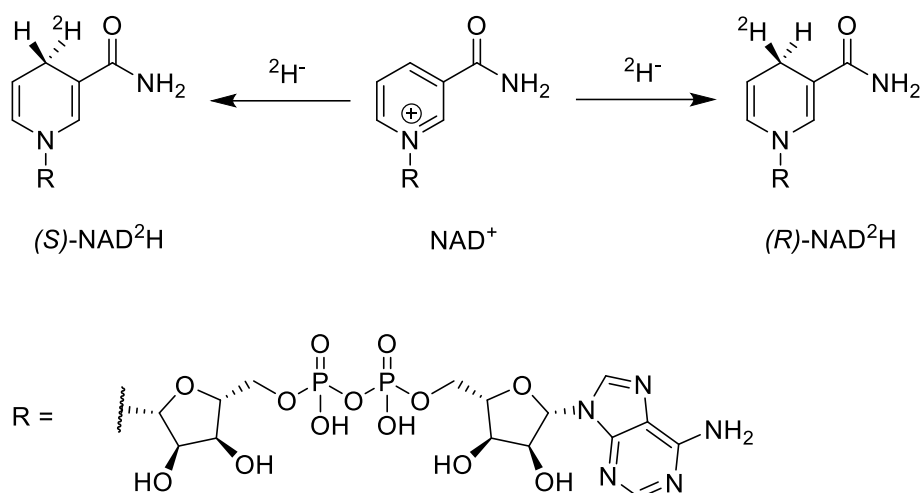
<http://dx.DOI.org/10.1039/c4ob02071e>

4.1 Abstract

Stereoselectively labelled isotopomers of NAD(P)H are highly relevant for mechanistic studies of enzymes which utilize them as redox equivalents. Whereas several methods are firmly established for their generation in high diastereomeric purity by enzymatic methods, alternative methods have so far not been investigated. This chapter presents the stereoselective deuteration of NAD⁺ at the 4-position (90% de) of the pyridinium-ring by means of an artificial metalloenzyme. The artificial metalloenzyme consists of a biotinylated iridium cofactor embedded in streptavidin isoforms and the resulting construct has been previously shown to be compatible with natural enzymes. Alternative methods for stereoselective NAD(P)⁺ reduction are expected to be of high interest for the mechanistic study of enzymes that accept NAD(P)H mimics and for the synthesis of structurally related fine chemicals.

4.2 Introduction

The coenzymes NAD(P)⁺ and NAD(P)H play a crucial role in the redox machinery of living systems. This relates to their ability to either accept a hydride at the C4-position of the pyridine ring in their oxidized form or to donate the respective hydride in the reverse-reaction (Scheme 4.1). When the hydride is replaced by a deuteride in the reduction step, two diastereoisomers can be formed due to the presence of the enantiopure adenine dinucleotide moiety. The diastereoisomers thus differ only in their configuration at C4. Stereoselective labelling of the coenzymes with deuterium or tritium yields precious mechanistic information for the corresponding enzymes. Methods for their preparation in high stereoisomeric purity are well established.^[1,2,3]



Scheme 4.1 — Deuteration of NAD^+ at the C4 position yields diastereoisomers.

Biocatalysis gains an ever increasing share in modern chemical manufacture, boosted by powerful protein engineering strategies.^[4] NAD(P)H or NAD(P)^+ mol equivalents are required in various biotransformations, including ketoreductases, alcohol dehydrogenases, Baeyer-Villiger monooxygenases, imine reductases, and P450s.^[5-8] These co-substrates are typically regenerated enzymatically in a catalytic concurrent fashion.^[9] However, alternative approaches employing *e.g.* chemocatalysis or electrochemical reduction have received increasing attention since they offer additional flexibility in process conditions and are readily transferrable to NAD(P) -mimics, which are substantially cheaper than their natural analogues.^[10]

One complex that has been frequently used in non-enzymatic regeneration systems for the transfer of reducing equivalents to NAD(P)^+ is the achiral $[\text{Cp}^*\text{Rh}(\text{bipy})(\text{H}_2\text{O})]^{2+}$.^[11] At least one report exists where an enantiopure complex was utilized.^[12] However, no labelling studies were undertaken and accordingly no diastereoselectivity for the reduction step studied. We recently reported on the application of an artificial transfer hydrogenase (ATHase) for the concurrent regeneration of NADH in a monooxygenase-coupled reaction.^[13] To generate the artificial metalloenzyme, a biotinylated iridium pianostool complex was incorporated into streptavidin (Sav) mutant S112A (Figure 4.1). The biotinylated ligand for the Cp^*Ir moiety is achiral in the vicinity of the metal center, and the respective complex has been shown to induce only negligible

stereocontrol in the reduction of prochiral imine substrates in the absence of streptavidin. However, upon incorporation into Sav, substantial stereocontrol can be achieved.^[14] Importantly, the concurrent process with the monooxygenase and other enzymes was only effective, when the complex was located inside Sav; otherwise dramatic deactivation of the monooxygenase and/or the artificial Ir-cofactor occurred.^[15]

We have previously shown that substrate reduction with ATHase derived from Sav mutants S112A and S112K lead to *R*- and *S*- enantiomers for both ketones and imines, respectively.^[14] The corresponding X-ray structures of $[\text{Cp}^*\text{Ir}-(\text{Biot-}p\text{-L})\text{Cl}] \subset \text{S112A}$ ^[14] and $[\text{Cp}^*\text{Ir}-(\text{Biot-}p\text{-L})\text{Cl}] \subset \text{S112K}$ ^[15] were recently reported and analysed: for S112A, the absolute configuration at $[\text{Cp}^*\text{Ir}-(\text{Biot-}p\text{-L})\text{Cl}]$ is (*S*) and for S112K, the absolute configuration is (*R*). Based on modelling studies, we hypothesise that the absolute configuration at Ir by-and-large determines the absolute configuration of the alcohol and amine products: we term this phenomenon “induced lock-and-key” whereby the protein determines which prochiral face of the substrates is reduced.^[15]

Herein we report on the diastereoselectivity of NAD deuteration employing the Ir-cofactor by itself and upon incorporation into two Sav-mutants (Figure 4.1).

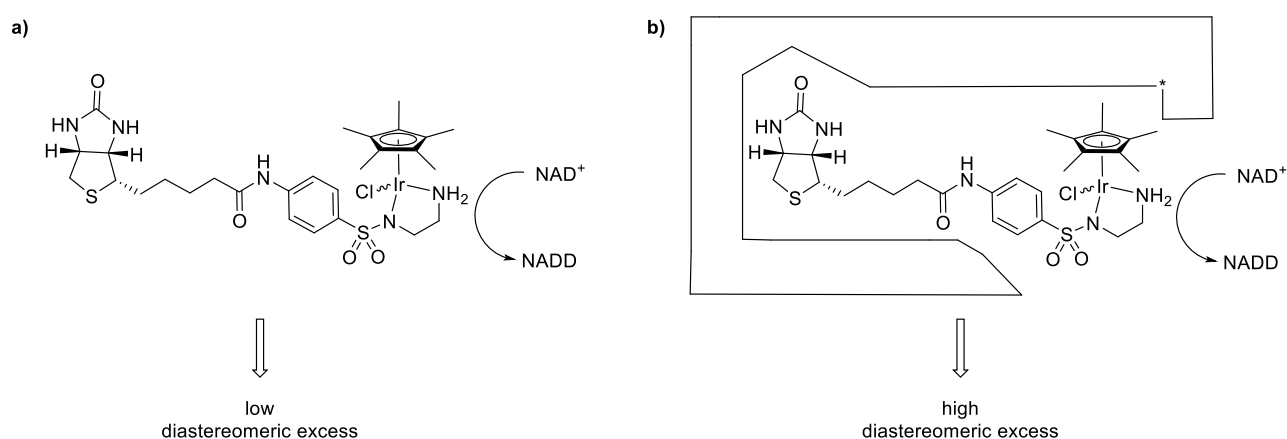


Figure 4.1 — NAD⁺ reduction, **a)** with a biotinylated Ir-complex and deuterated sodium formate in the absence of streptavidin mutants proceeds with low diastereoselectivity. **b)** Upon incorporation into streptavidin isoforms, the reduction proceeds with high diastereoselectivity. The star symbolizes a mutation in streptavidin.

4.3 Results and Discussion

To determine the diastereomeric ratio after reduction with deuteride, $^1\text{H-NMR}$ -spectroscopy offers a convenient means.^[16,17] This technique enables the direct determination of the diastereoselectivity in the reaction mixture without requiring isolation of the products. The only noteworthy differences to potential preparative reactions lies in the presence of a small amount of deuterium oxide (5%), the dissolution of the biotinylated Ir-complex in DMF-d_7 instead of DMF and a short centrifugation step. Based on catalysis results obtained in asymmetric imine reduction^[14] and NADH regeneration^[13] with artificial metalloenzymes, the selectivity with two representative mutants was investigated. Mutant S112A, employed previously for concurrent NADH regeneration, leads to superior enantiomeric excess and high turnover numbers in the reduction of 1-methyl-6,7-dimethoxy-3,4-tetrahydroisoquinoline yielding (*R*)-configured salsolidine (up to 96% *ee*).^[14] Reduction of the same substrate with the AME based on S112K, in contrast, leads to a bias in favour of the (*S*)-enantiomer (up to 78 % *ee*).^[14]

For the stereoselective NAD^+ reduction experiments, deuterated sodium formate was used as a deuteride source in the presence of $[\text{Cp}^*\text{Ir}(\text{biot-}p\text{-L})\text{Cl}]\text{C-S112A}$ and NAD^+ . Following centrifugation, the crude reaction mixtures were analyzed by $^1\text{H-NMR}$ spectroscopy. While background signals of the protein and other components of the crude reaction mixture prevented unambiguous integration of 1D $^1\text{H-NMR}$ data, a selective one-dimensional TOCSY NMR experiment using irradiation on H6 (5.89 ppm) yielded clean spectra with sufficient signal to noise ratio to reliably integrate the two resonances attributed to both diastereomers (Figure 4.1). As the TOCSY transfer occurs with slightly different efficiency for (*4R*- ^2H)-NADH and (*4S*- ^2H)-NADH, a calibration TOCSY experiment with commercial, non-deuterated NADH was performed (Figure 4.2a) and the resulting integrals (1.00 : 1.13 for H_{4s} : H_{4R}) were used to normalize the integrals of the deuterated species (Figure 4.2b-d). Due to the collapse of the $^2J_{\text{HH}}$

coupling constant of 18.1 Hz into a $^2J_{\text{HD}}$ of 2.8 Hz, both H4 resonances appear as broad singlets in the TOCSY spectrum and the fine structure is lost. The integration yielded a *de* of 87% for mutant S112A and a *de* of 90% for mutant S112K, while a *de* of 38% was obtained for the sample without Sav (all with an error margin of $\pm 1\%$), after 16 hours reaction time (Figure 4.2).

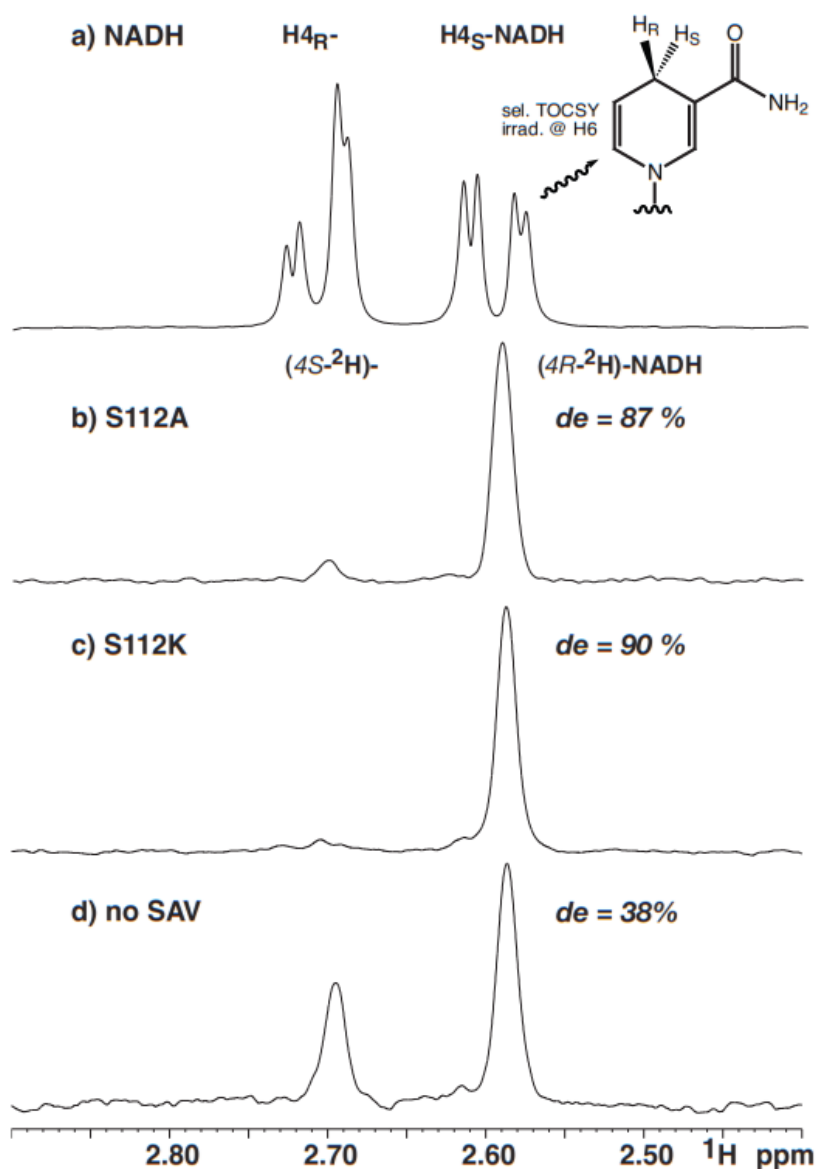


Figure 4.2 — Selected region from selective ^1H -TOCSY spectra of **a)** commercial NADH, and catalytic reduction of NAD^+ using $^2\text{HCOONa}$ with, **b)** S112A; **c)** S112K; **d)** no Sav.

The modest but significant diastereoselectivity observed in the absence of Sav arises most likely from substrate control considering the formation of basically racemic product from achiral starting materials in related transformations.^[13,14] Both mutants led to a significant improvement in the diastereomeric excess compared to the result obtained in the absence of streptavidin (Figure 4.2). Interestingly, for the NAD⁺ reduction, both S112A and S112K ATHases afford the same diastereomer preferentially. This observation stands in stark contrast with result previously reported for the ketone and imine reduction whereby S112A and S112K afford (*R*)- and (*S*)-reduction products respectively. In a matched-mismatched spirit, we speculate that the inherent chirality of the sugar moiety of NAD⁺ counterbalances the ATHase preference. This is supported by the inherent preference of the substrate in the absence of Sav. Alternatively, one NAD⁺ substrate could bind in the biotin vestibule in S112A, thus modifying the environment of the metal complex. Similar results were computed for the imine reductase with S112A.^[15] The preparation and screening of further mutants might provide guiding answer towards the design of ATHases with inverted selectivities for the reduction of NAD⁺.

4.4 Conclusions

The high chiral induction observed is promising for further applications such as the investigation of specificity in enzymes utilizing NAD(P)-mimics and the resulting information would be of interest for future enzyme engineering tasks. Furthermore, related prochiral structures can be envisaged, namely 3,4 substituted pyridinium ions, which would provide valuable building blocks upon asymmetric conversion.^[18]

4.5 Experimental part

Nicotinamide adenine dinucleotide hydrate (NAD⁺, contains 10% H₂O) was purchased from Sigma. ²HCOONa was purchased from ABCR. Streptavidin was prepared as previously reported.^[13] [Cp*Ir(biot-*p*-L)Cl] was a kind gift from Dr. Marc Dürrenberger

and prepared as reported in literature.^[19] NMR experiments were performed at 25°C (MeOH calibration) on a Bruker Avance III NMR spectrometer operating at 600 MHz proton frequency, equipped with a direct detection dual channel, broadband probe-head with z-gradient. Chemical shifts were referenced against proton solvent peaks (4.773 ppm for H₂O). The selective TOCSY experiment^[20,21] was performed using a MLEV17 spinlock sequence with a mixing time of 120 ms, trim pulses of 2.5 ms and a selective Gauss shaped refocusing pulse of 80 ms duration.

Stock solutions: buffer 1: sodium phosphate 50 mM, pH 7.5; buffer 2: ²HCOONa 200 mM, sodium phosphate 50mM, pH 7.5, {²HCOONa (138 mg) was dissolved in Milli-Q H₂O (5 ml), sodium phosphate buffer (0.5 ml, 1M) was added and the pH adjusted to 7.5 by addition of aq. NaH₂PO₄. Water was added to a total volume of 10 ml}; NAD⁺ stock solution: 10 mM in buffer 1 (NAD⁺ (29.9 mg, 405 μmol) was dissolved in buffer 1 (4.05 ml); Ir-stock solution: 10 mM [Cp*Ir(biot-*p*-L)Cl] (2.55 mg, 3.17 μmol) was dissolved in DMF-*d*₇ (317 μl).

Preparation of ATHase:

- Sav-mutant S112A (2.53 mg, assuming 3 free binding sites) was dissolved in buffer 1 (1.144 mL), and Ir-stock solution was added (11.6 μl).
- Sav-mutant S112K (2.65 mg assuming 3 free binding sites) was dissolved in buffer 1 (1.195 ml), and Ir-stock solution was added (12.1 μl).
- Sample without SAV mutant (intermediate solutions): buffer 1 (0.495 ml) and Ir-stock solution was added (5 μl). Mixing was achieved by means of a vortex mixer.

Reaction set up: To buffer 1 (125 μl) was added buffer 2 (250 μl; final concentration of ²HCOONa = 100 mM), ATHase (or intermediate solutions) (100 μl, final concentration of Ir = 20 μM) and NAD⁺ stock solution (25 μl, final concentration = 500 μM).

The reaction was incubated and agitated at 30°C and 200 rpm for 24h by means of a Thermomixer (HLC Biotech Model MHR 23).

Subsequently D₂O (50 μl) was added and the NMR spectra recorded.

4.6 References

- (1) Benson, T. E.; Marquardt, J. L.; Marquardt, A. C.; Etzkorn, F. A.; Walsh, C. T. *Biochemistry* **1993**, *32*, 2024–2030.
- (2) Viola, R. E.; Cooch, P. F.; Cleland, W. W. *Anal. Biochem.* **1979**, *96*, 334–340.
- (3) Ottolina, G.; Riva, S.; Carrea, G.; Danieli, B.; Buckmann, A. F. *Biochim. Biophys. Acta* **1989**, *998*, 173–178.
- (4) Bornscheuer, U. T.; Huisman, G. W.; Kazlauskas, R. J.; Lutz, S.; Moore, J. C.; Robins, K. *Nature* **2012**, *485*, 185–194.
- (5) Hollmann, F.; Arends, I. W. C. E.; Buehler, K.; Schallmeyer, A.; Bühler, B. *Green Chem.* **2011**, *13*, 226–265.
- (6) Hollmann, F.; Arends, I. W. C. E.; Holtmann, D. *Green Chem.* **2011**, *13*, 2285–2313.
- (7) Leipold, F.; Hussain, S.; Ghislieri, D.; Turner, N. J. *ChemCatChem* **2013**, *5*, 3505–3508.
- (8) Rodríguez-Mata, M.; Frank, A.; Wells, E.; Leipold, F.; Turner, N. J.; Hart, S.; Turkenburg, J. P.; Grogan, G. *ChemBioChem* **2013**, *14*, 1372–1379.
- (9) Wu, H.; Tian, C.; Song, X.; Liu, C.; Yang, D.; Jiang, Z. *Green Chem.* **2013**, *15*, 1773–1789.
- (10) Paul, C. E.; Arends, I. W. C. E.; Hollmann, F. *ACS Catal.* **2014**, *4*, 788–797.
- (11) Ruppert, R.; Herrmann, S.; Steckhan, E. *Tetrahedron Lett.* **1987**, *28*, 6583–6586.
- (12) Torres, M. De; Dimroth, J.; Arends, I. W. C. E.; Keilitz, J.; Hollmann, F. *Molecules* **2012**, *17*, 9835–9841.
- (13) Köhler, V.; Wilson, Y. M.; Dürrenberger, M.; Ghislieri, D.; Churakova, E.; Quinto, T.; Knörr, L.; Häussinger, D.; Hollmann, F.; Turner, N. J.; Ward, T. R. *Nat. Chem.* **2013**, *5*, 93–9.
- (14) Dürrenberger, M.; Heinisch, T.; Wilson, Y. M.; Rossel, T.; Nogueira, E.; Knörr, L.; Mutschler, A.; Kersten, K.; Zimbron, M. J.; Pierron, J.; Schirmer, T.; Ward, T. R. *Angew. Chem. Int. Ed.* **2011**, *50*, 3026–3029.
- (15) Robles, V. M.; Dürrenberger, M.; Heinisch, T.; Lledó, A.; Schirmer, T.; Ward, T. R.; Maréchal, J.-D. *J. Am. Chem. Soc.* **2014**, *136*, 15676–15683.

- (16) Brecker, L.; Ribbons, D. W. *Trends Biotechnol.* **2000**, *18*, 197–202.
- (17) Morawski, B.; Casy, G.; Illaszewicz, C.; Griengl, H.; Ribbons, D. W. *J. Bacteriol.* **1997**, *179*, 4023–4029.
- (18) Wu, J.; Tang, W.; Pettman, A.; Xiao, J. *Adv. Synth. Catal.* **2013**, *355*, 35–40.
- (19) Wilson, Y. M.; Dürrenberger, M.; Ward, T. R. In *Protein Engineering Handbook*; Lutz, S.; Bornscheuer, U. T., Eds.; Wiley-VCH Verlag GmbH & Co. KGaA, 2013; pp. 215–241.
- (20) Kessler, H.; Oschkinat, H.; Griesinger, C.; Bermel, W. *J. Magn. Reson.* **1986**, *70*, 106–133.
- (21) Bax, A.; Davis, D. G. *J. Magn. Reson.* **1985**, *65*, 355–360.

Chapter 5

Expanding the Chemical Diversity in Artificial Imine Reductases Based on the Biotin-Streptavidin Technology

Tommaso Quinto, Fabian Schwizer, Jeremy M. Zimbron, Albert Morina, Valentin Köhler and Thomas R. Ward

This chapter was published in: *ChemCatChem*, **2014**, *6*, 1010-1014.

DOI 10.1002/cctc.201300825

Reproduced by permission of the John Wiley and Sons

<http://dx.doi.org/10.1002/cctc.201300825>

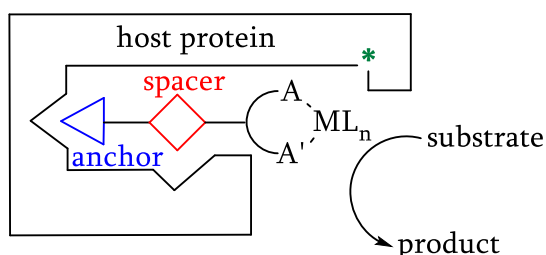
5.1 Abstract

We report on the optimization of an artificial imine reductase based on the biotin-streptavidin technology. With the aim of rapidly generation chemical diversity, a novel strategy for the formation and evaluation of biotinylated complexes is disclosed. Tethering the biotin-anchor to the Cp* moiety leaves three free coordination sites on a d⁶ metal for the introduction of chemical diversity by coordination of a variety of ligands. To test the concept, 34 bidentate ligands were screened and a selection of the 6 best was tested in the presence of 21 streptavidin (Sav) mutants for the asymmetric imine reduction by the resulting three legged piano stool complexes. Enantiopure α -amino amides were identified as promising bidentate ligands: up to 63% *ee* and 190 turnovers were obtained in the formation of 1-phenyl-1,2,3,4-tetrahydroisoquinoline with [biotinCp*Ir(L-ThrNH₂)Cl]⊂SavWT as a catalyst.

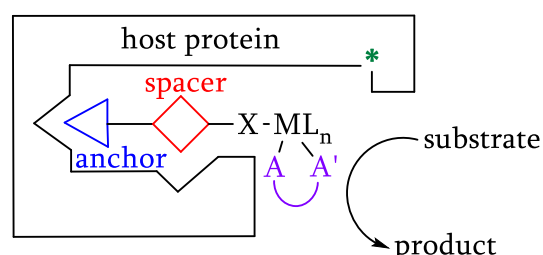
5.2 Introduction

Artificial metalloenzymes result from incorporation of an organometallic catalyst or catalyst precursor within a macromolecular scaffold (protein or oligonucleotide).^[1-19]The resulting hybrid catalyst can be optimized by using either genetic or chemical methods.^[1-8,18-21] In the context of artificial metalloenzymes based on the biotin-streptavidin technology, we and others have relied on synthesizing various biotinylated ligands to provide chemical diversity.^[1-4,15,20,21] To generate larger artificial cofactor libraries quickly, we reasoned that separating the necessary biotin anchor moiety and variable ligand elements would enable us to screen commercially available ligands in the presence of streptavidin (Sav; Scheme 5.1). To test the validity of this strategy, we selected the asymmetric transfer hydrogenation of prochiral imines catalyzed by biotinylated moieties (M = Rh, Ir).

a) Chemical diversity requires synthesis of a library of anchor-spacer-ligands



b) Dissociating the anchor from the variable ligand allows to rely on commercially available ligands to generate chemical diversity



Scheme 5.1 — Artificial metalloenzymes consist of an organometallic catalyst or catalyst precursor incorporated within a protein scaffold. The optimization of their catalytic performance is achieved either by mutating the protein (green star *) or by varying the bidentate ligand (A—A'). **a)** The recognition element (blue triangle Δ) and the variable bidentate ligand are covalently linked. **b)** The recognition element and the bidentate ligand (A—A') are distinct and thus allow to screen readily available ligands.

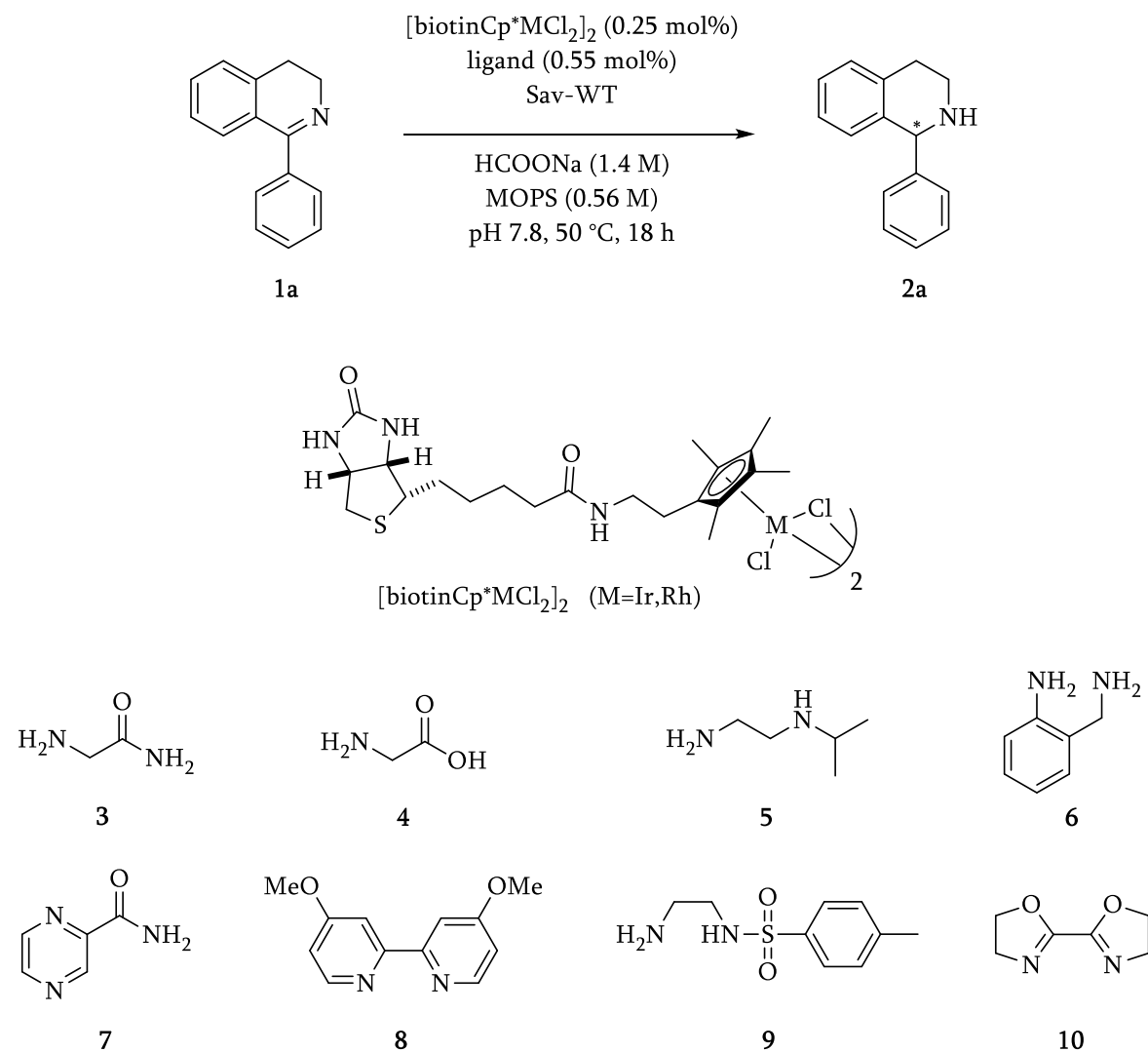
Considering the robustness of the Cp^{*}M moiety,^[22,23] we reasoned that for d⁶ transition metals tethering the biotin anchor to the Cp^{*} unit would leave three free coordination sites around the metal for further functionalization. It is widely accepted that three-legged piano stool complex-catalyzed asymmetric transfer hydrogenation proceeds via an outer sphere hydride transfer mechanism, which requires only one free coordination site around the metal for the reaction to proceed.^[24-27] This reaction is thus ideally suited to test the concept outlined in Scheme 5.1 b.

5.3 Result and Discussion

The synthesis of the biotinylated catalyst precursors [biotinCp^{*}MCl₂]₂ (M = Ir, Rh) is described elsewhere.^[12,19,28,29] The dimeric precursor was reacted *in situ* with a selection of commercially available bidentate ligands (Scheme 5.2). To identify suitable coordination conditions, the chiral ligand L-ProNH₂ was complexed *in situ* with the dinuclear catalyst precursors [biotinCp^{*}MCl₂]₂ (M = Ir, Rh) at different pH values within the buffer range of 3-(*N*-morpholino)propanesulfonic acid (MOPS). As the best

conversion for the asymmetric transfer hydrogenation of prochiral imine **1a** was observed at pH 7.8, this value was selected for all subsequent studies.

A preliminary screen was performed with eight commercially available bidentate ligands using $[\text{biotinCp}^*\text{MCl}_2]_2$ ($\text{M} = \text{Ir}, \text{Rh}$) for the reduction of 1-phenyl-3,4-dihydroisoquinoline **1a** with formate as hydride source. The results are presented in Table 5.1.



Scheme 5.2 — Initial selection of bidentate ligands (**3-10**) for the creation of artificial imine reductases based on the biotin-streptavidin technology.

The following trends emerged from these results:

1. The dinuclear catalyst precursor $[\text{biotinCp}^*\text{IrCl}_2]_2$, devoid of any additional ligands, demonstrates only low detectable artificial transfer hydrogenases

ATHase activity both in the absence and in the presence of Sav, whereas [biotinCp*RhCl₂]₂ displays significant activity only in the absence of Sav (Table 5.1, entry 1).

2. Although most ligands tested afford >60 turnovers (>30% yield) if combined with [biotinCp*RhCl₂]₂, only four ligands give rise to >60 turnovers with [biotinCp*IrCl₂]₂. Notably the widely used amino sulfonamide ligand scaffold (ligand **9**) performs only moderately in comparison to the best ligands under the experimental conditions adopted for this screening. With high throughput screening in mind, no particular effort was made to improve the performance of individual metal-ligand combinations.
3. Incorporation within Sav leads to a significant decrease in conversion in *all but two* metal-ligand combinations. Both glycine amide **3** and bisoxazoline **10** combined with [biotinCp*IrCl₂]₂ afforded more than 180 turnovers for the reduction of cyclic imine **1a**. Owing to the enantiopure environment provided by the Sav host, the corresponding amine **2a** is produced in enantioenriched form: (*S*)-**2a** in 43% *ee* with **3** and (*S*)-**2a** in 14% *ee* with **10** (Table 5.1, entries 2 and 9 with [biotinCp*IrCl₂]₂).

Table 5.1 Identification of the most suitable ligand for activating a biotinylated piano stool catalyst precursor for the reduction of imine **1a**.^(a)

Entry	Ligand	Yield (<i>ee</i>) ^(d) [%]			
		Ir ^(b)		Rh ^(c)	
		No protein	Sav-WT	No protein	Sav-WT
1	—	6 (-1)	3 (38)	81 (0)	5 (-5)
2	3	93 (0)	94 (43)	60 (0)	5 (7)
3	4	8 (-3)	2 (21)	51 (0)	4 (1)
4	5	0 (0)	0 (0)	34 (0)	3 (-1)
5	6	4 (-2)	0 (0)	16 (-1)	3 (-1)
6	7	31 (0)	13 (16)	35 (-1)	3 (-1)
7	8	44 (0)	0 (0)	6 (-1)	2 (-6)
8	9	16 (-1)	6 (13)	36 (0)	3 (1)
9	10	99 (0)	51 (14)	37 (0)	4 (0)

(a) The best results are highlighted in boldface. For full experimental details, see the Supporting information; (b) Metal catalyst precursor = [biotinCp*IrCl₂]₂; (c) Metal catalyst precursor = [biotinCp*RhCl₂]₂; (d) A positive *ee* value refers to the (*S*) enantiomer; a negative value refers to the (*R*) enantiomer of amine **2a**.

After identifying the α -amino amide scaffold as a promising activating ligand^[30-36] in the ATHase assembly for the reduction of imine **1a**, 28 commercially available amino amides were tested in conjunction with [biotinCp*IrCl₂]₂ in the presence of Sav-WT (Figure 5.1 and Table 5.2).

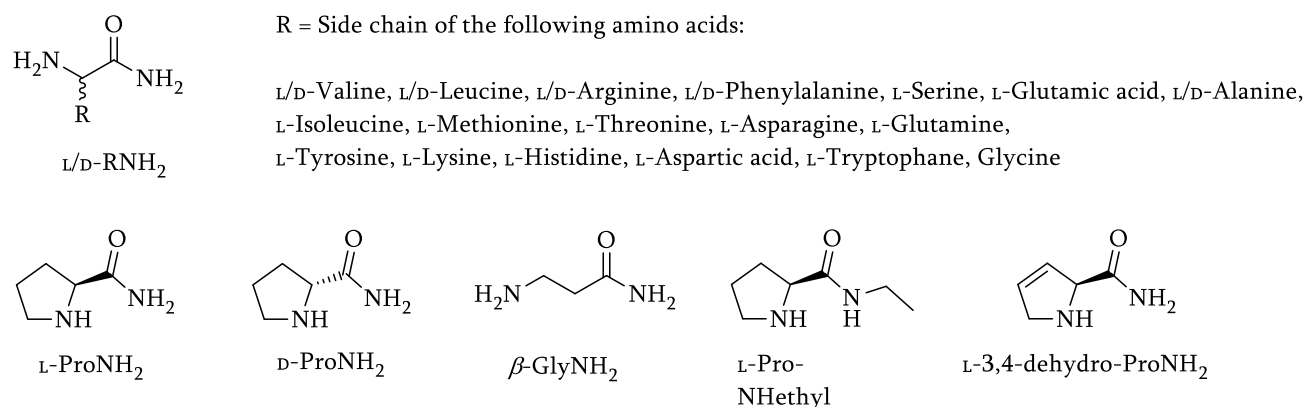


Figure 5.1 — Selection of amino amide ligands screened for the enantioselective reduction of imine **1a**.

The following trends emerge from these results:

1. In the absence of Sav, the enantiopure biotinylated piano stool complexes demonstrate up to 29% *ee* for the reduction of imine **1a**. The distant enantiopure biotin anchor does not significantly affect the enantioselectivity either in the presence of achiral ligands (Table 5.1) or in the presence of mirror-image amino amides. Accordingly (in the absence of Sav) L-PheNH₂ and D-PheNH₂ afford the amine (*S*)-**2a** in 17% *ee* and (*R*)-**2a** in 16% *ee* respectively (Table 5.2, entries 10 and 11).
2. In most of cases, the transfer hydrogenation activities in the absence and in the presence of Sav are comparable. However, incorporation within Sav leads to a significant increase in *ee* value for several combinations (Table 5.2, entries 1, 2, 4, 6, 8, 12, 18 and 20) or to an *inversion* of the preferred product enantiomer (Table 5.2, entries 5, 7, 9 and 17). In general, incorporation in Sav-WT shifts the stereoselectivity in favor of the *S* enantiomer.
3. Upon incorporation within Sav, >60% *ee* of (*S*)-**2a** and ≥170 turnovers are obtained with either L-LeuNH₂, D-ArgNH₂, L-IleNH₂ or L-ThrNH₂ (Table 5.2, entries 6, 9, 18 and 20). The α-amino amides bearing a softer donor side chain (e.g. L-MetNH₂ and L-HisNH₂, Table 5.2, entries 19 and 25) completely inhibit catalysis. We hypothesize that the binding mode of these potentially tridentate ligands may differ from the other amino amide ligands tested.^[34]
4. The absolute configuration of the amino amide has a modest impact on the enantioselectivity of the corresponding artificial metalloenzyme. In the isolated cases tested, the Δ*ee* value for the matched versus mismatched combinations differ by ≤ 20% in the protein (Table 5.2, entries 4 and 5, entries 6 and 7, entries 8 and 9, entries 10 and 11, entries 16 and 17), except in proline (Δ*ee*=75%; entries 2 and 3).

Table 5.2 Screening of different amino amide ligands for the reduction of imine **1a**, employing [biotinCp*IrCl₂]₂ (with or without Sav-WT) as complex precursor.^(a)

Entry	Ligand	Yield (ee) ^(b) [%]	
		no protein	Sav-WT
1	GlyNH ₂	93 (0)	94 (43)
2	L-ProNH ₂	99 (17)	47 (67)
3	D-ProNH ₂	99 (-29)	28 (-8)
4	L-ValNH ₂	99 (20)	70 (63)
5	D-ValNH ₂	99 (-12)	66 (45)
6	L-LeuNH ₂	97 (9)	96 (63)
7	D-LeuNH ₂	99 (-13)	96 (51)
8	L-ArgNH ₂	98 (7)	71 (52)
9	D-ArgNH ₂	71 (-12)	85 (61)
10	L-PheNH ₂	97 (17)	98 (33)
11	D-PheNH ₂	99 (-16)	96 (13)
12	L-SerNH ₂	99 (1)	98 (52)
13	L-GluNH ₂	99 (11)	94 (30)
14	L-Pro-NHethyl	83 (13)	5 (44)
15	L-3,4-dehydro-ProNH ₂	94 (24)	17 (58)
16	L-AlaNH ₂	57 (6)	87 (34)
17	D-AlaNH ₂	56 (-6)	88 (36)
18	L-IleNH ₂	98 (5)	89 (65)
19	L-MetNH ₂	0 (0)	0 (0)
20	L-ThrNH ₂	86 (6)	96 (63)
21	L-AsnNH ₂	85 (12)	91 (56)
22	L-GlnNH ₂	45 (12)	86 (39)
23	L-TyrNH ₂	70 (16)	90 (36)
24	L-LysNH ₂	99 (1)	89 (26)
25	L-HisNH ₂	0 (0)	0 (0)
26	L-AspNH ₂	66 (13)	94 (43)
27	L-TrpNH ₂	65 (20)	95 (37)
28	β-GlyNH ₂	7 (2)	3 (28)

(a) The best results highlighted in boldface. Reaction conditions: 35 mM substrate, 0.25 mol% [biotinCp*IrCl₂]₂, 0.55 mol% amino amide, 7.4 mg/ml Sav-WT, 0.56M MOPS, 1.4M formate, pH 7.8,

incubation for 18 h at 50°C. All listed results are the average of two runs; for full details see the supporting information; **(b)** A positive *ee* refers to the (*S*)-enantiomer, whereas a negative *ee* refers to the (*R*)-enantiomer of amine **2a**.

After identifying promising amino amide ligands, we proceeded to the genetic optimization of the ATHase activity. For this purpose, six amino amide ligands (L-ProNH₂, L-ValNH₂, L-LeuNH₂, L-IleNH₂, L-ThrNH₂ and GlyNH₂) were selected and screened in the presence of 21 Sav mutants for the reduction of cyclic imine **1a**. The corresponding results are presented as a fingerprint in Figure 5.2.

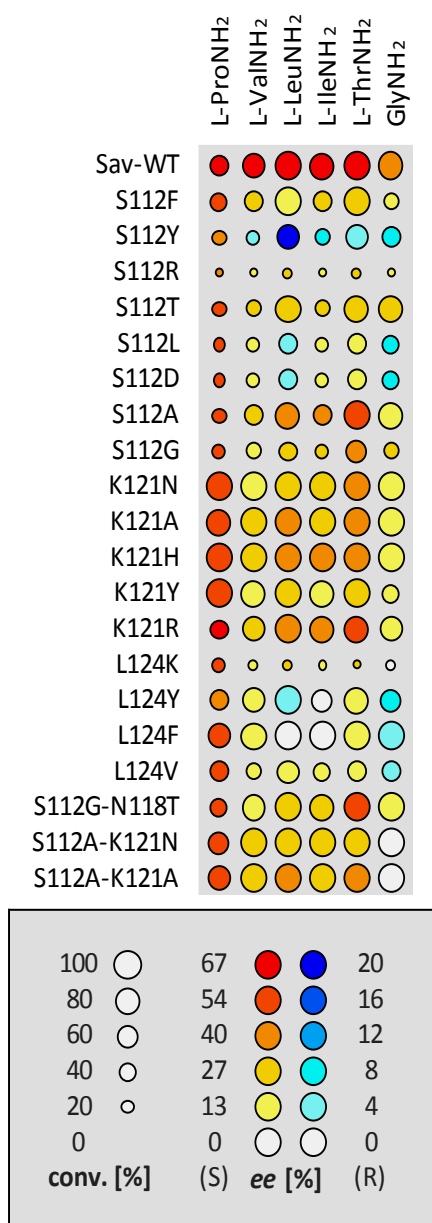


Figure 5.2 — Results of the chemogenetic optimization of ATHases for the asymmetric reduction of imine **1a**, which are presented in bubble-chart format. The size of the bubbles is proportional to the conversion (between 4% and 99%), and the color codes the *ee*. See Table 5.2 for experimental details. The numerical values (conversion, *ee*) are listed in the Table 5.4.

From the results presented in Figure 5.2, the following conclusions could be drawn:

1. The best results in terms of enantioselectivity for any ligand are obtained with Sav-WT.

- Mutating single residues at position S112 or K121, or mutating both residues simultaneously, lead to a decrease in enantioselectivity for all ligands tested. The S112Y mutant led, in combination with L-LeuNH₂, to an inversion of enantioselectivity compared to Sav-WT (63% *ee* of (*S*)-**2a** in Sav-WT and 20% *ee* of (*R*)-**2a** in the presence S112Y).
- All mutants at position K121 typically lead to high conversions with all amino amide ligand tested. In the presence of either L-ProNH₂ or L-ValNH₂, significantly improved conversions compared to Sav-WT were observed with mutants K121N, K121A, K121H and K121Y mutants.
- In the presence of L124K, L124Y or L124F mutant, a marked decrease in enantioselectivity compared with that in the presence of Sav-WT is observed for all ligands except L-ProNH₂. Conversions were generally good to excellent with the L124Y or L124F mutants.
- Good to excellent conversions were observed for all double mutant–ligand combinations, accompanied by a decrease in enantioselectivity (except L-ProNH₂).

Finally, the substrate scope of the artificial imine reductase was evaluated (Figure 5.3).

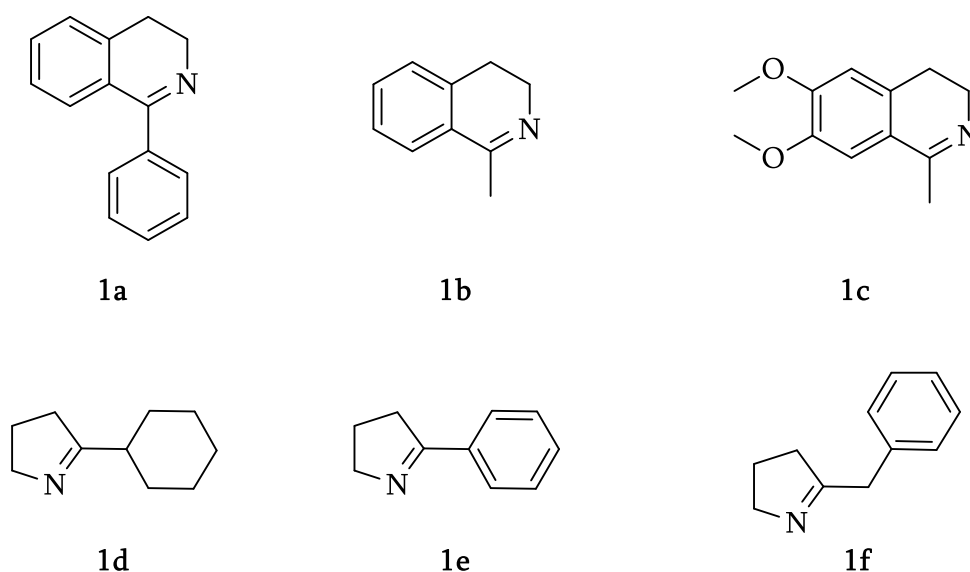


Figure 5.3 — Selection of substrates for the asymmetric transfer hydrogenation of cyclic imines.

For this purpose, six different prochiral cyclic imines were tested in the presence of artificial metalloenzymes [biotinCp*Ir(amino amide)Cl]⊂Sav-WT (amino amide = L-ProNH₂, L-ValNH₂, L-LeuNH₂, L-IleNH₂, L-ThrNH₂, GlyNH₂). The results of this screening are summarized in Table 5.3.

Table 5.3 Screening of different substrates for the [biotinCp*Ir(amino amide)Cl]⊂Sav-WT mediated transfer hydrogenation.

Entry	Ligand	Yield (ee) (a) [%]					
		1a	1b	1c	1d	1e	1f
1	L-ProNH ₂	47 (67)	99 (5)	100 (6)	69 (-32)	60 (-11)	100 (18)
2	L-ValNH ₂	70 (63)	100 (17)	100 (17)	84 (-44)	80 (-22)	86 (16)
3	L-LeuNH ₂	96 (63)	100 (3)	100 (18)	95 (-45)	96 (-31)	100 (20)
4	L-IleNH ₂	89 (65)	100 (20)	100 (43)	83 (-32)	79 (-22)	10 (18)
5	L-ThrNH ₂	96 (63)	100 (25)	100 (41)	98 (-57)	95 (-35)	91 (20)
6	GlyNH ₂	94 (43)	100 (4)	100 (18)	96 (-46)	94 (-9)	79 (2)

(a) A positive value corresponds to the (*S*)-enantiomer, whereas a negative value corresponds to the (*R*)-enantiomer. The absolute configuration of the amines **2d-f** was not determined. The best result are highlighted in bold face.

Variation of the substrate led to the following observations and trends:

1. Conversion of bulky substrate **1a** led generally to the highest observed enantioselectivities in favor of the (*S*) product.
2. Reducing the size of the substituent at position 1 of the dihydroisoquinoline moiety from phenyl to methyl resulted in a considerable decrease in enantioselectivity.
3. Introduction of methoxy substituents at position 6 and 7 of the dihydroisoquinoline moiety only moderately affected the selectivity.
4. With 2-substituted 1-pyrrolines, conversions were generally good to excellent.
5. The highest *ee* value for 1-pyrrolines was observed for the bulky substrate carrying a cyclohexyl substituent in combination with L-ThrNH₂. The *ee* values

for the benzyl- and phenyl-substituted substrates **1e** and **1f**, respectively were generally low.

5.4 Conclusion

To readily access large chemical diversity, a new artificial metalloenzyme design based on the biotin-streptavidin technology has been presented. Relying on three-legged piano stool complexes and tethering the biotin anchor on the Cp* moiety, allows to screen a variety of bidentate ligands for the asymmetric reduction of cyclic imines. An initial screen led to the identification of amino amides as versatile bidentate ligands in conjunction with the {biotinCp*Ir} moiety. Genetic diversity was introduced by site directed mutagenesis. Both chemical diversity and genetic diversity were shown to have a significant effect on the activity and the selectivity of the resulting artificial metalloenzyme.

By taking into account the versatility of the {Cp*ML_n} moiety in catalysis, we reasoned that the strategy disclosed herein will find wide application for the chemical optimization of artificial metalloenzymes. Current efforts are aimed at the structural and kinetic characterization of such hybrid catalysts.

5.5 Experimental Section

General procedure for the asymmetric transfer hydrogenation:

Buffer A (100 μ l; 0.6M in MOPS in Milli-Q H₂O at pH 7.8) was placed in a polypropylene (PP) tube, followed by the addition of the biotinylated metal complex [biotinCp*MCl₂]₂ stock solution (3.75 μ l; 5.0 mM in DMSO) and the ligand stock solution (3.75 μ l, 11 mM in Milli-Q H₂O or DMSO, depending on the ligand). The mixture was agitated for 30 min at 30°C and 600 rpm in a thermo mixer for precomplexation. The corresponding lyophilized Sav mutant (1.6 mg) was dissolved in buffer B (100 μ l, 0.6M in MOPS, 3.0M in HCO₂Na in Milli-Q H₂O at pH 7.8). Then, Sav-mixture (100 μ l) was added to the PP tube containing the metal complex and agitation was continued for 15 min at 30°C and 600 rpm, to ensure binding of the

biotinylated complex to Sav. Finally the substrate stock solution was added (7.5 μ l; 1M in DMSO) and the mixture was agitated at 50°C for 18 h. Subsequently, NaOH_(aq) (60 μ l 5M solution) was added to the reaction mixture, followed by addition of CH₂Cl₂ (1 ml). The phases were mixed thoroughly with a vortex mixer. The organic phase was separated through pipetting and transferred to another PP tube, which contained anhydrous Na₂SO₄. Solids were separated by centrifugation (2 min. at 21'100 *g*) and the supernatant analyzed by using HPLC or GC.

5.5 Supporting Information

General information

All amino acid amide ligands were purchased in their free form (H-L-ProNH₂, H-D-ProNH₂, H-L-PheNH₂, H-D-PheNH₂, H-L-GluNH₂, H-L-AspNH₂, H-L-LeuNH₂, H-D-LeuNH₂) or as their hydrochloride salts (H-L-ValNH₂·HCl, H-D-ValNH₂·HCl, H-L-ArgNH₂·HCl, H-L-ArgNH₂·HCl, H-L-SerNH₂·HCl, H-L-ProNH₂·HCl, H-L-3,4-dehydro-ProNH₂·HCl, H-L-AlaNH₂·HCl, H-D-AlaNH₂·HCl, H-L-IleNH₂·HCl, H-L-MetNH₂·HCl, H-L-ThrNH₂·HCl, H-L-AsnNH₂·HCl, H-L-GlnNH₂·HCl, H-L-TyrNH₂·HCl, H-L-LysNH₂·HCl, H-L-HisNH₂·HCl, H-L-TrpNH₂·HCl) from Bachem and used as received. H-GlyNH₂·HCl was purchased from Fluka. All other bidentate ligands were purchased from Aldrich, Acros and TCI. 3-(*N*-morpholino)propanesulfonic acid (MOPS) was purchased from Alfa Aesar. 1-methyl-3,4-dihydroisquinoline hydrochloride hydrate was purchased from Acros. Racemic standards were prepared by reduction of the corresponding imine or the hydrochloric salt thereof with NaBH₄ in methanol.

Streptavidin (Sav) mutants were expressed, purified and characterized as previously described.^[37] The synthesis of the biotinylated complexes [biotinCp*IrCl₂]₂ and [biotinCp*RhCl₂]₂ is described elsewhere.^[19] Substrate **1a**, **1d**, **1e** and **1f** (Scheme 5.3) were synthesized according to literature procedures.^[38,39]

Reaction mixtures were agitated with a thermo mixer (HLC Biotech Model MHR 23). HPLC measurements were performed on Agilent (or hp) machines equipped with

modules from the 1100 and 1200 series and diode array detectors (if not indicated otherwise). HPLC columns were used with the appropriate guard columns. Column and conditions are indicated for each compound separately. GC measurements were performed on Agilent GCs of the 6890 series equipped with FIDs.

Preparation of stock solutions

Reaction buffer A was prepared by dissolving MOPS (final conc. 0.6 M) in Milli-Q H₂O; the pH was adjusted to 7.8 with aq. 10N NaOH. Reaction buffer B was prepared by dissolving MOPS (final conc. 0.6 M), NaHCO₂ (final conc. 3.0 M) in Milli-Q H₂O; the pH was adjusted to 7.8 with 10N aq. NaOH. The [biotinCp*IrCl₂]₂ and [biotinCp*RhCl₂]₂ stock solutions (5.0 mM) were prepared by dissolving the complexes in appropriate amounts of DMSO. The ligand stock solutions (11 mM) of the amino amides H-L-ProNH₂, H-D-ProNH₂, H-L-LeuNH₂, H-D-LeuNH₂, H-L-PheNH₂, H-D-PheNH₂ and β-GlyNH₂ were prepared by dissolving these compounds in DMSO. All other amino amides were dissolved in Milli-Q H₂O. All non-amino acid amide ligands were dissolved in DMSO to a final concentration of 11 mM. The substrate stock solutions were prepared by placing the corresponding substrate in a volumetric flask (1 ml), followed by addition of DMSO to a final concentration of 1 M.

General procedure for the asymmetric transfer hydrogenation

Complexation:

Buffer A (100 μl) was placed in a 1.5 ml PP-tube, followed by addition of the biotinylated metal complex stock solution (3.75 μl) and the ligand stock solution (3.75 μl). The mixture was agitated for 30 min at 30°C and 600 rpm in a thermo mixer to allow the formation of the complex.

Preparation of ATHase:

The corresponding lyophilized Sav-mutant (1.6 mg for 100 μ l buffer; final concentration in the reaction = 7.4 mg/ml) was dissolved in buffer B (note: three free binding sites (fbs) per tetramer were assumed to ensure the presence of sufficient fbs; the actual number of fbs is usually higher).

After complexation, 100 μ l of the prepared ATHase solution were added to the former PP-tube (containing the prepared metal complex), and agitation was continued for 15 min at 30°C and 600 rpm (to allow the binding of the biotinylated complex to Sav). Finally the substrate stock solution was added (7.5 μ l; final concentration in the reaction = 35 mM) and the mixture was agitated at 50°C for 18 h. Subsequently aq. NaOH (60 μ l of a 5 M solution) was added to the reaction mixture followed by addition of CH₂Cl₂ (1 ml).

The phases were thoroughly mixed by means of a Vortex mixer. The organic phase was separated by pipetting and transferred to another PP-tube, which contained anhydrous Na₂SO₄. Solids were separated by centrifugation (2 min at 21'100 g) and the supernatant analyzed by HPLC or GC.

Substrates 1a and 1b:

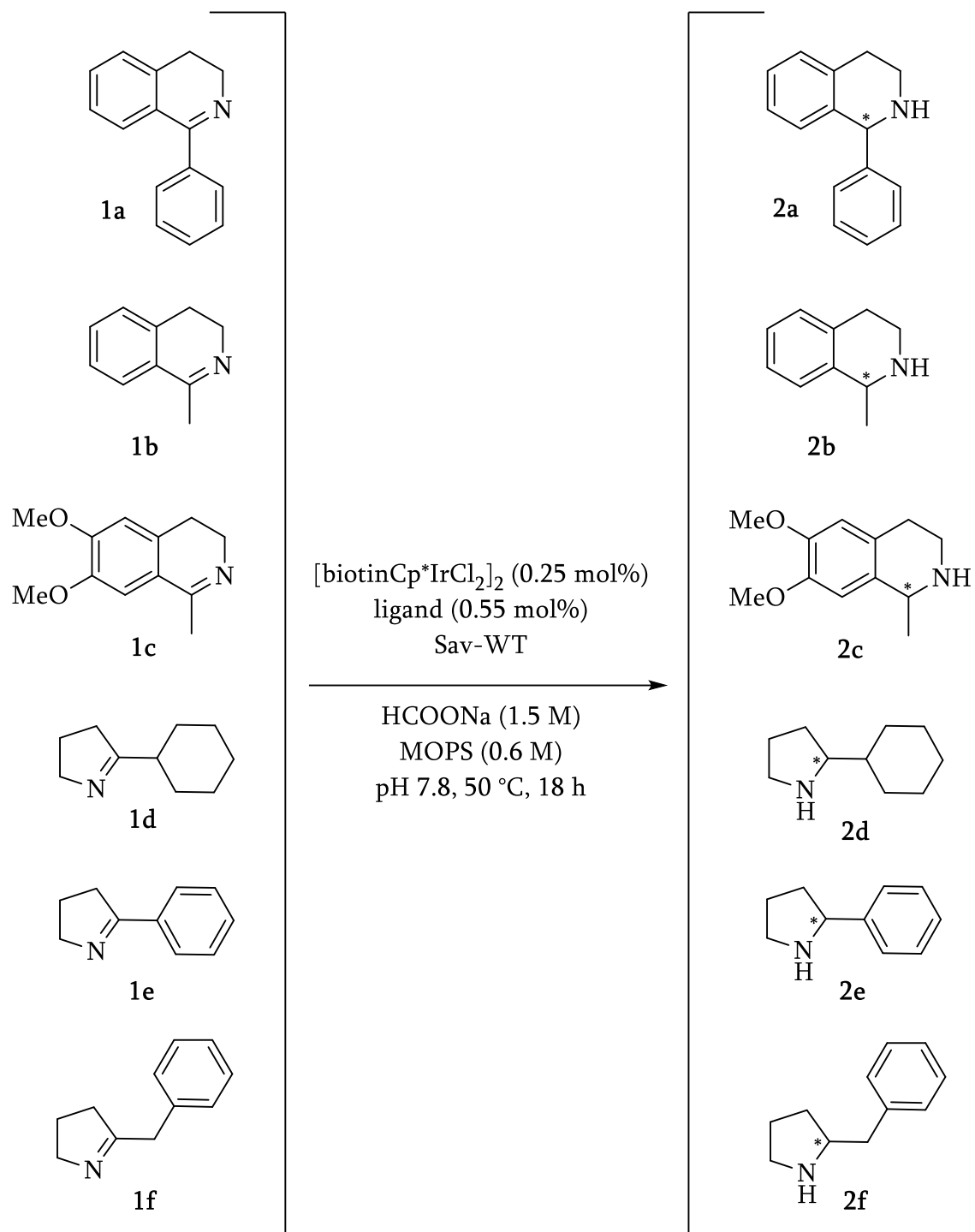
Chiral stationary phase HPLC (chiralpak IC 250 \times 4.6 mm, 5 μ m; hexane/*i*-PrOH/HNEt₂ 97:3:0.06, 1 ml/min, 25°C, detection at 265 nm). Conversion of substrate **1a**: T_{ret} = 7.6 min ((*S*)-**2a**), T_{ret} = 10.5 min ((*R*)-**2a**), T_{ret} = 16.0 min (starting material **1a**). Conversion of substrate **1b**: T_{ret} = 10.6 min ((*S*)-**2b**), T_{ret} = 11.4 min ((*R*)-**2b**), T_{ret} = 17.9 min (starting material **1b**). The absolute configuration of amine **2a** was assigned by comparison with a commercial sample of (*S*)-1-phenyl-1,2,3,4-tetrahydroisoquinoline (Fluorochem). The absolute configuration of amine **2b** was assigned by comparison with literature data.^[40] Conversions for substrates **1a** and **1b** were determined by comparison of the signal area of product and substrate peaks under consideration of the experimentally determined response factors.

Substrate 1c:

Chiral stationary phase HPLC (chiralpak IC 250 × 4.6 mm, 5 μm; CH₂Cl₂/*i*-PrOH/HNEt₂ 98:2:0.1, 1 ml/min, 25°C, detection at 265 nm). Conversion of substrate **1c**: T_{ret} = 5.6 min ((*S*)-**2c**), T_{ret} = 6.1 min ((*R*)-**2c**), T_{ret} = 7.8 min (starting material **1c**). The absolute configuration of amine **2c** was assigned by comparison with literature data.^[20] Conversions for substrate **1c** were determined by comparison of the signal area of product and substrate peaks under consideration of the experimentally determined response factors.

Substrates 1d-f:

For substrates **1d**, **1e** and **1f** the conversion was determined by GC-FID (Agilent J&W CAM, 30 m × 0.32 mm, 0.25 μm; 150 °C isothermal, 1.7 ml He/min; injector: 250°C, split 100; detector: 240°C). Conversion of substrate **1d**: T_{ret} = 3.6 min (amine **2d**), T_{ret} = 3.3 min (imine **1d**). Conversion of substrate **1e**: T_{ret} = 7.72 min (amine **2e**), T_{ret} = 8.7 min (imine **1e**). Conversion of substrate **1f**: T_{ret} = 6.4 min (amine **2f**), T_{ret} = 9.2 min (imine **1f**). For *ee*-determination, products **2d**, **2e** and **2f** were converted to their corresponding trifluoroacetamides. Trifluoroacetic anhydride (TFAA, 200 μl) was added to the GC-samples used for conversion determination and volatiles were removed to near dryness in a gentle stream of N₂. The residue was dissolved in a small amount of CH₂Cl₂ (30-100 μl) and analyzed by GC-FID on a chiral stationary phase (Agilent CP-Chirasil-DEX CB, 25 m × 0.25 mm, 0.25 μm; 140°C isothermal, 1.7 ml He/min; injector: 300°C, split 100; detector: 275°C). Product **2d**: T₁ = 9.6 min, T₂ = 9.9 min; Product **2e**: T₁ = 10.7 min, T₂ = 11.0 min; Product **2f**: T₁ = 16.4 min, T₂ = 17.0 min. The absolute configuration of products **2d-f** was not determined.



Scheme 5.3 — List of all substrates screened and the corresponding reduced products (standard conditions).

Table 5.4 Results of the chemogenetic optimization of ATHase for the asymmetric reduction of imine **1a**.^(a)

entry	mutant	L-ProNH ₂		L-ValNH ₂		L-LeuNH ₂		L-IleNH ₂		L-ThrNH ₂		GlyNH ₂	
		conv	ee ^(b)	conv	ee ^(b)	conv	ee ^(b)	conv	ee ^(b)	conv	ee ^(b)	conv	ee ^(b)
		[%]	[%]	[%]	[%]	[%]	[%]	[%]	[%]	[%]	[%]	[%]	[%]
1	Sav-WT	47	67	70	63	96	63	89	65	96	63	94	43
2	S112F	41	60	47	28	96	14	54	33	96	23	34	10
3	S112Y	28	46	24	-3	68	-20	34	-7	69	-6	48	-7
4	S112R	9	45	8	20	14	21	9	20	13	31	8	11
5	S112T	29	58	32	22	91	26	31	30	86	29	93	25
6	S112L	21	50	27	14	52	-6	25	13	52	11	40	-7
7	S112D	21	50	27	14	52	-6	25	13	52	11	40	-7
8	S112A	27	57	52	30	84	36	53	35	97	54	89	13
9	S112G	26	54	34	16	46	33	23	24	55	39	30	22
10	K121N	97	60	97	15	99	25	99	30	98	41	99	14
11	K121A	86	58	97	25	99	39	97	29	97	40	98	15
12	K121H	95	59	97	22	99	38	98	34	97	34	98	11
13	K121Y	97	59	89	13	98	25	89	20	94	31	42	13
14	K121R	44	61	72	27	96	40	82	36	93	51	76	17
15	L124K	26	53	13	15	13	21	10	17	9	21	10	0
16	L124Y	53	45	75	8	95	-3	59	3	87	9	58	-10
17	L124F	70	58	91	7	98	4	94	4	97	15	97	-5
18	L124V	50	52	32	13	67	16	38	20	50	13	48	-6
19	S112G-N118T	42	60	79	18	97	27	91	27	97	49	97	18
20	S112A-K121N	61	53	95	22	98	25	97	29	99	25	97	-2
21	S112A-K121A	68	59	95	23	97	35	95	28	97	35	95	1

(a) See Table 5.2 for experimental details. (b) A positive value corresponds to the (*S*)-enantiomer, whereas a negative value corresponds to the (*R*)-enantiomer of amine **2a**.

5.6 References

- (1) Wilson, M. E.; Whitesides, G. M. *J. Am. Chem. Soc.* **1978**, *100*, 306–307.
- (2) Rosati, F.; Roelfes, G. *ChemCatChem* **2010**, *2*, 916–927.
- (3) Zastrow, M. L.; Pecoraro, V. L. *Coord. Chem. Rev.* **2013**, *257*, 2565–2588.
- (4) Ward, T. R. *Acc. Chem. Res.* **2011**, *44*, 47–57.
- (5) Lu, Y.; Yeung, N.; Sieracki, N.; Marshall, N. M. *Nature* **2009**, *460*, 855–862.
- (6) Ueno, T.; Tabe, H.; Tanaka, Y. *Chem. Asian J.* **2013**, *8*, 1646–1660.
- (7) Deuss, P. J.; den Heeten, R.; Laan, W.; Kamer, P. C. J. *Chem. Eur. J.* **2011**, *17*, 4680–4698.
- (8) In *Coordination Chemistry in Protein Cages: Principles, Design and Applications*; Ueno, T.; Watanabe, Y., Eds.; Wiley: Hoboken, 2013.
- (9) Chevalley, A.; Salmann, M. *Chem. Comm.* **2012**, *48*, 11984–11986.
- (10) Podtetenieff, J.; Taglieber, A.; Bill, E.; Reijerse, E. J.; Reetz, M. T. *Angew. Chem. Int. Ed.* **2010**, *49*, 5151–5155.
- (11) Fujieda, N.; Hasegawa, A.; Ishihama, K.; Itoh, S. *Chem. Asian J.* **2012**, *7*, 1203–1207.
- (12) Reiner, T.; Jantke, D.; Marziale, A. N.; Raba, A.; Eppinger, J. *ChemistryOpen* **2013**, *2*, 50–54.
- (13) Esmieu, C.; Cherrier, M. V.; Amara, P.; Girgenti, E.; Marchi-Delapierre, C.; Oddon, F.; Iannello, M.; Jorge-Robin, A.; Cavazza, C.; Ménage, S. *Angew. Chem. Int. Ed.* **2013**, *52*, 3922–3925.

- (14) Onoda, A.; Fukumoto, K.; Arlt, M.; Bocola, M.; Schwaneberg, U.; Hayashi, T. *Chem. Comm.* **2012**, *48*, 9756–9758.
- (15) Lin, C.; Lin, C.; Chan, A. S. C. *Tetrahedron: Asymmetry* **1999**, *10*, 1887–1893.
- (16) Mayer, C.; Gillingham, D. G.; Ward, T. R.; Hilvert, D. *Chem. Commun.* **2011**, *47*, 12068–12070.
- (17) Allard, M.; Dupont, C.; Muñoz Robles, V.; Doucet, N.; Lledós, A.; Maréchal, J.-D.; Urvoas, A.; Mahy, J.-P.; Ricoux, R. *Chembiochem* **2012**, *13*, 240–251.
- (18) Hyster, T. K.; Knörr, L.; Ward, T. R.; Rovis, T. *Science* **2012**, *338*, 500–503.
- (19) Zimbron, J. M.; Heinisch, T.; Schmid, M.; Hamels, D.; Nogueira, E. S.; Schirmer, T.; Ward, T. R. *J. Am. Chem. Soc.* **2013**, *135*, 5384–5388.
- (20) Dürrenberger, M.; Heinisch, T.; Wilson, Y. M.; Rossel, T.; Nogueira, E.; Knörr, L.; Mutschler, A.; Kersten, K.; Zimbron, M. J.; Pierron, J.; Schirmer, T.; Ward, T. R. *Angew. Chem. Int. Ed.* **2011**, *50*, 3026–3029.
- (21) Reetz, M. T.; Peyralans, J. J.-P.; Maichele, A.; Fu, Y.; Maywald, M. *Chem. Commun.* **2006**, 4318–4320.
- (22) Wu, X.; Li, X.; Zanotti-Gerosa, A.; Pettman, A.; Liu, J.; Mills, A. J.; Xiao, J. *Chem. Eur. J.* **2008**, *14*, 2209–2222.
- (23) Wu, X.; Xiao, J. In *Metal-Catalyzed Reactions in Water*; Dixneuf, P. H.; Cadierno, V., Eds.; WILEY-VCH: Weinheim, 2013; pp. 173–242.
- (24) Martins, J. E. D.; Clarkson, G. J.; Wills, M. *Org. Lett.* **2009**, *11*, 847–850.
- (25) Palmer, M. J.; Wills, M. *Tetrahedron: Asymmetry* **1999**, *10*, 2045–2061.

- (26) Clapham, S. E.; Hadzovic, A.; Morris, R. H. *Coord. Chem. Rev.* **2004**, *248*, 2201–2237.
- (27) Haack, K.-J.; Hashiguchi, S.; Fujii, A.; Ikariya, T.; Noyori, R. *Angew. Chem. Int. Ed. Engl.* **1997**, *36*, 285–288.
- (28) Reiner, T.; Jantke, D.; Raba, A.; Marziale, A. N.; Eppinger, J. *J. Organomet. Chem.* **2009**, *694*, 1934–1937.
- (29) Leusen, D. Van; Beetstra, D. J.; Hessen, B.; Teuben, J. H. *Organometallics* **2000**, *19*, 4084–4089.
- (30) Verzijl, G. K. M.; De Vries, J. G.; Broxterman, Q. B. WO0190396A1 **2001**.
- (31) Sheldrick, W. S.; Heeb, S. *J. Organomet. Chem.* **1989**, *377*, 357–366.
- (32) Pelagatti, P.; Carcelli, M.; Calbiani, F.; Cassi, C.; Elviri, L.; Pelizzi, C.; Rizzotti, U.; Rogolino, D. *Organometallics* **2005**, *24*, 5836–5844.
- (33) Pelagatti, P.; Bacchi, A.; Calbiani, F.; Carcelli, M.; Elviri, L.; Pelizzi, C.; Rogolino, D. *J. Organomet. Chem.* **2005**, *690*, 4602–4610.
- (34) Severin, K.; Bergs, R.; Beck, W. *Angew. Chemie, Int. Ed.* **1998**, *37*, 1634–1654.
- (35) Ahlford, K.; Ekström, J.; Zaitsev, A. B.; Ryberg, P.; Eriksson, L.; Adolfsson, H. *Chem. Eur. J.* **2009**, *15*, 11197–11209.
- (36) Mayer, C.; Hilvert, D. *European J. Org. Chem.* **2013**, 3427–3431.
- (37) Humbert, N.; Zocchi, A.; Ward, T. R. *Electrophoresis* **2005**, *26*, 47–52.
- (38) I. Iantos, D. Bhattacharjee, D. S. E. *J. Org. Chem.* **1986**, *51*, 4147–4150.
- (39) Starr, D. F.; Bulbrook, H.; Xixon, R. M. *J. Am. Chem. Soc.* **1932**, *54*, 3971–3976.

- (40) Köhler, V.; Wilson, Y. M.; Dürrenberger, M.; Ghislieri, D.; Churakova, E.; Quinto, T.; Knörr, L.; Häussinger, D.; Hollmann, F.; Turner, N. J.; Ward, T. R. *Nat. Chem.* **2013**, *5*, 93–99.

Chapter 6

Conclusion and outlook

The subject of this work was the creation of artificial metalloenzymes as a promising approach to combine the favourable aspects of biocatalysis and homogeneous catalysis. Based on the biotin/(strept)avidin technology and Cp*Ir and Cp*Rh derived organometallic moieties, ATHases (Artificial Transfer Hydrogenases) were generated. With the ultimate goal of performing efficient *in vivo* catalysis, potential interactions between the catalyst and the biological environment were considered.

Biotransformation often requires cofactor regeneration, which is performed by a second enzyme. The development of alternative non-enzymatic NADH regeneration methods is still an active field of research. In the chemical method for NADH regeneration, the mutual inhibition between the organometallic catalyst and the natural enzymes is a common issue. We observed that [Cp*Ir(biot-*p*-L)Cl] is a better catalyst (TOF 4.6 min⁻¹) compared to [Cp*Rh(bipy)H₂O]²⁺ (TOF 0.27 min⁻¹) in terms of activity for NADH regeneration. To overcome the mutual inhibition challenge, we incorporated the organometallic catalyst [Cp*Ir(biot-*p*-L)Cl] into streptavidin (Sav) to create an artificial transfer hydrogenase (ATHase).

The resulting ATHase showed a TOF higher than [Cp*Rh(bipy)H₂O]²⁺, and was successfully coupled with HbpA to convert 2-phenylphenol to phenylcatechol. Only the desired product was generated in the presence of Sav, while in the absence of Sav-shielding, less than 5% of product was formed. The presence of Sav efficiently shielded the iridium complex from interaction with HbpA and subsequent mutual inhibition, demonstrating the applicability of concurrent cascade reactions. The concurrent reaction could also be carried out under biphasic conditions, illustrating the versatility of the ATHase in terms of reaction conditions.

Further studies should address the optimization of the ratio ATHase/HbpA to improve the reaction rates, as well as the dependence of the NADH regeneration system on the formate concentration. The immobilization of the entire enzyme cascade or the coupling of the ATHase for NADH regeneration with different redox NADH dependent enzymes should be investigated to demonstrate the general applicability of the regeneration system.

The diastereoselectivity of NAD⁺-reduction at the C4-position was also investigated. In the absence of Sav, 38% *d.e.* was observed, due to substrate control (NAD⁺). However in the presence of mutants S112K and S112A, diastereomeric excesses of 90% and 87%, respectively, were obtained for the (*R*)-diastereomer. Additional work should be carried out to design and identify mutants, which will provide the opposite enantiomer for the reduction of NAD⁺, and allow to gain mechanistic information for the corresponding ATHase.

The scope and potential of ATHases were investigated further. Taking into account the stability of three legged piano stool complexes based on IrCp* and RhCp*, the biotin anchor was tethered to the Cp* moiety, leaving three free coordination sites for screening various bidentate ligands. This methodology enabled the rapid generation of a large library of artificial cofactors, and led to the identification of α -amino amides as functional bidentate ligands in combination with the [biotinCp*IrCl₂]₂ for transfer hydrogenation. A range of 28 commercial available α -amino amides was screened, and the best six were combined with 21 streptavidin variants. Up to 63% *ee* and 96% yield (190 TON) were obtained in the presence of [biotinCp*Ir(L-ThrNH₂)CL]₂-SavWT. These findings demonstrate that both chemical- and genetic diversity have significant effect on the activity and selectivity in the reduction of cyclic imines. Screening of a wider library of mutants will aim to improve the selectivity of the reaction, and the characterization of this novel hybrid catalyst will allow a better understanding of its mechanism.

These studies revealed the potential and versatility of the created artificial transfer hydrogenases for different reactions in terms of activity and selectivity. Further

investigation will aim at structural, mechanistic and kinetic characterization of the created ATHases to better understand their operational mode, and expand their application by combining them with natural enzymes for biotechnological purposes.

Tommaso Quinto

Gasstrasse 37, 4056 Basel, Switzerland

Tel. +41 78 725 40 56 (CH)

+39 333 94 70 615 (IT)

e-mail: tomquinto@yahoo.it

Linkedin: <https://ch.linkedin.com/pub/tommaso-quinto/37/483/366>

Profile

Organometallic and bioinorganic chemist, well organized and detail-oriented, with experience in interdisciplinary research and working environment. I'm interested in career opportunities in a fast-paced environment with high-potential for a personal and professional growth, where I can apply and develop my skills.

Professional experience

- Apr. 2014 **Traineeship**
Dec. 2014 Syngenta, Stein, Basel — Switzerland
Multistep organic synthesis of different classes of compounds (aromatic ether, amine, acid, spiro compound) up to 50 gr scale, as potential fungicides.
Advisor: Dr. Martin Pouliot
- Jul. 2012 **Traineeship**
Sep. 2012 Dr Reddy's Chiretech Technology Limited, Cambridge — United Kingdom
(Marie Curie, BIOTRAINS, grant travel)
Stereoselective reduction of ketone as precursor of relevant pharmacological substrates, employing the artificial metalloenzyme technology with high-throughput screening (HTS).
Advisor: Dr. Richard Lloyd
- Aug. 2011 **Traineeship**
Sep. 2011 TU Delft, University of Technology, Delft — Netherlands
(Marie Curie, BIOTRAINS, grant travel)
Employing artificial metalloenzymes technology for NADH regeneration in enzymatic cascade reactions.
Advisor: Dr. Frank Hollmann
- Jun. 2010 **Traineeship**
Two weeks University of Graz, Graz — Austria
(Marie Curie, BIOTRAINS, grant travel)
Synthesis of biotinylated catalysts for enantioselective imine and ketone reduction.
Advisor: Prof. Dr. Wolfgang Kroutil

Education

- Oct. 2009 **Ph.D. in Chemistry**
May 2015 University of Basel – Switzerland
(Marie-Curie Fellowship, BIOTRAINS ITN-238531)
“Artificial Transfer Hydrogenases based on Biotin Streptavidin Technology”
Advisor: Prof. Dr. Thomas R. Ward
- Oct. 2006 **MSc. in Advanced chemical Methodologies**
Mar. 2009 University of Bologna – Italy
“New intramolecular Au-Catalysed Friedel-Craft reactions of indoles with alcohols”
Advisor: Prof. Dr. Achille U. Ronchi
- Sep. 2001 **BSc. In Chemistry**
Jul. 2006 University of Bologna – Italy
“Synthesis of new chiral heterogeneous catalyst and their use in the stereocontrol of organic transformations”
Advisor: Dr. Marco Bandini

Soft Skills

Languages — ITALIAN, native speaker. ENGLISH, proficient. GERMAN, beginner (A2 level)

Informatics — MS Office, Chemdraw, Graph-Pad Prism, Mendeley, Scifinder, Reaxys.

Communications — teaching assistant and coordinator (analytical and organometallic chemistry). Expertise in presenting challenging scientific concept and results to general audience including international conferences. Proficient at generating scientific reports.

Initiative — Organisation of an International conference “Marie Curie ITN Biotrains” for 20 international students, their PI’s and ten representative from renewed pharmaceutical and chemical companies

Technical Skills

Organic and organometallic chemistry, homogeneous and heterogeneous catalysis, organic synthesis, protein chemistry, Schlenk line technique, high throughput screening (HTS), NMR and IR spectroscopy, HPLC, ESI-MS, glove box usage for synthesis and handling of sensible compounds.

Conferences — Oral presentations

Biotrains Meeting, Copenhagen, (DK)	19 Sep. 2012
Biotrains Meeting, York, (UK)	07 Feb. 2012
Frontiers in White Biotechnology, Delft (NL)	20 Jun. 2011
Biotrains Meeting, Basel, (CH)	04 Dec. 2010
Biocatalysis for Chemical Synthesis, Graz (A)	20 Mar. 2010

Publications

Quinto, T., Häussinger, D., Köhler, V., Ward, T. R., *Org. & Biomol. Chem.* **2015**, *13*, 357-360.
Quinto, T., Schwizer, F., Zimbron, J. M., Morina A., Köhler V., Ward, T. R., *ChemCatChem.* **2014**, *6*, 1010-1014.
Quinto, T., Köhler, V., Ward, T. R., *Topic & Catal.*, **2014**, *57*, 321-331.
Köhler, V., Wilson, Y. M., Dürrenberger, M., Ghislieri, D., Churakova, E., Quinto, T., Knörr, L., Häussinger, D., Hollmann, F., Turner, N. J., Ward, T. R., *Nat. Chem.*, **2013**, *5*, 93–99.
Bandini, M., Eichholzer, A., Gualandi, A., Quinto, T., Savoia, D., *ChemCatChem.*, **2010**, *2*, 661–665.
Bandini, M., Benaglia, M., Quinto, T., Tommasi, S., Umani-Ronchi, A., *Adv. Synth. Cat.*, **2006**, *348*, 1521–1527.

Personal Interests

Travelling, language and foreign culture, cycling, cooking, reading, agriculture, football, volunteer.

References

Academics:

Prof. Dr. Thomas R. Ward (Thomas.ward@unibas.ch)

Dr. Frank Hollmann (F.Hollman@tudelft.nl)

Industry:

Dr. Chris Cobley (ccobley@drreddys.com)

Dr. Richard Lloyd (rlloyd@drreddys.com)

Dr. Martin Pouliot (Martin.Pouliot@Syngenta.com)

Appendices

Figure S1: ^1H with water suppression of NADH

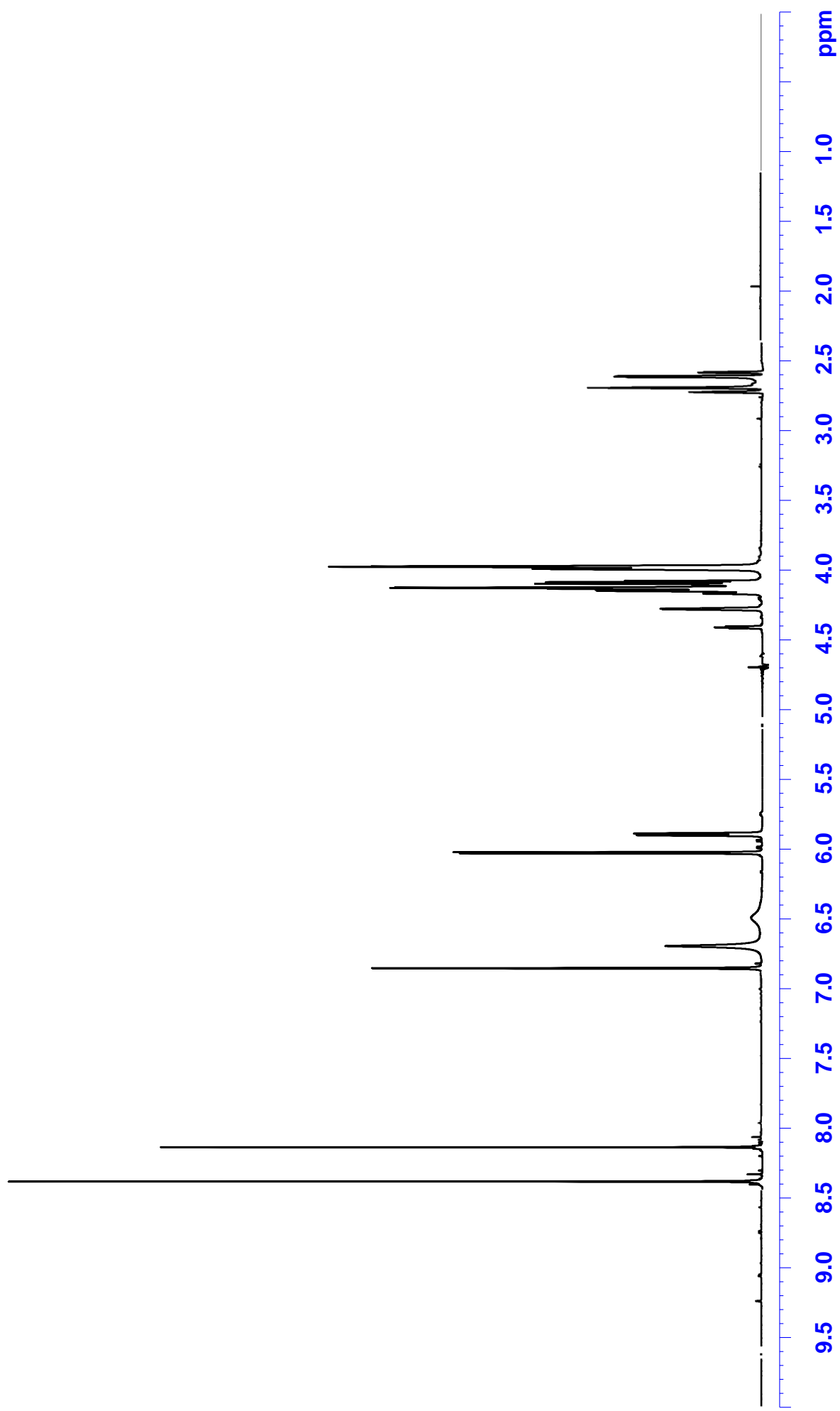


Figure S2: ^1H with water suppression of NAD^2H from the reaction involving Sav-S112A

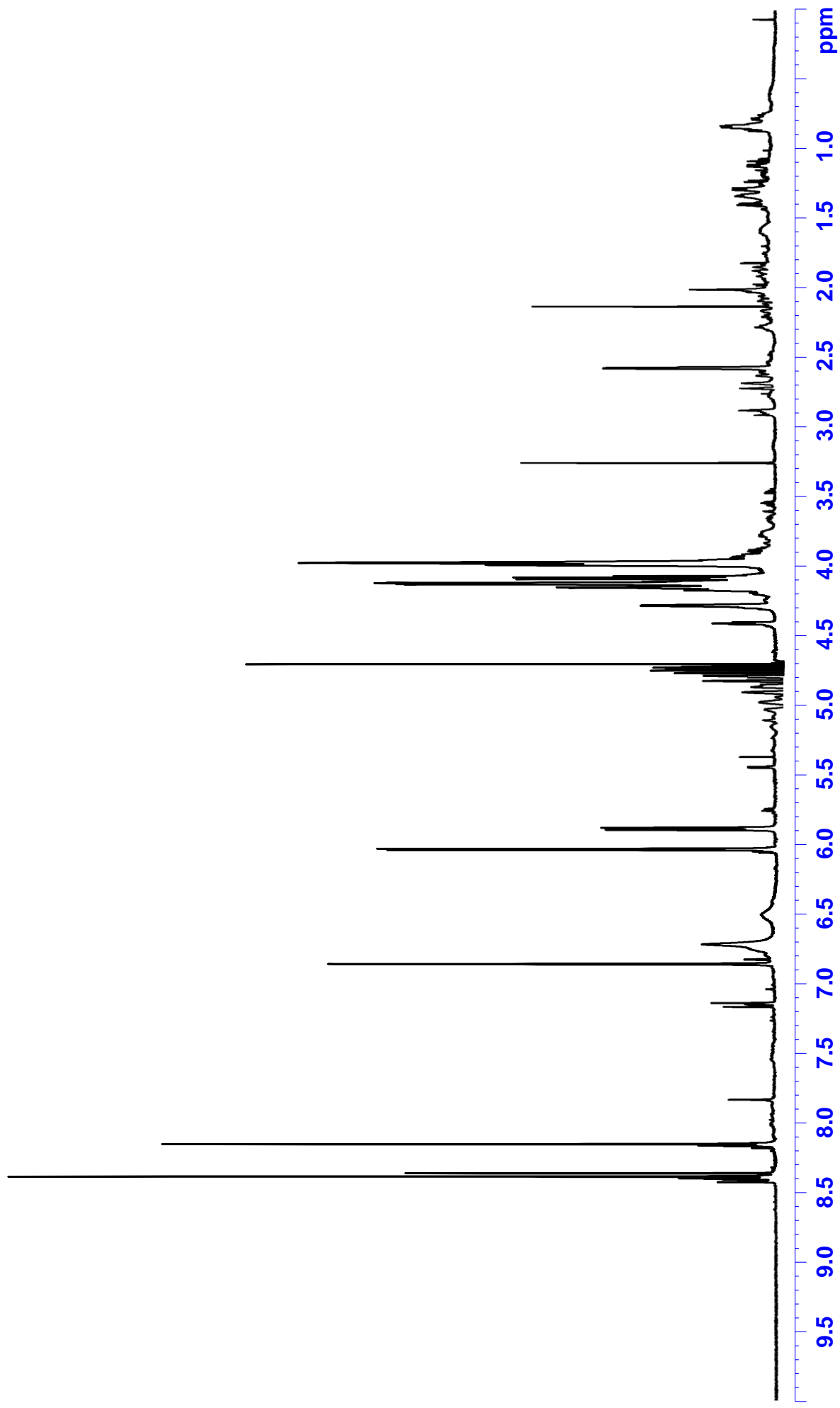


Figure S3: ^1H with water suppression of NAD^2H from the reaction involving Sav-S112K

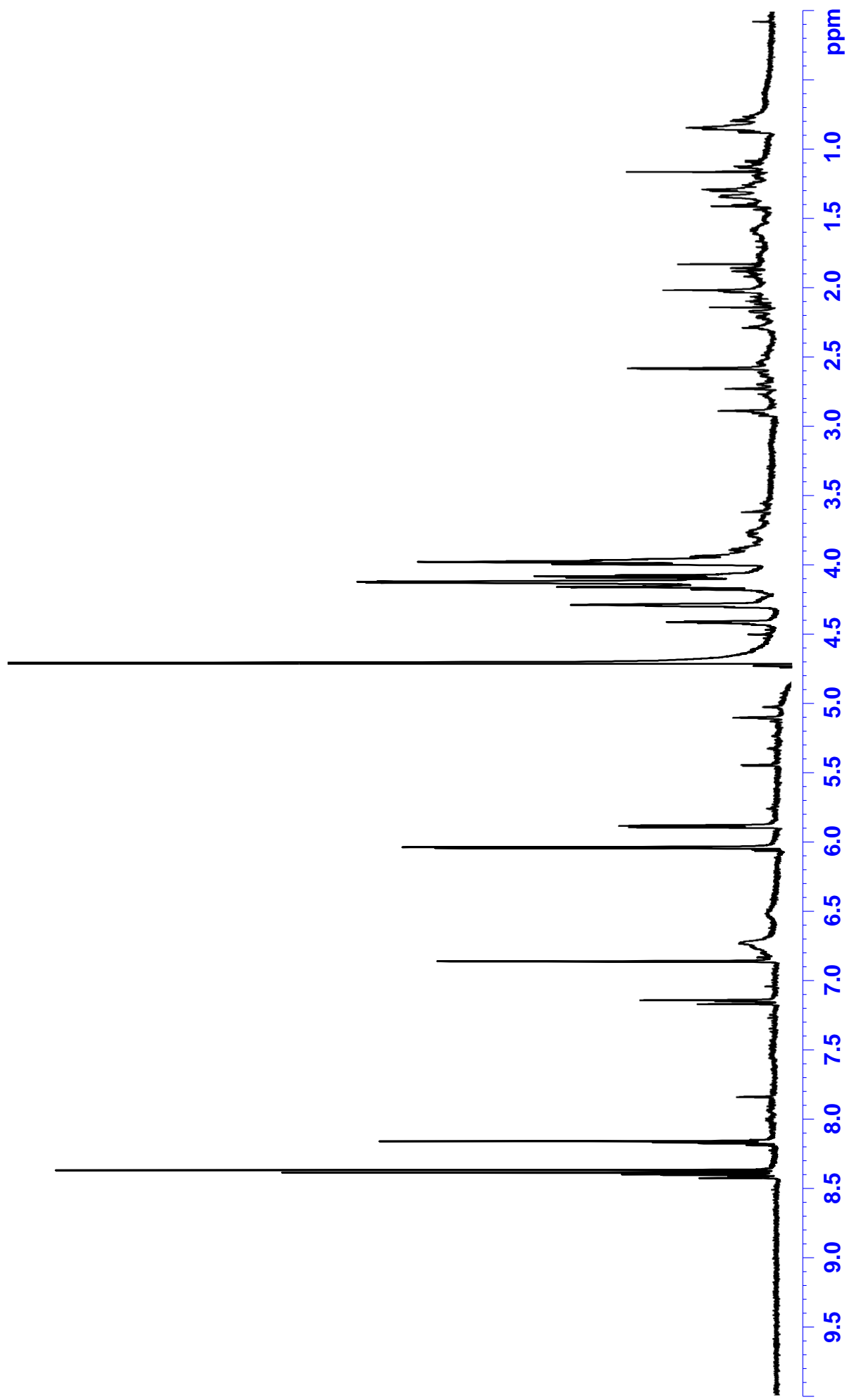


Figure S4: ^1H with water suppression of NAD^2H from the reaction without Sav

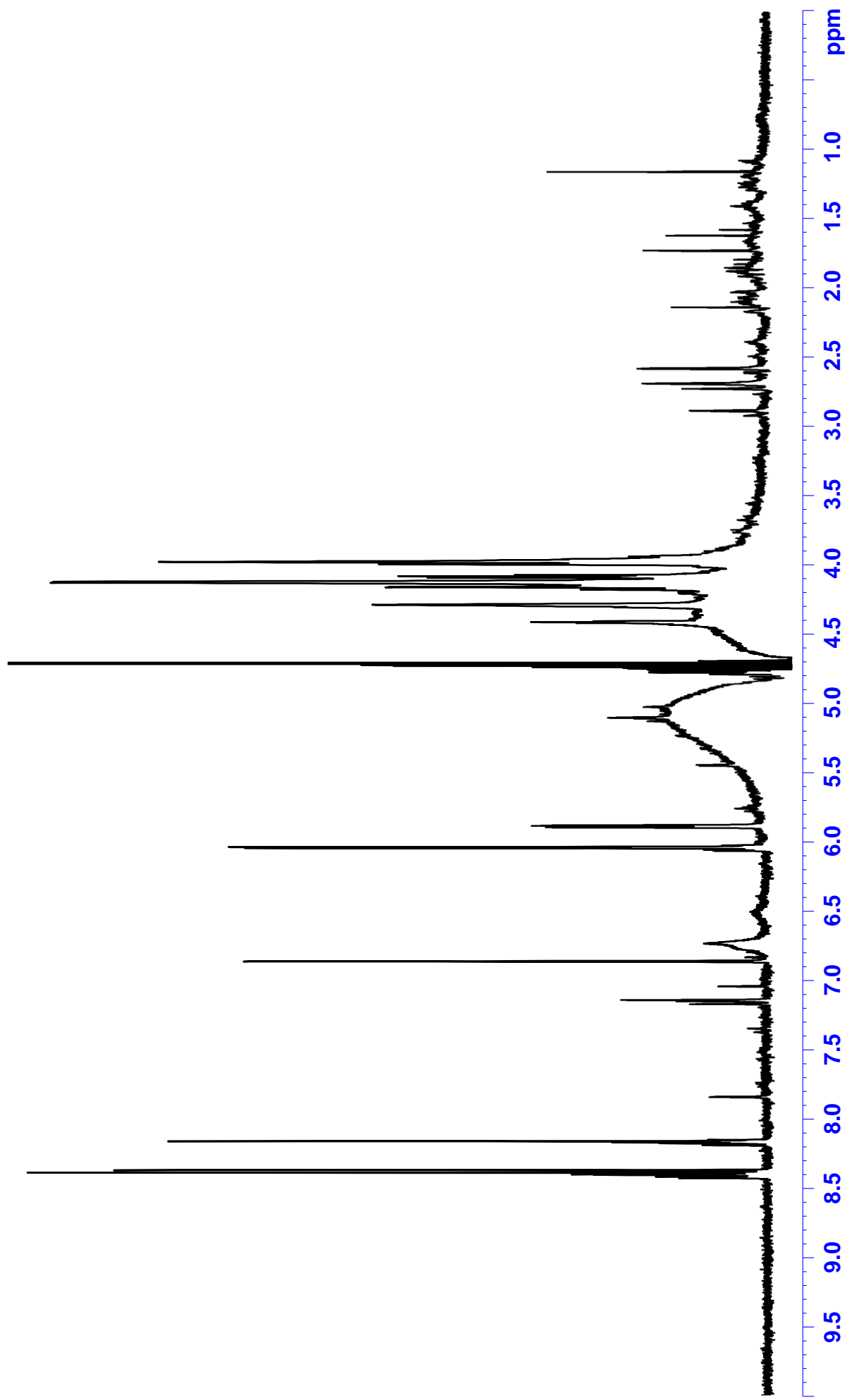


Figure S5: Selective tocsy of NADH

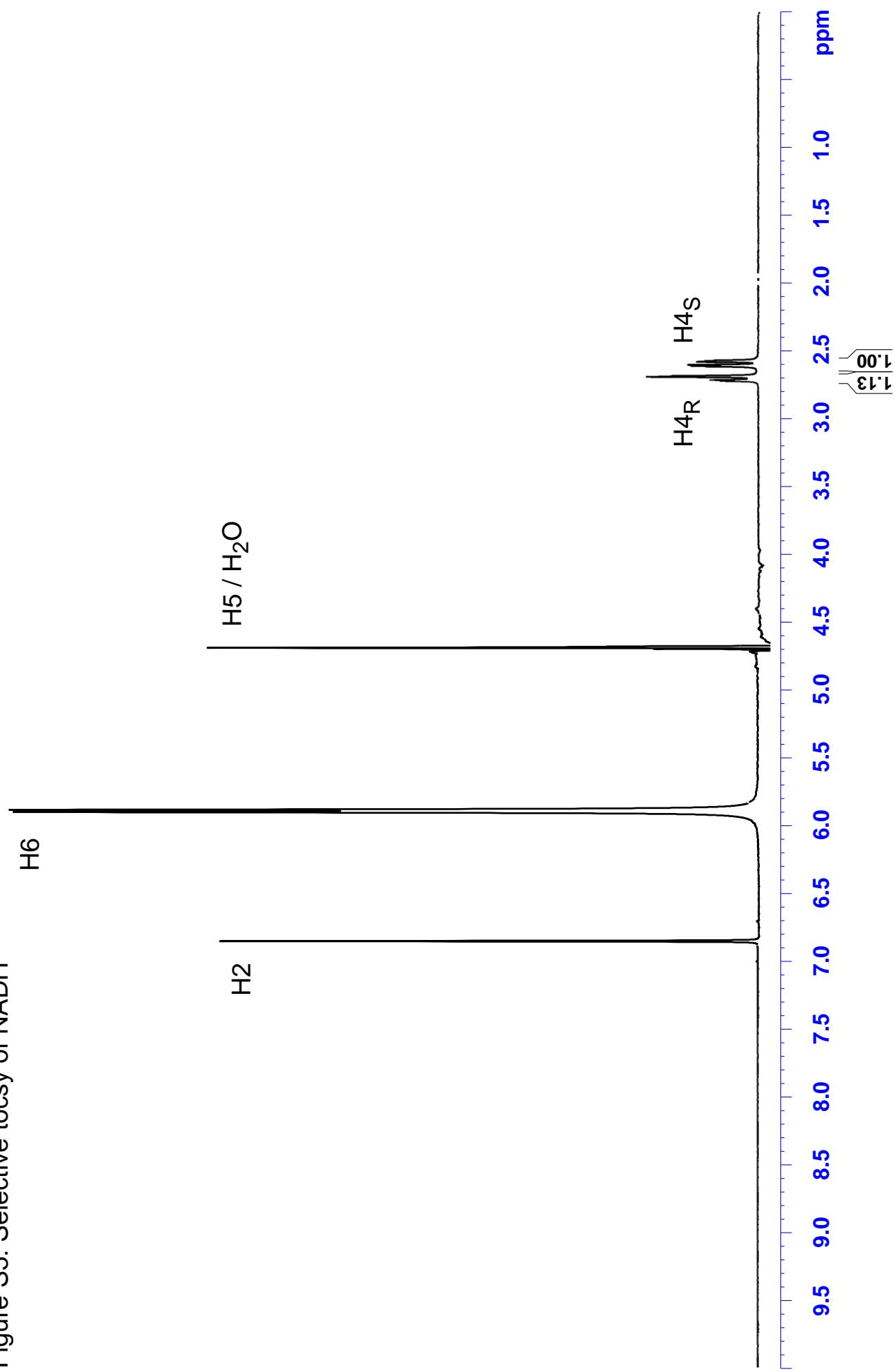


Figure S6: Selective tocsy of NAD²H from the reaction involving Sav-S112A

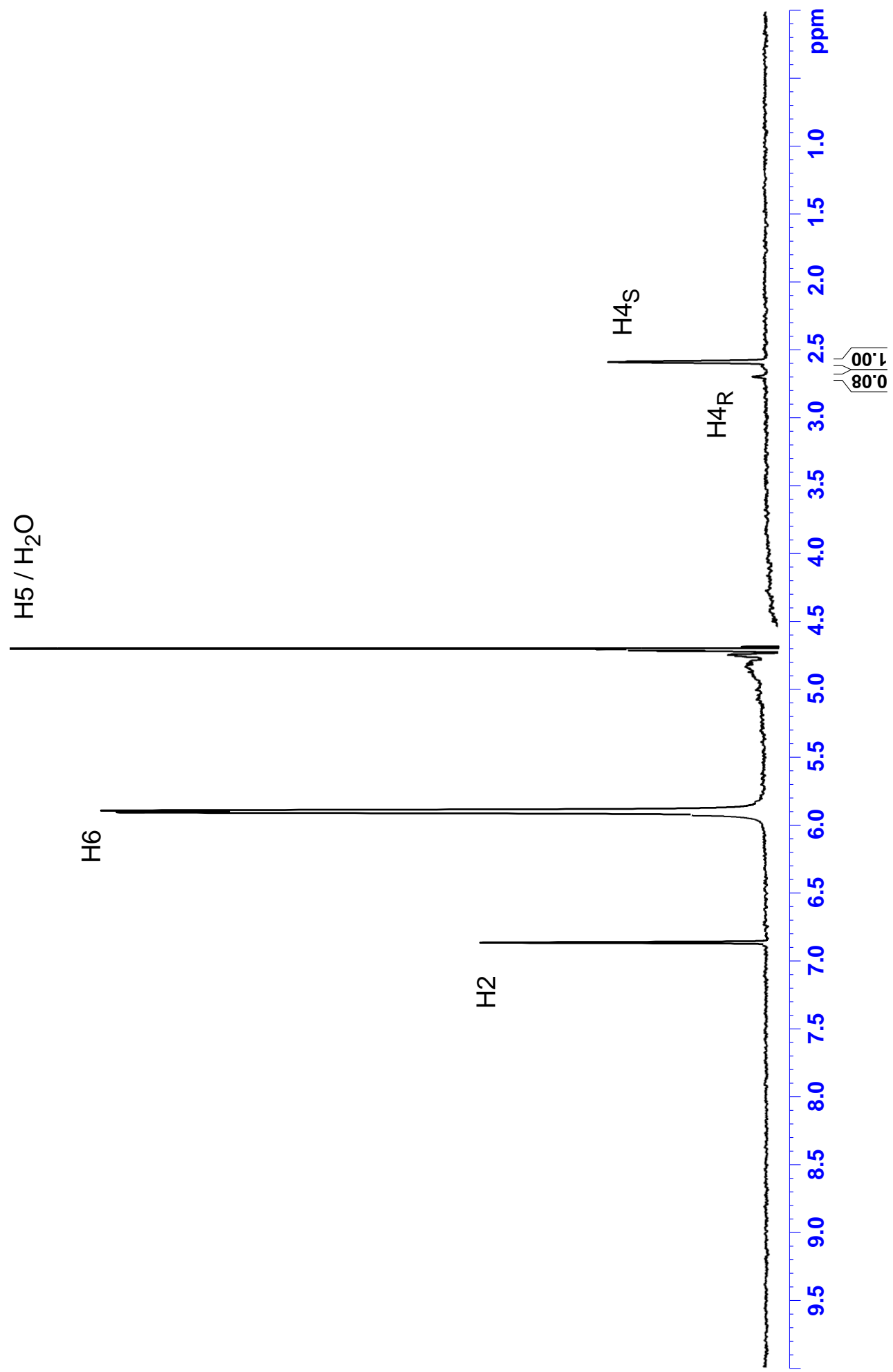


Figure S7: Selective tocsy of NAD²H from the reaction involving Sav-S112K

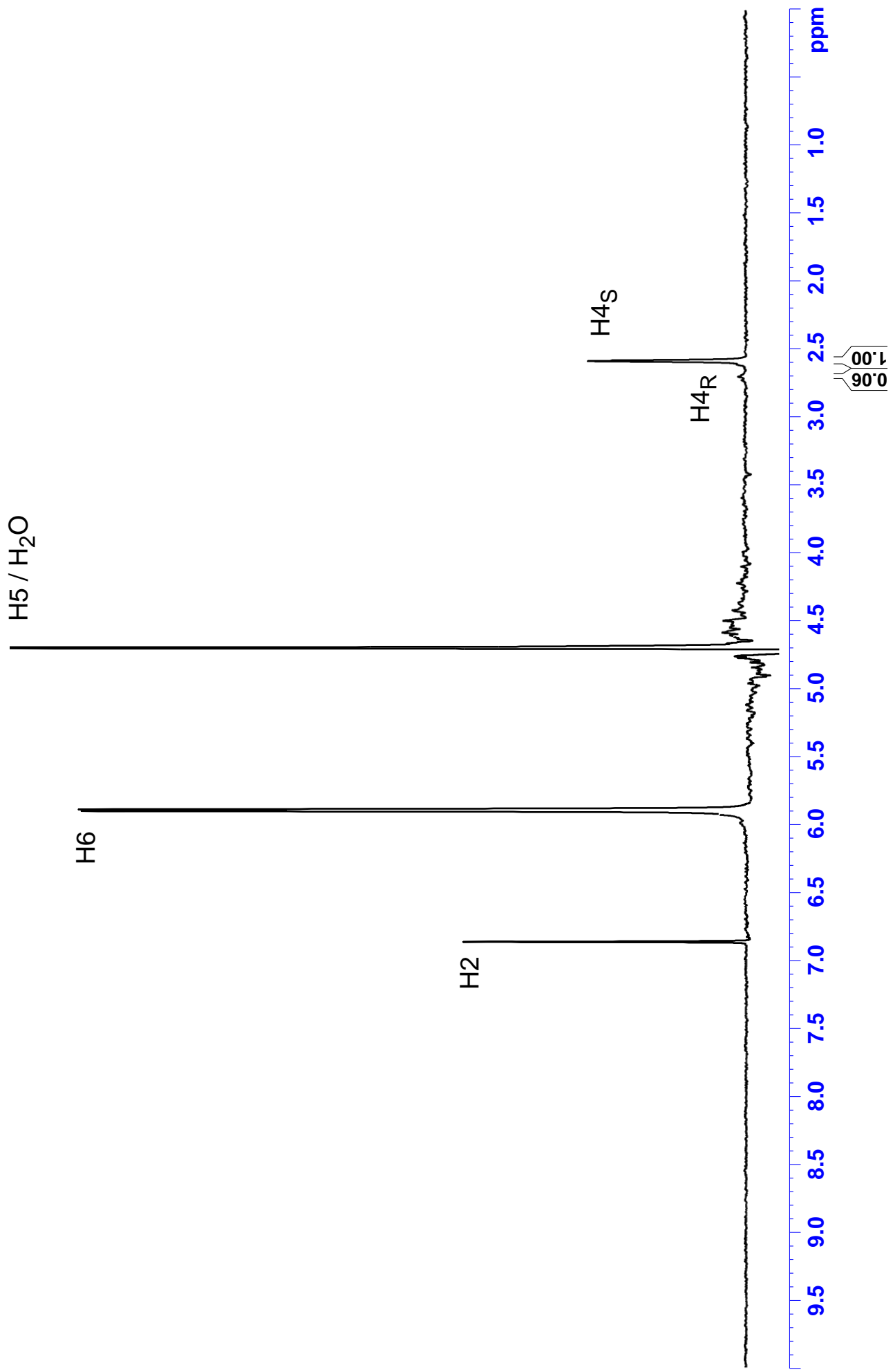


Figure S8: Selective tocsy of NAD²H from the reaction without Sav

